1994

Self-consistent Theory For Magnetic Properties In High-temperature Superconductors

Ravi Prakash Singh

Self Consistent theory for Magnetic Properties in High Temperature Superconductors

by

Ravi Prakash Singh

Department of Physics

Submitted in partial fulfillment
of the requirements for the degree of
Doctor of Philosophy

Faculty of Graduate Studies
The University of Western Ontario
London, Ontario
December 1993

ISBN 0-315-90567-0

ABSTRACT

It is now widely known that the new high-temperature superconductors are antiferromagnetic insulators in their normal state. Experimental results indicate that layered cuprates such as $La_{2-x}Sr_xCuO_4$ and $YBa_2Cu_3O_{6+x}$ go from antiferromagnetic to superconducting state as x changes in the stoichiometry with doping. This suggests a possible correlation between the properties of antiferromagnetism and superconductivity in these materials. Also, the magnetic properties in the normal state such as Neel temperature, it's dependence on doping, the sublattice magnetization etc. have an unusual behaviour which is not yet fully understood. The existing theories are not able to explain these magnetic properties. The aim of this thesis, therefore, is to understand the magnetic properties of these compounds in the antiferromagnetic insulating state.

We have developed a theory which takes into account the antiferromagnetic correlations present within the CuO_2 layers and also the weak but finite interlayer coupling between these CuO_2 planes. Our theory is based on the Green's function approach by which we have obtained an expression for the Neel temperature, it's doping dependence, the sublattice magnetization, the magnetic susceptibility and the magnetic correlation length. We have obtained self-consistent expressions for sublattice magnetization and susceptibility. We have found analytical expressions for some of these magnetic properties which would prove extremely helpful to the experimentalists. We have compared our theoretical results to the experimental result for doping dependent Neel temperature, sublattice magnetization, magnetic susceptibility and the magnetic correlation length. It is shown that the theory gives

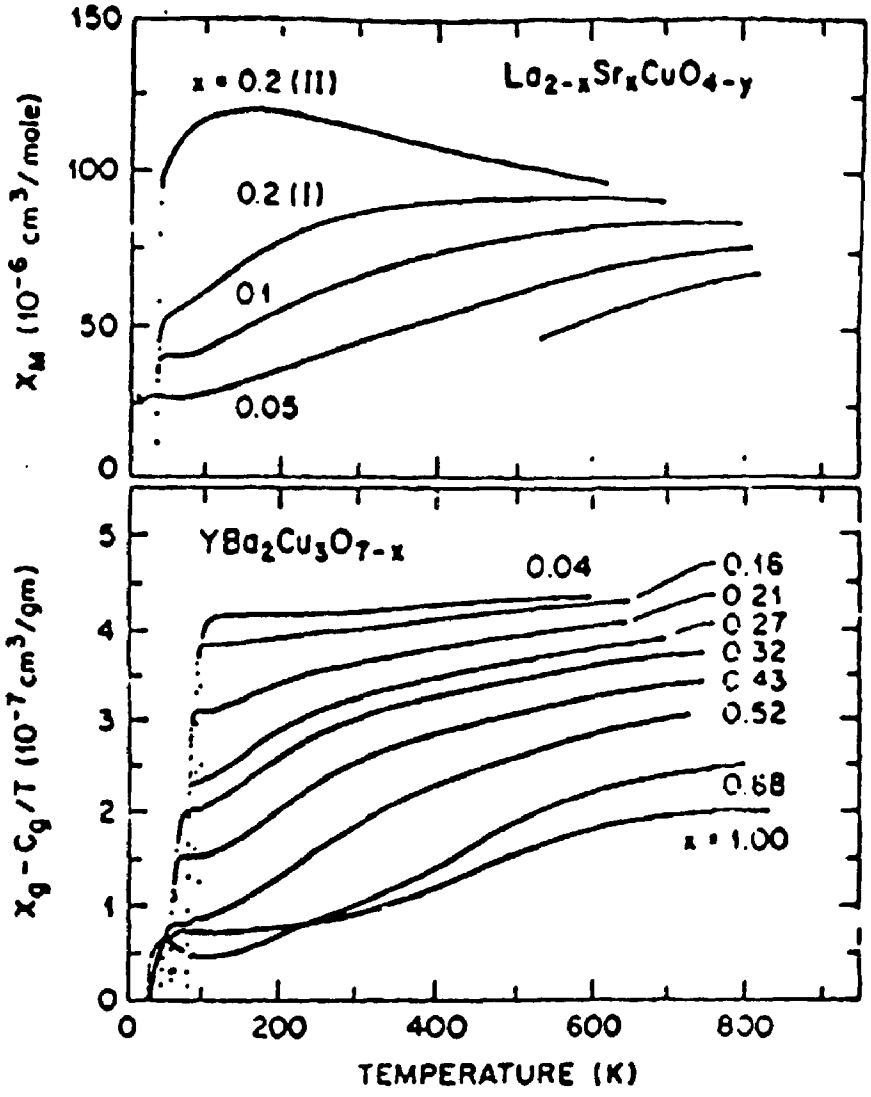

Figure 3.3: (a) Magnetic susceptibility χ vs. temperature for 2-1-4. (b) Corrected magnetic susceptibility χ_g - C/T vs. temperature for 1-2-3 compound.

To my parents

ACKNOWLEDGEMENTS

It was the ingenuity, wisdom and deep insight of my supervisor Prof. Mahi Singh which over the years has given me the courage and perseverance to stay with a topic as diverse and mystifying as High temperature Superconductors. I'm greatly indebted to him for the long hours and uncanny foresight which he rendered to me during my research. I find myself fortunate to have a rich and fruitful association with a person of his calibre.

I'm thankful to my examining committee comprising of Profs. Mike Cottam and John Nuttal who helped me during critical stages and shaped the course of my study at Western. Their input and their persona has always been a driving force behind this endeavor.

The environment of the Physics dept. has always been conducive to some great research and all my Professors have been marvellous. In particular, Prof. P.K John who always made it a point to talk to me about my research and helped immensely throughout. Prof. Graham Rose, ex-Graduate Chairman, for all the encouragement through the tough times. Prof. Dick Holt, current Graduate Chairman, during the later part of the thesis, for his interest and for taking care of all the necessary formalities. Prof. Phillip Tong for his interest and for introducing the topic to me. I'd be ever so grateful to you all.

I've been lucky to find Dr. Zhi Chao Tao who not only collaborated with me on a couple of projects but has always made himself available for discussion and provided some exquisite pointers. I'm thankful to Mr. Naser Tweel, my office-mate and my colleague, for all the subtleties of the topic which we figured out together.

I'm thankful to my friends Ashok, Narayan, Rajat, Sudhir, Vijay and countless others, for their valued advice which has helped me complete this thesis with my sanity intact.

Finally, my deepest regards and appreciation for the two most important people in my life, my parents, for their continued support, love and affection without which this work would have been a life long ambition. I'm fortunate to have achieved that ambition with their help and for me there is no turning back.

Contents

List of Tables

List of Figures

List of Abbreviations

AFM:	Antiferromagnetic
FSW:	Free spin-wave
HTS:	High-temperature superconductors
MES:	Mossbauer effect spectroscopy
MRPA:	Modified random phase approximation
μSR:	Muon spin resonance
NQR:	Nuclear quadrupole resonance
NS:	Neutron scattering
PAC:	Perturbed angular correlation
RPA:	Random phase approximation
SBMFT:	Schwinger boson mean field theory
SF:	Spectral function

Chapter 1

Introduction

1.1 Historical Background

The very first indication that metals when cooled below a certain temperature showed zero resistivity was found by H. Kamerlingh-Onnes[1]. This phenomenon, initially observed in mercury and later in other metals, was termed Superconductivity. In 1913, Kamerlingh-Onnes was awarded the Nobel Prize for his pioneering work on the properties of matter at low temperatures. It was a startling discovery except that the temperature required to do so was 4K. The importance of the discovery was no doubt recognised and hoards of activities have taken place since then [2-14].

Prior to 1986, superconductivity saw at least two periods of high activity [1-6]. It started with the discovery of superconductivity and the existence of critical current and critical magnetic field. H.K.Onnes during 1911-1914 also did the persistent current experiments. In the years that followed, a variety of metals and metallic alloys were found which showed superconductivity at varying transition temperatures. Apart from finding these materials with higher transition temperatures a

lot of other important developments occurred in this field before 1986. In 1933, Meissner and Ochsenfeld revealed the diamagnetic character of superconductors[2]. The discovery led to the formulation of Gorter-Casimir theory of the thermodynamics [3] of superconductors in 1934 and then the London theory of electromagnetic behaviour [4] in 1935.

More recent discoveries involve the development of the Ginzburg-Landau theory [5] in 1950 and the discovery of the Isotope Effect in the same year. The theoretical attempts for the elucidation of the microscopic mechanism responsible for the properties of Type II superconductors resulted in BCS theory in 1957 by John Bardeen, Leon Cooper and Robert Schrieffer, for which they won a Nobel Prize in 1972. They proposed that electrons interact with each other by means of distortions in the lattice and they form a bound state called Cooper pair. It was then shown that this attractive interaction between electrons was responsible for Superconductivity. This was the first comprehensive theoretical attempt to describe the superconducting phenomenon in superconductors [6].

Later in the 1960's, Ivar Giaever was the first to study the single particle tunnelling in superconductors. Other major theoretical development came in 1962 when Brian Josephson predicted that Cooper like pairs can tunnel between weakly linked superconductors. In recognition of these theoretical and experimental development in superconducting tunnel junctions both Brian Josephson and Ivar Giaever were awarded the 1974 Nobel prize along with Esaki who studied tunnelling in semiconductors. These discoveries were important from the technological point of view since they formed the basis for a diverse electronic application of superconductors, such as the production of SQUIDS and multilayers, which would be required to produce integrated circuits.

1986 saw one of the most important discoveries of this century. In the early part of 1986, Bednorz and Müller [7] found a ceramic material La-Ba-Cu-O, which showed some interesting properties and a transition temperature of 30K. It was conceived, for the first time that a ceramic material could show a transition temperature (T_c) of 30K. These materials are now famously known as 2-1-4 compounds. It is to be understood here that ceramics are Insulators. Prior to 1986, all the superconducting materials discovered were either metals or metallic alloys. This discovery fetched them the 1987 Nobel prize in Physics. Never before in the history of Nobel prize has anyone been awarded this singular recognition in such a short time following their discovery. As a consequence of this discovery, a renewed interest grew in superconductivity and in the ensuing years people all over the world engaged themselves in finding materials with higher transition temperatures. Paul Chu [8] and his group in early part of 1987 came up with a new class of superconducting compound, Y-Ba-Cu-O, called 1-2-3 compounds, showing a T_c of 90K. In 1988, H. Maeda and his group found yet another compound, Bi-Sr-Ca-Cu-O, which showed a transition temperature of 115K [9]. Later in the same year, the trend was continued by Z. Z. Sheng and A. M. Herman who escalated the transition temperature to 125K in Tl-Ba-Ca-Cu-O [10].

In 1993, after a gap of almost five years, Andreas Schilling has reported finding Hg-Ba-Ca-Cu-O which shows a transition temperature of nearly 133.5K [11]. Recently, in a span of less than two months, following this discovery, Paul Chu et al. have reported observing superconductivity above 150K in $HgBa_2Ca_2Cu_3O_{8+\delta}$ under high pressures which is the highest reported T_c to date [12]. It is interesting to realize that the transition temperatures in these high-temperature superconductors (HTS) is more than the boiling point of Liquid Nitrogen (77K) which has the

advantage of being much cheaper than the liquid Helium which was widely used to observe superconductivity prior to 1986. The only problem with the last two of these ceramics is that they are highly toxic in nature and hence pose severe problems in the study of their properties. Fig 1.1 shows the manner in which the transition temperature has grown during this century. The list of High-temperature superconductors and their transition temperatures are presented in Table 1.1.

Although, the field of High temperature superconductivity is still in it's infancy but already, these discoveries have made an everlasting impression on the scientific research by bringing Physics, Chemistry and Engineering together. From the applications point of view, it has been recognised that these discoveries are so vital that the enhancement of T_c to somewhere near the room temperature would revolutionize the basic structure of the world we live in. The efforts to achieve that ever so elusive goal is still underway.

In this thesis, Superconductors among metals and metallic alloys discovered prior to 1986 are called **Conventional Superconductors** while those discovered after 1986 in layered copper oxides would be called **High temperature Superconductors**. The difference in the nomenclature is important since before the advent of High temperature superconductivity in ceramics it was believed that due to the presence of the quantized lattice vibrations in solids (phonons), there was attractive interaction between electrons and they formed Cooper pairs which were responsible for the onset of superconductivity. BCS theory gave an upper limit to the transition temperature, below which there is no residual resistivity in the material, of nearly 30K. Now, in the post 1986 era, the highest transition temperature has gone to almost 150K and BCS theory is no longer applicable to the High temperature superconductors. It hence becomes imperative to look for different mechanisms and

theories that could explain such high transition temperatures in these new oxides.

High temperature superconductors are different in the sense, that they have a highly unusual phase diagram, for example, in $La_{2-x}Sr_xCuO_{4-y}$ and $YBa_2Cu_3O_{6+x}$, the material undergoes a structural change from tetragonal to orthorhombic as x changes in the stoichiometry. This changing x in the stoichiometry is also accompanied by an insulator to superconductor transition. This rich phase diagram, a very distinct insulator to metal transition and various structural instabilities have given different approaches for possible mechanisms. On top of all this, rather unusual magnetic and electronic properties have contributed significantly to the notion that a completely different type of mechanism may well be playing part in the superconductivity. Some of these have gathered enough support both theoretically and by experimental revelations. Initial suggestion of Anderson[13, 14] that a novel quantum spin fluctuation in CuO_2 layers may be responsible for HTS has received considerable attention. This theory has been called the Resonating Valence Bond (RVB) theory. Further, it was found that the 3-D Neel temperature in 2-1-4 compounds showed a sensitive dependence on the doping concentration of oxygen [15] and later strong 2-D correlations were observed in these materials[16, 17]. These observations led Anderson to conjecture that these fluctuations may play decisive role in destroying the long range antiferromagnetic order in the ground state, thereby, producing a new quantum 'spin-liquid' state. How does this spin-liquid state manifests itself in —bringing out the superconducting properties in these layered superconducting ceramics is still a matter of great debate.

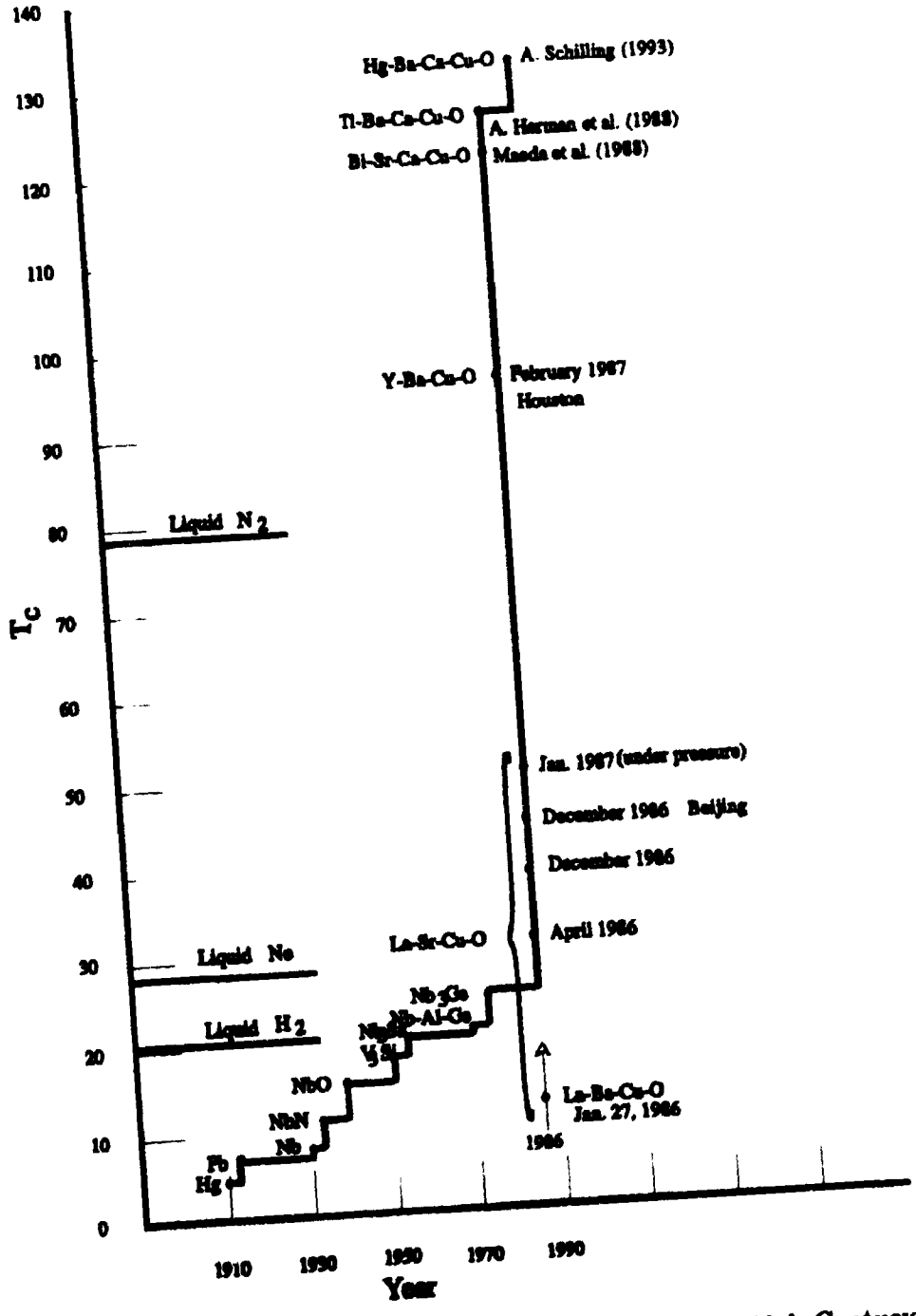

Figure 1.1: Advances in Superconductivity in the 20th Century

Table 1.1:

LIST OF HIGH T_c OXIDE SUPERCONDUCTORS		
Compound	T_c	Discovered by
La-Ba-Cu-O		J. G. Bednorz, K. A. Muller (1986)
$(La_xBa_{1-x})_2CuO_4$	30K	
$La_{1.85}Sr_{.15}CuO_4$	45K	
Y-Ba-Cu-O		W. K. Wu, C. W. Chu (1987)
$YBa_2Cu_3O_7$	90K	
$YBa_2Cu_3O_8$	85K	
Bi-Sr-Ca-Cu-O		H. Maeda et al. (1988)
$Bi_xSr_2Ca_2Cu_2O_y$	85K	
$Bi_xSr_2Ca_2Cu_3O_y$	115K	
Tl-Ba-Ca-Cu-O		Z. Z. Sheng, A. M. Herman (1988)
$Tl_xBa_2CaCu_2O_y$	100K	
$Tl_xBa_2CaCu_3O_y$	120K	
$Tl_2Ba_2Ca_2Cu_3O_10$	125K	
Hg-Ba-Ca-Cu-O	133.5K	Andreas Schilling (1993)
$HgBa_2Ca_2Cu_3O_{8+\delta}$	150K	C. W. Chu et al. (1993)
$Ba_xK_{1-x}BiO$	30K	R. J. Cava et al. (1988)
$Nd_{2-x}Ce_xCuO_4$	20K	Y. Tokura, H. Takagi and S. Uchida (1989)

Until 1986, superconductivity was observed in metals and metallic alloys. The layered copper oxides on the other hand are Insulators in the normal state. Study of these insulators in their normal state has revealed some very unusual properties and a very strong antiferromagnetic correlation. It is believed that the normal state of these high-temperature superconductors (HTS) holds the key to the mystery enveloping superconductivity in these compounds. It is in this context that a study of the magnetic properties in the normal state takes utmost importance.

Various studies on HTS [15, 16, 17] suggest that their structure is highly anisotropic and they undergo a phase transformation from tetragonal to orthorhombic superconducting state when doped. In the case of $La_{2-x}Sr_xCuO_{4-y}$, the doping of oxygen as well as doping of Sr affects the phase transition. As x changes from 0.0 to 0.02 the compound is an AF insulator. At $x \sim 0.04$ the compound becomes a superconductor. Similarly, in $YBa_2Cu_3O_{6+x}$, the parent compound is an antiferromagnetic insulator at no doping. With $x > 0.4$, the compound goes under a phase transformation from AF insulator to superconductor[35, 36, 37]. As far as superconductivity is concerned, it has also been found that substitution of 'Y' in 1-2-3 by other rare earths doesn't change the transition temperature much. However, the transition temperature is strongly suppressed by substitution of zinc but at the same time, iron and cobalt have very little effect. Substitution of oxygen in these compounds enhances the superconducting nature and the transition temperature is increased but substitution of p-holes contributes towards a strong Antiferromagnetic ordering in CuO_2 planes.

The copper spins in these materials have a magnetic moment and they are arranged antiferromagnetically within the two dimensional layers and also perpendicular to it. Some earlier experiments suggested that the maximum staggered

magnetization in the Neel state is approximately $0.5\mu_B$/Cu. Above the Neel temperature no long range order exists [16]. Experiments on these materials have shown that the Neel temperature is highly dependent on oxygen and rare earth metal doping [21, 38]. For undoped 2-1-4 and 1-2-3 compounds the Neel temperature is found to be 340K and 500K respectively. The Neel temperature and the effect of doping are dealt with in Chapter IV.

In the normal state, the sublattice magnetization depends crucially on the temperature. The sublattice magnetization decreases as the temperature is increased and eventually disappears at the Neel temperature. Undoped materials at zero temperature do not behave as saturated sublattices. Due to zero point quantum fluctuations, the average spin value is less than half. We discuss these subtleties in considerable detail in Chapter V. The sublattice magnetization has different temperature dependences in different regimes. Also, it has been observed that with doping the sublattice magnetization shows a crossover from 3-D to quasi-2D behaviour [74]. The temperature dependence of sublattice magnetization is still a very controversial topic and we address this problem when we deal with magnetization in Chapter V.

The magnetic susceptibility in HTS depends crucially on the method of preparation of the materials. It has been found that the susceptibilities in these compounds are anisotropic [40, 41]. The contributions to the susceptibility come primarily from the spatial orientation of the Cu orbitals and the spin. The spin susceptibility for 1-2-3 is found to be 2-3 times larger than the insulating antiferromagnet, below the neel temperature. The temperature variations of susceptibility are more or less governed by the Curie Weiss law. Below the Neel temperature the magnetic susceptibility is a linear function of temperature for quasi-2D case and it varies as T^2 for the 3-D case [42]. We address these points in greater detail in

Chapter VI.

The Magnetic correlation length has been studied by various authors. Experimental results on 2-1-4 compounds suggest that the correlation length decreases as the temperature is increased [17, 114, 61]. Doping of Sr in 2-1-4 has been shown to have far reaching implications on the magnetic correlation length. Even a small concentration of excess holes was found to alter the magnetic correlation length to a large extent [61]. Theoretical attempts to explain these experiments for undoped and doped samples haven't been very successful. We discuss some of these attempts when we calculate the magnetic correlation length from our theory in Chapter VIII.

1.2 Scope of the Thesis

It is now known that the normal state of these HTS is an antiferromagnetic insulator possessing strong correlations between spins in the 2-dimensional copper oxide planes. Also, there exists a weak interlayer coupling between the planes which plays a very crucial role in most of the magnetic properties such as Neel temperature, sublattice magnetization, magnetic susceptibility and magnetic correlation length.

Our aim is to build a theory for quasi-two dimensional antiferromagnets including the antiferromagnetic correlations within the planar CuO_2 layers and also between these layers. We wish to study the magnetic properties such as the Neel temperature, it's dependence on doping, the sublattice magnetization, the magnetic susceptibility and the magnetic correlation length. We would also study the crossover behaviour of the magnetic properties in 1-2-3 and 2-1-4 compounds with doping and with the change in temperature. We would then compare our theoretical results with the experimental results available for the above mentioned properties.

The theoretical results obtained with this theory would be compared with other theoretical attempts that have been made to explain these properties.

A study like this is important since, recently, it has been argued based on some experimental revelations that the antiferromagnetic correlations present in the normal state persist through the superconducting transition. The inter correlation between antiferromagnetism and superconductivity has been one of the most important questions in the post 1986 superconductors. We present this study with the hope that the results achieved through this theory would go a long way in understanding the the antiferromagnetic phase of $La_{2-x}Sr_xCuO_4$ and $YBa_2Cu_3O_{6+x}$.

The thesis has been divided into nine chapters. The first chapter of the thesis deals with the historical background concerning Superconductivity and most of the important developments that have occurred over the years. We have tried to give a brief introduction of some major developments in the field until recently. We have also introduced the magnetic properties of the High temperature superconductors in their normal state.

The second Chapter covers some startling differences between the conventional and high-temperature superconductors and some of the important structural properties and phase diagram of HTS. Our intention is to establish here, that the properties are so diverse that the theoretical model for conventional superconductors are no more valid for HTS. Also, we start to look into some important structural aspects and the phase diagram of HTS which would give us crucial information that would be used in formulation of a theory for normal state magnetic properties.

A brief review of the experimental results on the magnetic properties of high-temperature superconductors are given in Chapter III. We have focussed our study

on two compounds namely $YBa_2Cu_3O_{6+x}$ (1-2-3) and $La_{2-x}Sr_xCuO_{4-y}$ (2-1-4). We have reviewed all those magnetic properties that are calculated in chapters ahead. So, this chapter would also establish some facts that are used later to test our theory on.

In the fourth chapter, we have laid down the self-consistent theory and have derived an expression for the Neel temperature for antiferromagnets. Theoretical results obtained from the theory are presented and the results are compared with experiments. We have also studied the role of interlayer coupling and doping on the Neel temperature in HTS.

This theory is shown to provide a self-consistent expression, in the fifth chapter, for the sublattice magnetization. The expression thus obtained is evaluated numerically and the results are compared with the experimental results. We have compared our results specifically with the linear spin-wave theory and have shown that under specific approximations on the self-consistent theory, spin wave results can be obtained. The theory is shown to give results which are in excellent agreement with experiments.

The sixth chapter contains a novel approach for the evaluation of magnetic susceptibility by the spectral function of spin waves. The magnetic susceptibility and it's dependence over temperature is studied and the results are again compared with the available experimental results. Our theoretical results are shown to explain the experimental results at high temperatures. At low temperatures, there is a disagreement between theory and experiments which is discussed.

We have studied the r-dependent and T-dependent crossover in the seventh chapter. The sublattice magnetization is shown to undergo a crossover which occurs

at a critical value of the anisotropy parameter. The results obtained are compared with other theoretical results. It is also shown, by a general use of the spectral function that at a temperature T$\sim 2J_{||}\sqrt{2r}/k_B$, the sublattice magnetization undergoes a 3-dimensional to quasi-two dimensional character.

We have evaluated the magnetic correlation length in the eighth chapter. The dependence of magnetic correlation on doping is also studied. It is shown that the expression for the magnetic correlation length is doping dependent. The results are compared with some of the recent experimental results and good agreement has been obtained. We have also compared our theoretical results with other theoretical models which have been used to explain the magnetic correlation length.

We have presented all the results and the salient features of the self- consistent theory in the last chapter. A brief summary of our work is presented here.

A short review of the Green's function approach is added in the appendix I since the self-consistent theory has emerged out of this approach. In appendix II, we have shown by using the second quantization method that the Heisenberg hamiltonian is a consequence of exchange effects in solids.

Chapter 2

Properties of HTS

The advent of High-temperature superconductivity in layered copper oxides has triggered widespread interest in the study of the nature and the properties of these materials. The most important reason for such an upsurge of interest was the realization that the properties, both in the normal and superconducting state, in these ceramic materials differed from their predecessors. We will try to give here a brief outline of some basic properties in Conventional and High-temperature superconductors (HTS) since, it not only gives us a better understanding about these novel materials but would also help others to appreciate the need for a comprehensive theory that could solve the mystery which encompasses the field of High-temperature superconductivity today.

This chapter gives the definition of superconductors and then the basic differences between conventional and high-temperature superconductors. We then discuss the structural properties of High temperature superconductors, mainly 1-2-3 and 2-1-4. Structural anisotropy in the High temperature superconductors is the reason behind a lot of interesting properties in the normal state of these layered copper oxides. At the end of this chapter, we have focussed our attention to the phase dia-

gram of two widely studied High temperature superconductors, namely La-Sr-Cu-O and Y-Ba-Cu-O.

The aim of this chapter is twofold. First, we want to establish that the properties of conventional and High temperature superconductors are so different that the theoretical model used to explain superconductivity prior to 1986 is no longer valid. Second, we would review the structural properties and phase diagram of High temperature superconductors in order to gather some basic information which might help us in developing a theory for explaining the magnetic properties.

2.1 What are superconductors ?

A superconductor when cooled below a certain temperature, called the transition temperature $\mathbf{T_c}$, has **zero electrical resistivity**. This alone does not guarantee a solid to be superconductor. At the transition temperature, a superconductor, should expel all magnetic field. This phenomenon of perfect diamagnetism exhibited by superconductors is called the **Meissner Effect**. At high enough fields, however, the superconductivity vanishes and the field fully enters the sample. The critical field, H_c, where the superconductivity is destroyed is also an intrinsic property of superconductivity. It has been found that in some superconducting materials the loss of the diamagnetic character happens at a sharp value of magnetic field and in others there is a partial diamagnetism after a lower critical field H_{c1} and total loss at an upper critical field H_{c2}. The materials showing former behaviour are called **Type I Superconductors** while the latter **Type II Superconductors**. Most of the HTS are known to be Type II superconductors.

2.2 Comparison between Conventional and HTS

Here, we give a brief outline of some of the salient differences between Convention. l and High temperature Superconductors.

Resistivity

Resistivity in normal metals is given by $\rho \approx A + B\,T$ where $T \geq 0.2\,\theta_D$. Here θ_D, is called the Debye temperature and A and B are constants. In this temperature range, the T-dependent resistivity is dominated by the electron-electron interactions. However, in the low temperature regime, electron-phonon scattering plays the dominant part in the resistivity and is given by the form $\rho \approx C + D\,T^5$. Here, C and D are constants. These constants in the above form for resistivity is a consequence of the electron scattering from point or line defects, impurities etc. [18]. In case of High temperature superconductors, due to the structural anisotropy, the resistivity too has an anomalous anisotropic temperature dependence. At low temperatures, the resistivity along the ab-plane, ie. within the CuO_2 planes, ρ_{ab}, changes linearly with temperature which is unusual since we expect a T^5 behaviour [19]. In the direction perpendicular to the planes, along the c-axis, $\rho_c \propto T^{-\alpha}$, where $\alpha \approx 0.61$ [20]. The perpendicular resistivity is nearly two to five orders of magnitude larger than the inplane resistivity ie. ρ_c/ρ_{ab} ~500 - 10^6. These differences in the inplane and interplane resistivities in 1-2-3 compounds is shown in fig.(2.1). This anomalous behaviour of resistivity is still unclear with unknown reasons.

Carriers

In case of conventional superconductors which were metals or metallic alloys, the charge carriers were always electrons. In retrospect, the recent Hall Effect and other measurements suggest that the carriers in case of 1-2-3 and 2-1-4 are holes [21, 22].

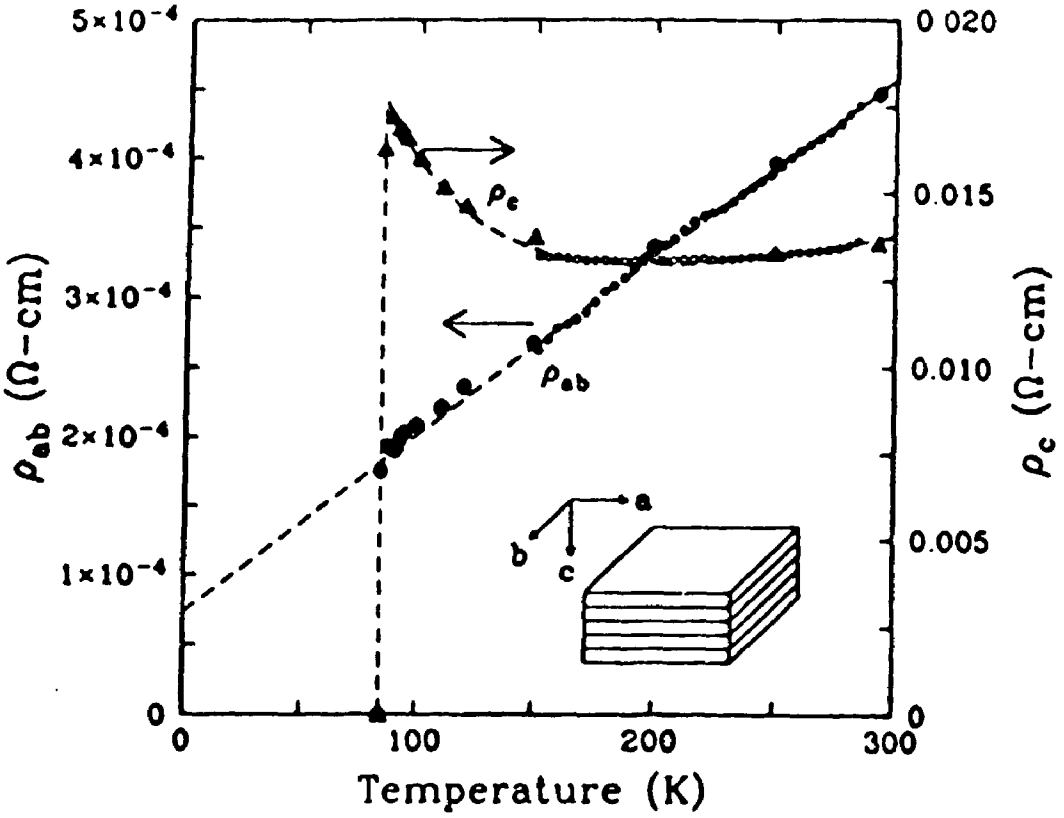

Figure 2.1 : The intraplane and interplanar resistivities in 1-2-3 compounds.

Energy gap

The conventional superconductors have an energy gap in the superconducting state. BCS theory predicts such a gap and gives the relationship between the critical temperature T_c and the Energy Gap Δ as $2\Delta/k_B T_c = 3.53$. In HTS, different experimental techniques have shown that in 1-2-3, there is an Energy gap similar to the one in conventional superconductors [23, 24, 25]. Most of these identify a range of 3.0 to 6.0 for $2\Delta/kT_c$. This range of values reflect a highly anisotropic gap in case of 1-2-3. Tsai et al. [24] have studied tunnelling in directions parallel and perpendicular to the c-axis on 1-2-3 films. They have concluded that the gaps in two principal directions had the values $\Delta_{ab} = 5.9 \pm 0.2kT_c$ and $\Delta_c = 3.6 \pm 0.2kT_c$. The energy gap for 1-2-3 has also been measured from various other techniques by van Bentum et al. [23]. The values obtained from some of these measurements range from 12.5 to 14.0 meV.

Characteristic Lengths (ξ and λ)

ξ, the Coherence Length, is the spatial range or the decay distance of the superconducting wavefunction. λ is the penetration depth. Unlike the conventional counterparts the coherence length in HTS is very small and highly anisotropic, for example in La-Sr-Cu-O $\xi_o \sim 20\mathring{A}$. Coherence Length for 1-2-3 is of the order of 10Åas compared to 1000Åin other type II superconductors. Braginsky et al. [26] have obtained both coherence length and the penetration depth for the a-b plane and along the c-axis. They found λ = 1800 $\mathring{A}$ and 270 $\mathring{A}$ and ξ = 2 - 4 $\mathring{A}$ and 16 - 30 $\mathring{A}$ along the c-axis and within the ab-plane respectively.

Heat Capacity

Like conventional superconductors, HTS too show a jump in Heat capacity at $T=T_c$

which is indicative of a phase transformation. Also, at T=0 unlike the normal metals which have a linear T term in heat capacity, no such linear dependence has been found in HTS nor in Conventional superconductors. In the Heat capacity measurements, the sharp jump is replaced by a more gradual change with a tail extending well above the transition temperature.

Isotope Effect

In conventional superconductors, it was observed that the doping of isotopes enhanced the transition temperature. The transition temperature was found to depend on the Isotopic mass by the relation $T_c \propto M^{-\alpha}$ where α was almost 1/2 within experimental error [27]. Measurements on HTS like 1-2-3, shift of transition temperature was sought after a major fraction of O^{16} was replaced by O^{18}. Interestingly enough, no shift in transition temperature was observed [28, 29]. This observation is taken to imply that the phonon contribution to the coupling is minor and hence BCS theory is not valid for these compounds.

Having understood some basic differences between conventional and High temperature superconductors, we would now move on to the study of some characteristic properties of layered copper oxides. From here on, it's our intention to discuss those characteristics only, which have significant implications on the magnetic properties of HTS. Also, from here onwards, we would avoid the properties of conventional superconductors altogether.

2.3 Crystal Structure

There has been a lot of indications that lead us to believe that the mystifying properties of HTS originate due to certain type of structure of these superconductors.

We will during the course of this thesis focus our attention on two famous materials viz. $YBa_2Cu_3O_{6+x}$ called 1-2-3 and $La_{2-x}Sr_xCuO_{4-y}$ called 2-1-4. These have the advantage of being extensively studied and most clearly understood among all other materials that exhibit high temperature superconducting behaviour. These two materials belong to the class of compounds known as perovskites.

2.3.1 Perovskite Structure

The structure of superconducting materials has been studied by various experimental techniques like X-ray, Neutron-diffraction, Electron Microscopy etc.[43, 44, 45, 46, 47]. These studies suggest that their structure is related to the ideal perovskite structure ABX_3. The unit cell in ideal perovskite has a cubic ABX_3 structure where A and B are cations and X is an anion. The structure of an ideal perovskite is shown in fig.(2.2). Almost all of these compounds are insulators except when A and B both are heavy non-transition metals.

2.3.2 Structure of 2-1-4

The parent compound in the $La_{2-x}Sr_xCuO_{4-y}$ series is the compound La_2CuO_4 which forms as the tetragonal K_2NiF_4 structure. The basic structure of these A_2BX_4 compounds have their B atoms lying in planes and are octahedrally coordinated by X atoms while the A atoms are about nine-fold coordinated. La-Ba-Cu-O system is a variation on the perovskite ABX_3 structure where A=La or Ba and B=Cu. Neutron and X-ray diffraction [48, 43] have found the structure of 2-1-4 having two K_2NiF_4 form ula units per unit cell. At the center of the cell is a CuO_4 octahedron surrounded by La or Ba atoms. Each copper atom is at the center of

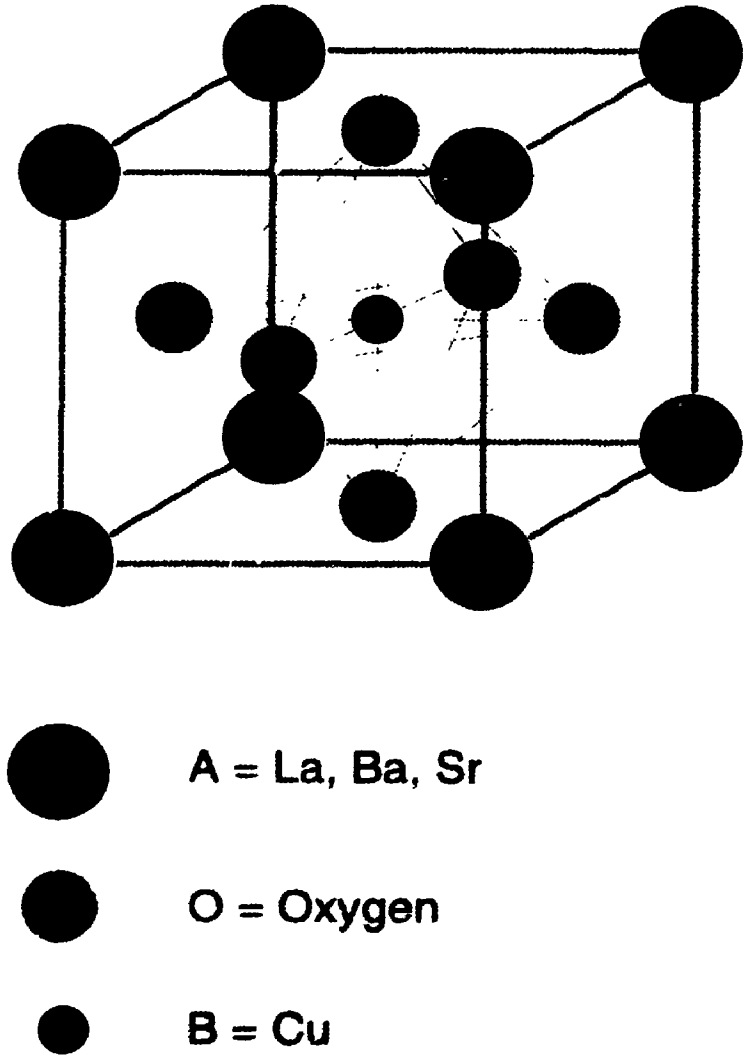

Figure 2.2: Structure of ABX_3 : Ideal perovskite

the octahedron surrounded by four oxygen in the square planar arrangement and two other oxygen are situated above and below the plane at a larger distance. This results in the cubic perovskite structure being elongated along the 'c' direction of the cell. Above and below this is another layer of elongated perovskites that are shifted along the'a' and 'b' axes by half a unit cell thus forming a CuO_4 octahedra situated at the corners of unit cell of $(La_{1-x}Ba_x)_2CuO_4$. This kind of distortion is called Orthorhombic distortion. This kind of structure almost always results in the formation of a planar CuO_2 layer which is conjectured to be playing decisive role in the onset of superconductivity in these materials. These planar CuO_2 layers have strong antiferromagnetic correlation between the neighbouring Cu spins and infact these correlations are responsible for the host of unusual magnetic properties in the normal state. The unit cell of La-Ba-Cu-O system is shown in fig.(2.3).

2.3.3 Structure of 1-2-3

The Y-Ba-Cu-O system which shows a transition temperature of 90K has a more intricate structure although more or less similar to La-Ba-Cu-O. In 1-2-3, stacking of three ABX_3 type perovskites make a unit cell. The A element in this case is either Y or Ba and there are two key oxygen atoms missing in the unit cell structure. The oxygen atoms at the center of c axis and the corners of 'ab' plane surrounding the Y site are missing. Also, the oxygen located at the top and bottom plane along the 'a' direction is missing causing an orthorhombic distortion in the unit cell. The absence of oxygen in the top and the bottom plane destroys the planar structure and instead forms a one dimensional periodic chains of Cu-O along the b-direction. Also, the oxygens between the chain and the plane moves towards the CuO chain thus weakening the bonding between it and the Cu on the CuO_2 plane.

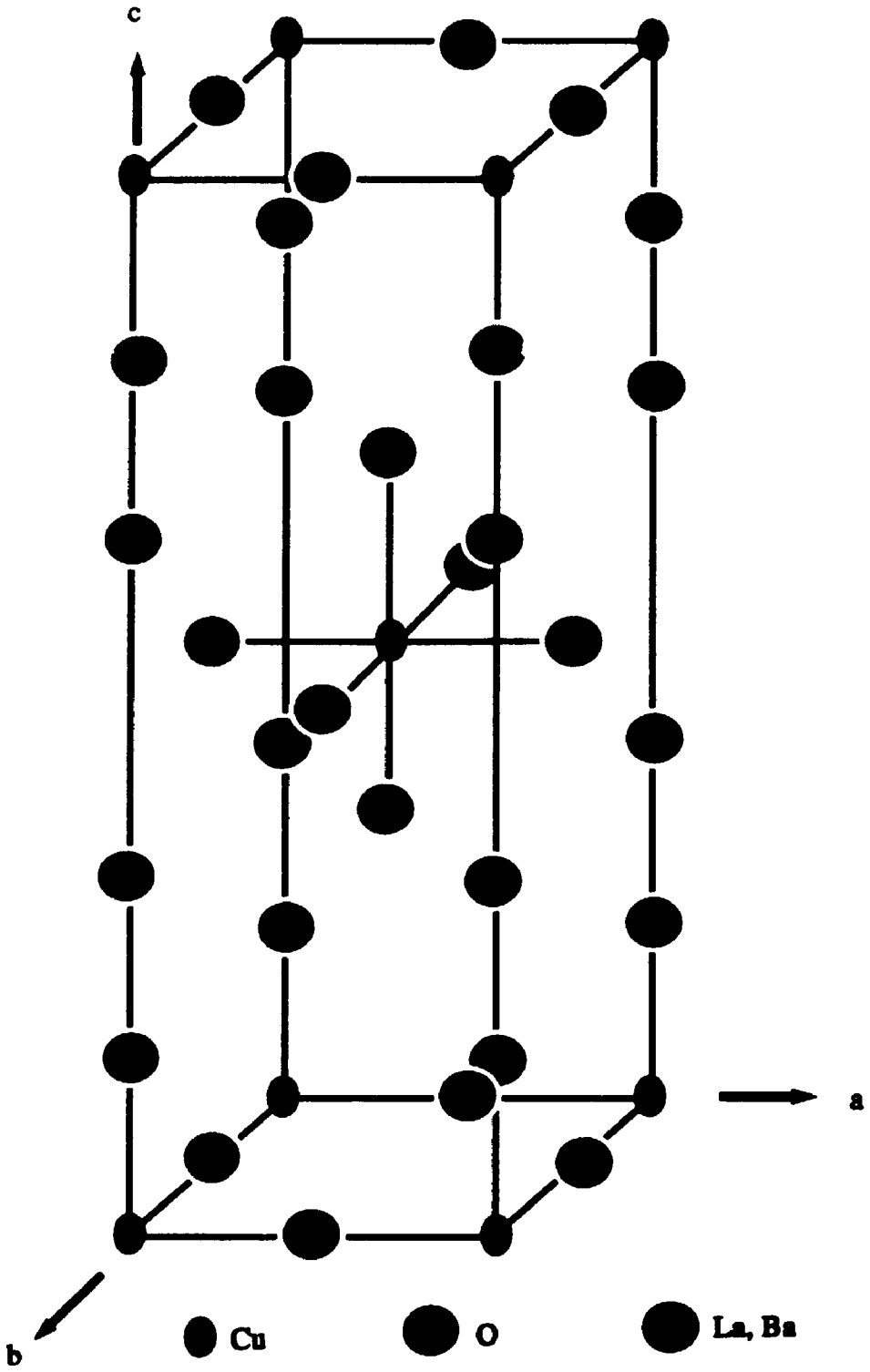

Figure 2.3 : Structure of 2-1-4

This produces a planar effect between the copper and the remaining oxygens. The unit cell hence contains two of these CuO_2 planes, in apparent contrast to La-Ba-Cu-O which contains only one of these layers. When oxygen is added to the system, they go first to the chain layers where the Cu[1+] ions are changed to Cu[2+] and hence we get holes in these layers. This is the reason why these layers are also called the *charge reservoir layers*. The planar layers on the other hand are not affected by the addition of the oxygen in the stoichiometry. Most of the conduction takes place in these planar layers and they are also termed as the *conduction layers*. The location of these planar and chain layers are depicted in fig.(2.4). Most of the magnetic properties are associated with the interactions within and between these planar layers. We would discuss the significance of these layers on the magnetic properties in the normal state of these materials in Chapter IV.

The basic structure corresponds to a cubic perovskite with one of the axes triply elongated. This is an oxygen deficient structure. Along the b-axis there are Cu1-O1 chains with each Cu1 having two O1 neighbours at 1.94Åand two O4 at 1.85Å. Above about $500°C$, the b-axis contracts while the a-axis elongates, and finally both become almost equal and the structure becomes tetragonal. The unit cell dimensions of this tetragonal Y-Ba-Cu-O system is a= 3.86 Å, b=3.86 Å, and c=11.82 Å.

Over the years it has been well established that the Cu[1] and Cu[2] atoms have a 2+ valence ($3d^9$) configuration in the fully oxygenated x=1 compound [135]. Evidences of oxygen holes in the planes and chain layers in 1-2-3 has also been obtained by different experimental techniques [50, 51]. Superconductivity occurs when a sufficient concentration of holes is present in these materials. In case of 1-2-3 it is now known that the transition from the tetragonal to the orthorhombic

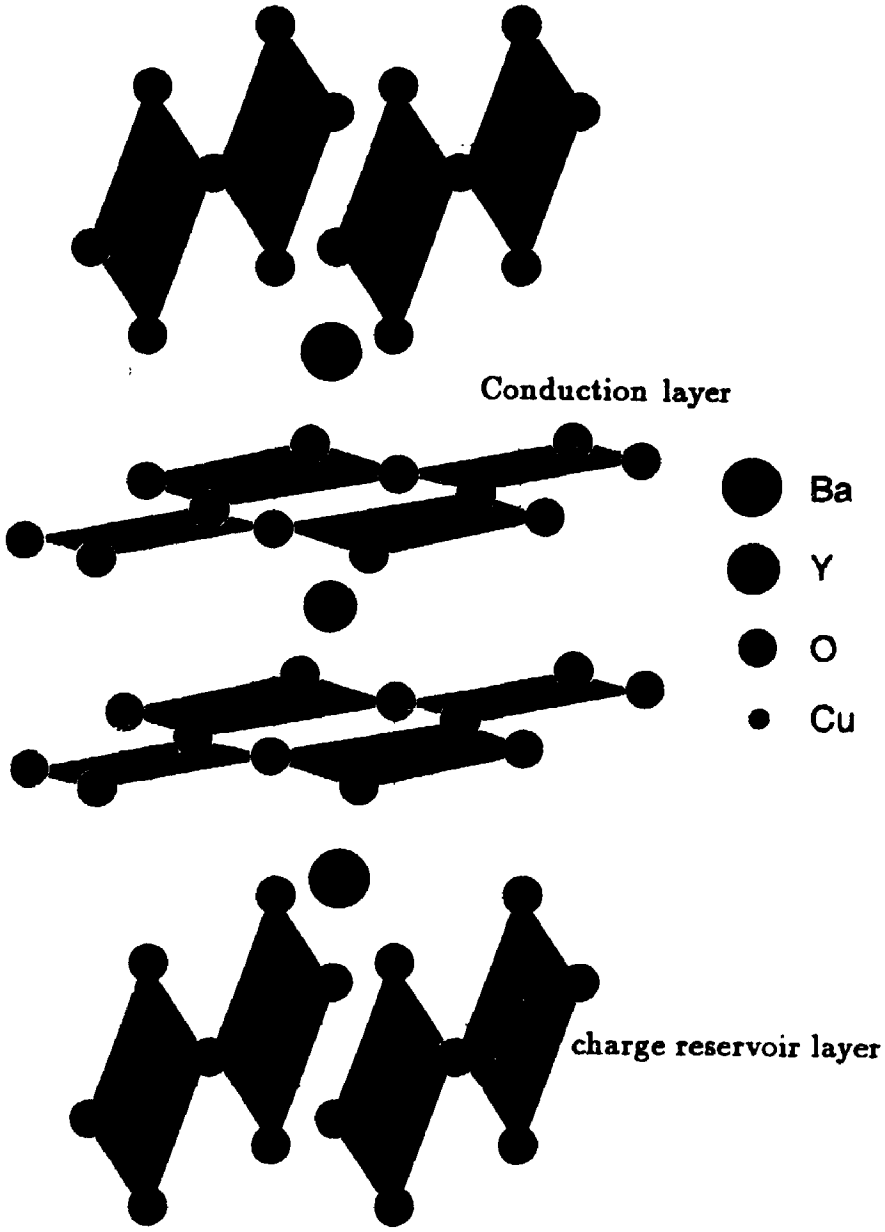

Figure 2.4: High temperature superconductor 1-2-3 showing the alternating layers of conduction and reservoir of charges. Conduction layers comprise of two CuO_2 layers separated by Y atom while the charge reservoir layers consist of CuO_x chains along 'b' with barium and oxygen atoms. The oxygen content near the copper atoms in the chain layer is variable with x ranging from 0 to 1

phase is controlled by the orientational ordering of the chain segments. The antiferromagnetic ordering, however, in the tetragonal phase is dominated by the localized Cu moments in the CuO_2 layers.

2.4 Phase Diagram

Neutron diffraction [35, 52, 16, 53, 17] and muon spin precession experiments [54, 55] have confirmed that the oxygen doping in these materials produces a phase transformation from tetragonal to orthorhombic structure. Fig.(2.5) shows the phase diagram for 1-2-3 compounds. With no oxygen doping the undoped compound is a tetragonal antiferromagnetic insulator with Neel temperature of nearly 500K. As the oxygen concentration changes from x=0 to x=0.4 the Neel temperature decreases and eventually becomes zero. For x$\leq$ 0.4 in $YBa_2Cu_3O_{6+x}$, Cu^{2+} spins are antiferromagnetically aligned on the CuO_2 planes and also along the tetragonal axis. At $x > 0.5$ the compound becomes superconducting and the transition temperature starts increasing. This phase is orthorhombic superconductor with transition temperatures getting to a maximum at x=1.0. The phase diagram also shows that if the temperature is increased at a particular doping concentration of oxygen beyond x=0.5 the orthorhombic superconductor changes to an orthorhombic metal.

The properties of $La_{2-x}Sr_xCuO_{4-y}$ also change drastically with oxygen doping and also with the doping of Sr. With no oxygen doping, y=0, and varying the concentration of Sr, 2-1-4 changes from orthorhombic superconductor to orthorhombic antiferromagnetic insulator. The phase diagram in fig.(2.6) shows the dependence of Sr doping on the Neel temperature. At x=0, with no oxygen doping the parent compound is La_2CuO_4 which is an antiferromagnetic insulator with Neel

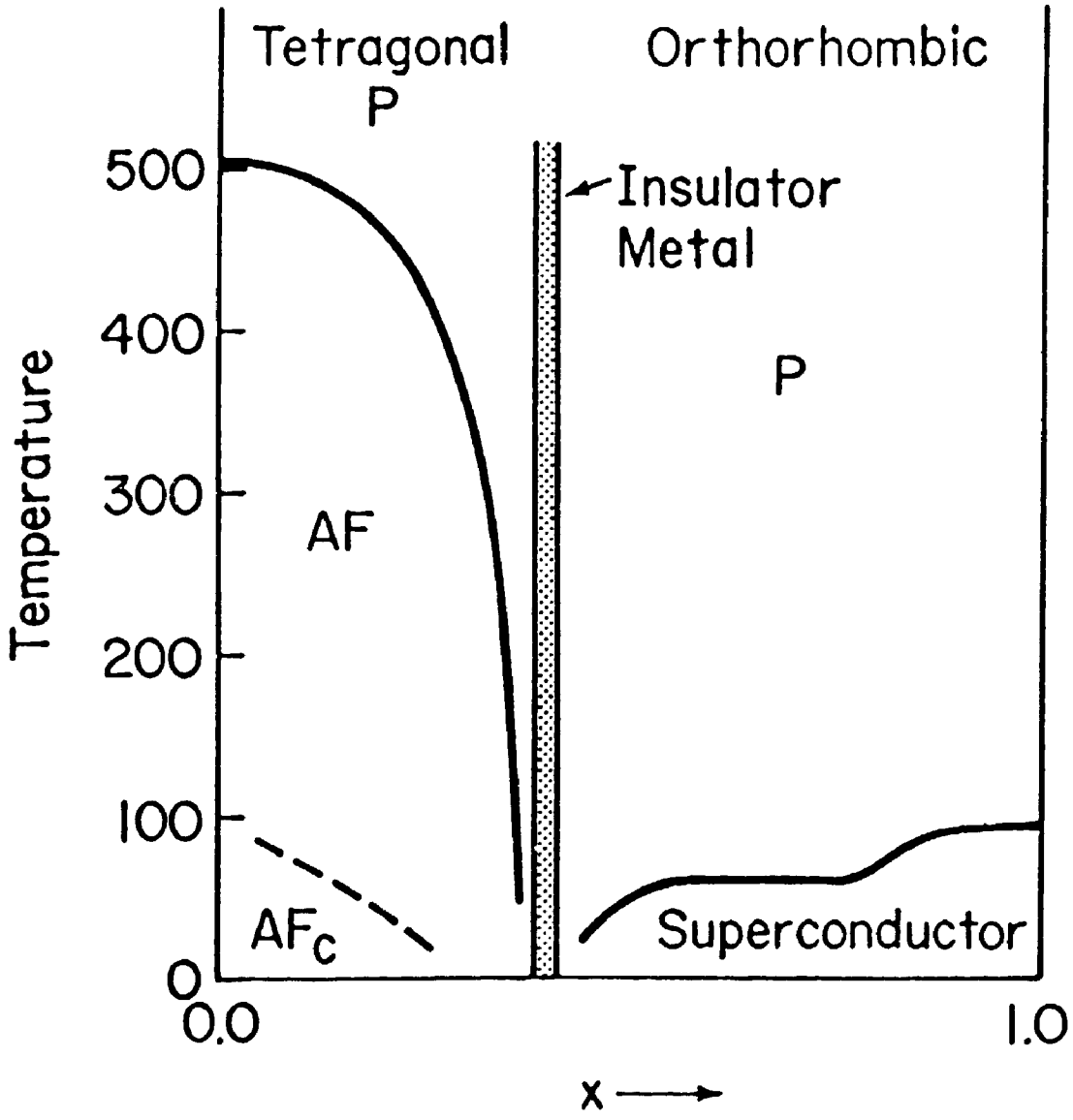

Figure 2.5: Phase diagram of 1-2-3

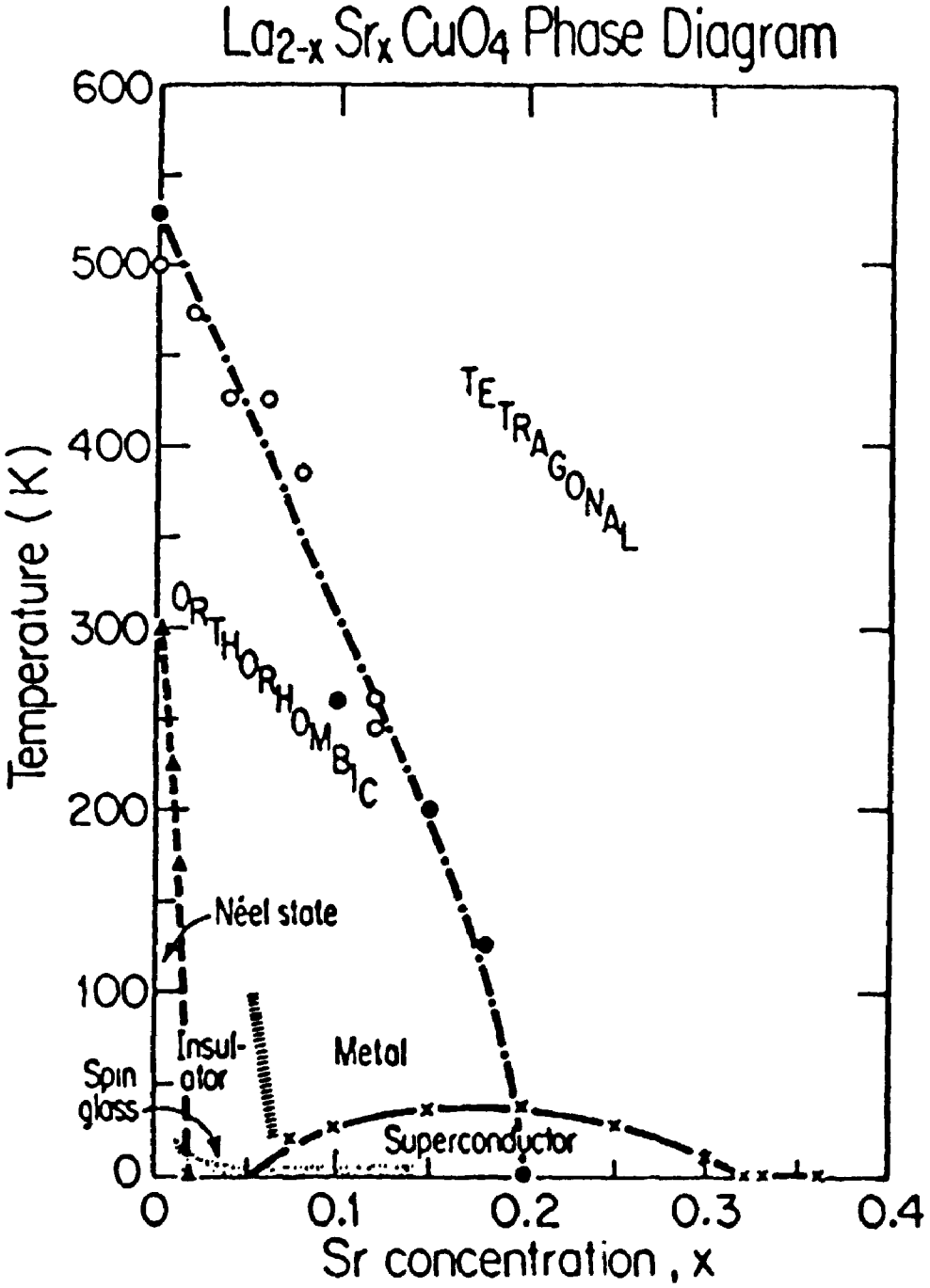

Figure 2.6: Phase diagram of 2-1-4

temperature of 300K. As the concentration of Sr changes from $0 < x < 0.02$ the Neel temperature of La-Sr-Cu-O decreases from 300K and eventually becomes zero. At this Sr concentration further doping makes the system undergo an antiferromagnetic to superconducting transition. Sandwiched between these two states there is a spin-glass state, the properties of which are beyond the scope of this thesis. The material becomes superconducting for $0.05 \leq x \leq 0.35$ with maximum transition temperature of about 35K. The superconductivity is destroyed if the temperature is increased at these concentrations of Sr doping. The subsequent phase is an orthorhombic normal metal. It has also been found that the Neel temperature in 2-1-4 is extremely sensitive to oxygen concentration as well.

2.5 Conclusions

Through this chapter we have established a few facts which would emerge to be of immense help later when we start developing a theory for the magnetic properties. We have established here that

- The properties of conventional and HTS are very different and hence the older models can not be used to explain the properties of HTS.
- These layered copper oxides are antiferromagnets in their normal state and the magnetic nature is due to the Cu spin.
- Strong magnetic correlations exist in the planar CuO_2 layers and a much weaker correlation also exists between these planar layers. These planar layers are identified as playing important role in the magnetic properties of HTS.

- They undergo a phase transformation from Insulator to Superconductor as they are doped.

We have now familiarized ourselves with some of the basic properties of these layered copper oxides. We would now study in detail, the magnetic properties for 1-2-3 and 2-1-4 as obtained from different experimental methods, in the next chapter.

Chapter 3

Magnetic Properties of the Normal state

Now that we have reviewed the crystal structure and the phase diagram of 1-2-3 and 2-1-4 compounds, we are in a better position to understand some of the magnetic properties in the normal state of these layered copper oxides. Most of these properties are a direct consequence of the highly anisotropic crystal structure and a complex yet rich phase diagram which we have already discussed in Chapter II. Here, we are going to review some of the important experimental results on some vital magnetic properties such as the Neel temperature, the sublattice magnetization, susceptibility and magnetic correlation length. In the chapters ahead, we will develop a theory to explain these experimental results.

3.1 Antiferromagnetism

Before we discuss the magnetic properties of these AFM insulators, let's first understand what exactly is an antiferromagnet. It's a material in which the ionic spins are arranged antiparallel to each other. Supposing we have a crystal whose constituent

atoms can be resolved into two sublattices 'A' and 'B' such that the nearest neighbours of the atoms of 'A' are the atoms of 'B' and vice-versa. The cubic and bcc are both of this type with a negative exchange interaction. The exchange energy of two atoms is a minimum if their spins are antiparallel. This type of material is called an Antiferromagnet.

Below a certain temperature the magnetic moment of one sublattice is oriented in one direction. However, as we reach the transition temperature the spins start orienting randomly and consequently the magnetization becomes zero. The temperature at which this happens is called the Neel temperature. Hence, an antiferromagnet can be viewed as two interpenetrating ferromagnetic lattices with the nearest neighbour of any spin lying on a different sublattice. The orientation of spins in a crystal lattice is the effect of a purely quantum phenomenon called *Exchange Interaction.* Fig.(3.1) shows the alignment of spins in a general antiferromagnet. A classical antiferromagnet would have perfect Neel order at zero temperature, but, in a quantum mechanical antiferromagnet, spin waves are present even at T=0, which correspond to the zero point fluctuation of the spins, and hence there is deviation from the perfect order.

Most of our knowledge about the high-temperature superconductors is based on the experimental results that have been achieved over the last six years. Most of the time it has been observed that one single experiment is not conclusive enough and hence a different more sophisticated experiment becomes a necessity. During our discussion we will mention some of these experiments with the understanding that in most cases, although the basic understanding about these magnetic properties may not have changed, some of the numbers are continuously being improved. With this in mind, let's now review some of the magnetic properties of $YBa_2Cu_3O_{6+x}$ and

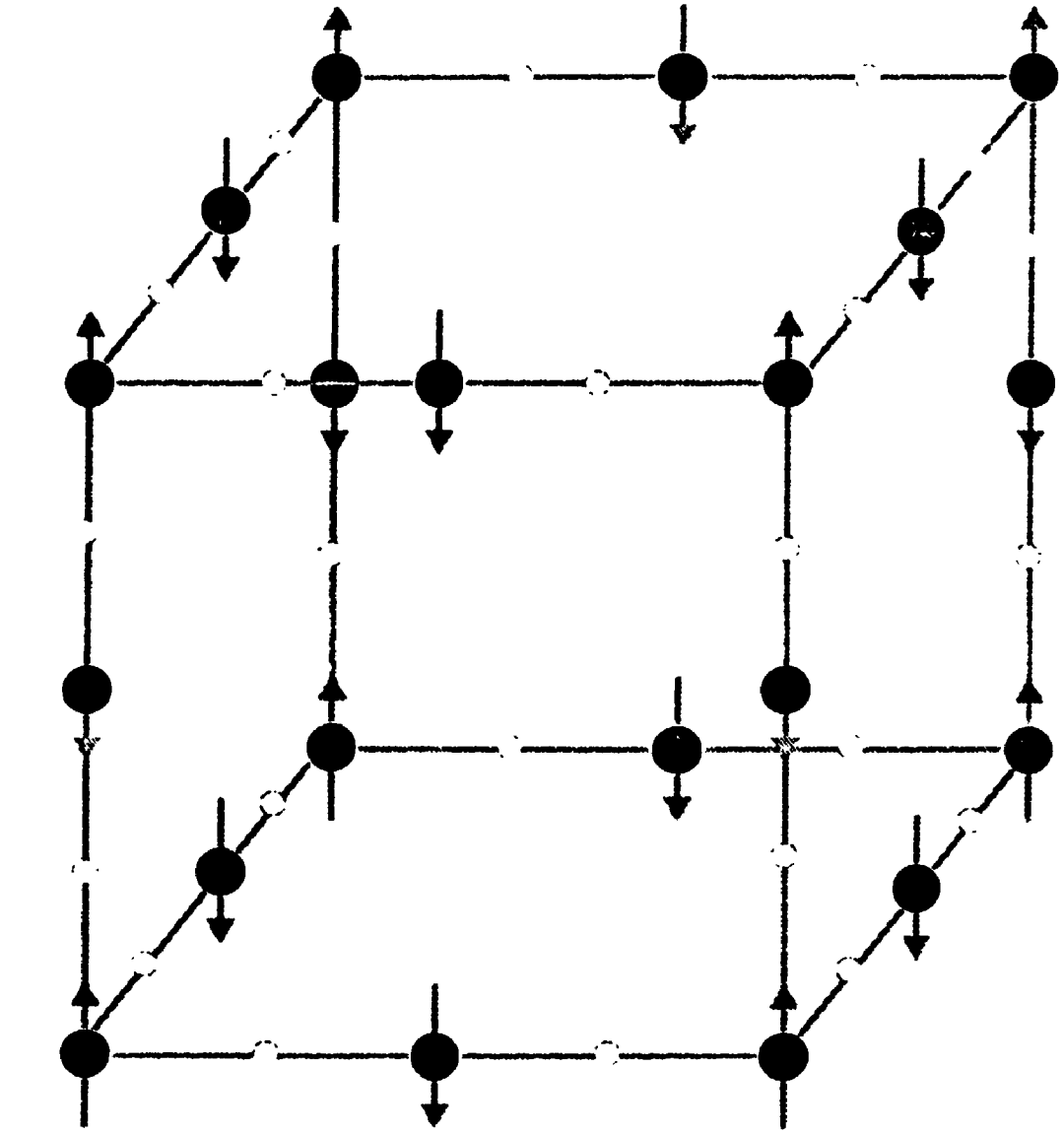

Figure 3.1: Spin alignment in an Antiferromagnet

$La_{2-x}Sr_xCuO_4$ in their normal state.

3.2 Magnetic Moment

In the case of both 2-1-4 and 1-2-3 compounds, antiferromagnetic ordering has been observed by neutron diffraction studies [16, 17, 52]. In both these oxides, there is about $0.5\mu_B$ spins per Cu atom [16, 17]. In the 2-1-4 series, the parent compound is an antiferromagnet with copper spins aligned along the ab-plane and also perpendicular to this plane. Muon spin rotation experiments done on $La_2CuO_{4-\delta}$ found that in the presence of a zero external magnetic field, below the Neel temperature there were clear long lived signals of muon spin precession [54]. The muon precession signal suggested that the ordering of Cu spins occurs with microscopic homogenous spin distribution. It was also interpreted from this experiment that the Cu atoms in 2-1-4 have the same distribution of magnetic moments on all the Cu sites. Some first hand calculations with the assumption that only 50% ordering takes place resulted into an upper limit of $S \leq 0.6\mu_B$ where S is the average ordered moment per copper spin.

Neutron diffraction studies done on the samples of 1-2-3 also show AFM ordering as the oxygen concentration is changed in the samples. A single AFM structure has been observed for 1-2-3 with a maximum Neel temperature of 500K and average ordered moment of $(0.66 \pm 0.07)\mu_B$ per magnetic copper atom at no oxygen doping [37].

It has been interpreted from these experiments that both the HTS, Y-Ba-Cu-O (1-2-3) and La-Sr-Cu-O (2-1-4) are magnetic in nature in their ground state since they contain copper in the $3d^9$ state In the ionized state, there is one unpaired Cu

spin. The alignment of this spin is instrumental in providing the magnetic nature to these materials.

3.3 Doping Effects and the Neel temperature

Positive muon spin rotation and relaxation experiments have revealed local antiferromagnetic order in the defect perovskite $YBa_2Cu_3O_{6+x}$ for the oxygen concentration ranging between 6.0-6.4 [57]. It is found that with increasing concentration of oxygen, the Neel temperature decreases rapidly *. The magnetic ordering in these materials can be found by applying an external magnetic field transverse to the muon polarization direction. If the external magnetic field is less than the local field at the site of the muon, the amplitude of muon precession at external magnetic field frequency contains information about the nonmagnetically ordered spins. Hence the muon precession amplitude gives us the paramagnetic fraction of the spins. For spins that lie in the antiferromagnetic fraction they experience a local field due to the neighbouring spins and for these the external field is only a small perturbation. The results from this experiment have indicated that the mean Neel temperature, at which almost half of the spins are ordered, decreases with the increase in oxygen concentration. The Neel temperature was found to decrease sharply around x=0.25 and after that it is followed by a tail at higher value of 'x' [57].

Neutron Scattering results of Tranquada et al. [36, 37] have reached almost the same conclusions. The results for 1-2-3 indicate that as 'x' increases, the Neel temperature changes slowly until the tetragonal-to-orthorhombic transition is ap-

*These experiments also suggest a possible correlation between Antiferromagnetism and superconductivity. The positive muon is very useful in studies like this since it serves as a probe of the local magnetic environment and it is quite sensitive to and can differentiate between antiferromagnetism and superconductivity.

proached, at which point it quickly falls to zero. With increasing x, oxygen enters the Cu[1] layer and creates some $Cu[1]^{2+}$. This was confirmed by the fact that the Neel temperature remains high over a large range of x. As a result for 1-2-3, the magnetic ordering is not destroyed until the tetragonal-orthorhombic phase boundary is reached, in contrast to $La_{2-x}Sr_xCuO_{4-y}$ in which even a small amount of doping destroys the long range order even before the phase boundary is reached [56]. For 2-1-4, Neel order exists only for $x \leq 0.02$ and within this region the charge carriers are strongly localized, and the electronic conduction is closely similar to that of conventional lightly doped semiconductors [58, 59]. All these results have resulted in a phase diagram of the type shown in fig.(2.5) and fig.(2.6), for 1-2-3 and 2-1-4 respectively.

Neutron scattering experiments on pure and doped samples of 2-1-4 have also established that the pure system is very close to being an ideal realization of the 2D spin-1/2 Heisenberg model [17]. Strong magnetic correlations exist in these pure systems. Within the 2-D layers, the strong antiferromagnetic superexchange provides the relevant antiferromagnetic interaction between the neighbouring Cu sites [56]. But, apart from these strong two-dimensional correlations there is a small but finite interlayer coupling which makes these systems quasi- two dimensional. Elastic neutron scattering studies have now confirmed that the parent compound of 2-1-4 does behave as a quasi-two dimensional quantum Heisenberg antiferromagnet [63].

3.4 Sublattice Magnetization

The staggered magnetization is proportional to the average spin $< S >$ and a value of M= $g\mu_B < S > \sim 0.65\mu_B$ was observed at low temperatures [60]. Assuming a g$\sim$2.2 for spin $\frac{1}{2}$ Cu[2+] ion one gets a value of $< S > \sim 0.3$. After some of these initial reports for magnetization, various experimental techniques have been used to study sublattice magnetization in these layered cuprates. Among them, Mossbauer experiments are one of the most widely used. The principle underlying this method is simple. Earlier studies have suggested that in the layered oxides, doped Fe usually occupies the Cu sites and the Fe spin is coupled antiferromagnetically to the Cu spins [118, 117]. The hyperfine field splits the nuclear ground state and the first excited state of Fe which have spins of $\frac{1}{2}$ and $\frac{3}{2}$ respectively. Below the Neel temperature, transitions between these two states with a dipole selection rule results in a completely split out sextet which can be easily observed by Mossbauer spectra. Through this the magnetic hyperfine field is determined which is proportional to the sublattice magnetization. Low levels of doping ensure that the property of the parent compound is not altered considerably. The temperature dependence of the hyperfine field at the Fe nucleus in the lattice hence gives the temperature dependence of the sublattice magnetization of the antiferromagnetic Cu-spin system.

The temperature variation of sublattice magnetization in La_2CuO_4 from such a technique has revealed that there's a weak dependence which increases to almost a linear fall off as the temperature increases. Mossbauer spectroscopic studies with about half a percent of doped ^{57}Fe on La_2CuO_4 have provided these results[116].

Other experimental techniques have been used to study the phase diagram of La_2CuO_4 including Perturbed $\gamma\gamma$ angular correlation experiments (PAC) using

^{111}In atoms as probes to find out about the mean field exponent for magnetization [140]. Inhomogeneous samples of 2-1-4 were doped with $\leq$ 10 ppm of radioactive ^{111}In on oxygen gas at 1273K and annealed for 3-4 hours in vacuum at 773K. It was found that the In settles at the La site. The Fourier lines of the PAC data were found to split by a weak magnetic field, B_{hf}(T), which were shown to fit to a power law

$$\frac{B_{hf}(T)}{B_{hf}(0)} = D\,(1 - T/T_N)^{\beta} \tag{3.1}$$

where $\beta = 0.50$ and $T_N = 316.7$K. We recall that the hyperfine field is proportional to the sublattice magnetization. This value of $\beta = 0.5$ corresponds to the mean field value thus implying that ordering in 2-1-4 is dominated by long range interactions. However, a different set of PAC experiments have found that the β has a value of 0.27 [123].

The above mentioned mean field nature of the sublattice magnetization assumes a homogenous Neel temperature throughout the sample. In reality however, the Neel temperature in 2-1-4 is inhomogeneous as shown by ^{139} La nuclear quadrupole resonance (NQR) [154] and ^{57} Fe Mossbauer measurements[122]. The effect of inhomogeneity on the value of β has recently been demonstrated by ^{57}Fe Mossbauer experiment of Imbert et al. [122]. It was shown that at each temperature below about 230K all the probes that were doped in the 2-1-4 material experienced the same Hyperfine field. As the temperature was increased above 230K, fractions of the probes crossover into the nonmagnetic state thus giving a clear signature of inhomogeneity in the Neel temperature. This happened due to the fact that with these inhomogeneities some parts of the material reach their Neel temperature at 230K and the probes in this part of the material becomes nonmagnetic while others still occupy a position in parts which reach their Neel temperatures at about 316K.

Typically the highest Neel temperature of these segments where local magnetic order exists is almost 318K. The thermal evolution of the sample average of the hyperfine field obtained by weighting over the magnetic and nonmagnetic fractions was also calculated. It was shown that these averaged data points correspond to those values which would be obtained by experimental procedures, like the one explained above, which are not sensitive to local inhomogeneities. They fit very well with β=0.5. But, in reality, since inhomogeneities are present in the samples, this value is fictitious and much larger than the real local value.

The Neutron scattering experiments of M(T) reveal that 2-1-4 follows a mean-field magnetization curve, unlike the results obtained from hyperfine field $B_{hf}(T)$ from Mossbauer-effect spectroscopy (MES) of dilute ^{57}Fe in these compounds. Fig. (3.2a) and fig.(3.2b) show the temperature dependence of normalized magnetization from different experimental and theoretical predictions. The criticism of these MES [see fig.(3.2b)] data too has been subject of debate for a while now [124]. It seems that the discrepancy observed in the M(T) observed through NS and $^{57}FeB_{hf}(T)$ [see fig.(3.2a)] is due to incorrect explanation of MES data. The hyperfine field of a probe impurity such as ^{57}Fe, which has a local magnetic moment, is not directly proportional to M(T) and hence it's description over entire temperature range below the Neel temperature for 2-1-4 is incorrect [124].

3.5 Susceptibility

The other important magnetic property in 2-1-4 and 1-2-3 compounds is the static susceptibility. Variations in the static susceptibility can be found when the chemical modifications induce the insulator to superconducting transition in these com-

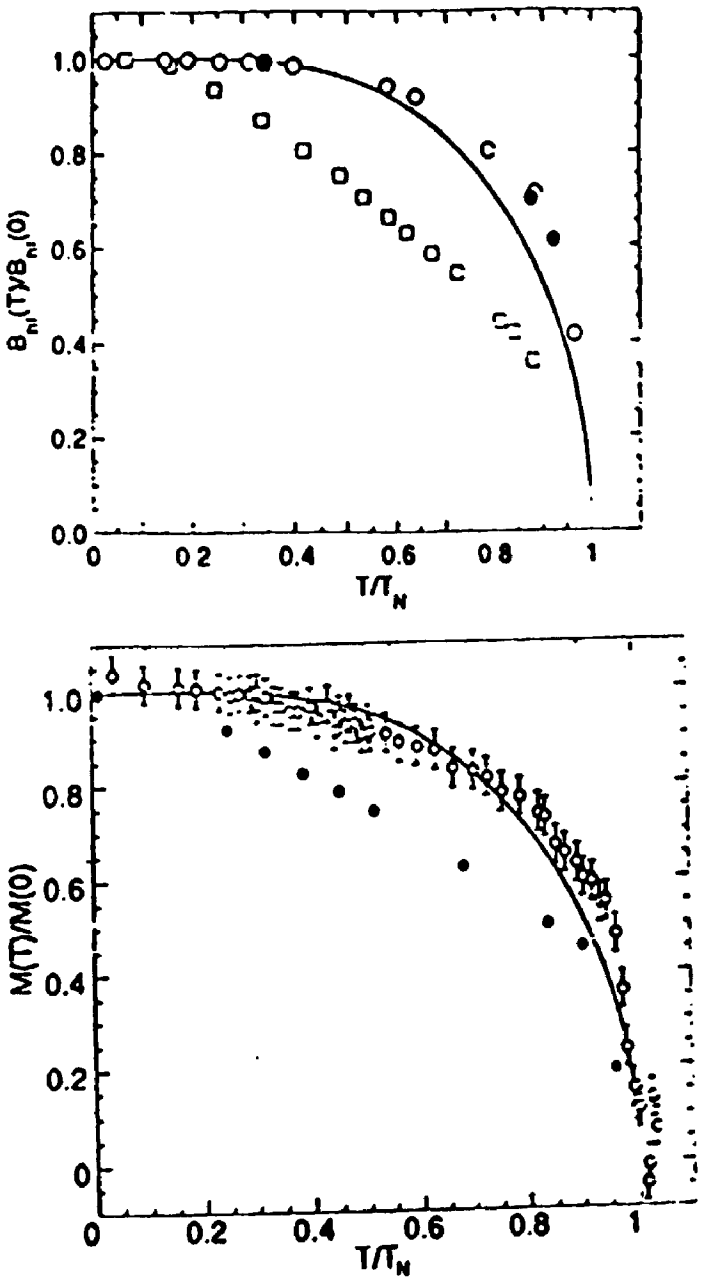

Figure 3.2: (a) Normalized Hyperfine field vs. Temperature of CuO from μSR (o), ^{100}Rh PAC (•) and ^{57}Fe MES (□); (b) Temperature dependence of normalized magnetization (o) and ^{57}Fe hyperfine field (•) for 2-1-4 via NS and MES respectively.

pounds. In 1-2-3 the variation of susceptibility with temperature depends crucially on the method of preparation of oxygen deficient samples. One of the common problems with the calculation of susceptibility from experiments is the presence of paramagnetic contributions from intrinsic impurities. Johnston et al. [125] have shown that these paramagnetic impurities tend to dominate at low enough temperatures. After separating the contributions from impurities they found that the magnetic susceptibility scales universally with temperature normalized to the temperature at which susceptibility has a maximum.

Tranquada et al.[37] have shown that the intrinsic signal for magnetic susceptibility can be obtained by subtracting a Curie-like contribution (C_g/T). When they fitted a term like C_g/T to the susceptibility data they found that the shapes of the residual curves were not sensitive to the precise value of C_g or to the replacement of the Curie term by a Curie-Weiss form $C_g/(T-\theta)$. They hence wrote the corrected term as $\chi^{corr} = \chi_g - (C_g/T)$. We show the corrected susceptibility data for both 1-2-3 and 2-1-4 compounds in fig. (3.3a and 3.3b). Each curve is dominated by a broad maximum at temperature $\geq$ 800K and the susceptibility is found to decrease with decreasing temperature [130].

Interestingly, the spin susceptibility for the 90K superconductor is 3 to 4 times larger than the insulating antiferromagnet below the Neel temperature. The same tendency is also observed in $La_{2-x}Sr_xCuO_4$, but the quantitative analysis is not quite straight. However, a best estimate gives a ratio of $\sim$ 1.5 - 1.9 for the low temperature spin susceptibilities of x=0.15 and x=0. This ratio incidentally is only half of that in 1-2-3 [62]. Discounting the contributions due to long range order, there is a peculiarity in the low temperature spin susceptibility of 2-1-4 and 1-2-3. For both these compounds, spin susceptibility is close to 1 x 10^{-5} emu per one mole

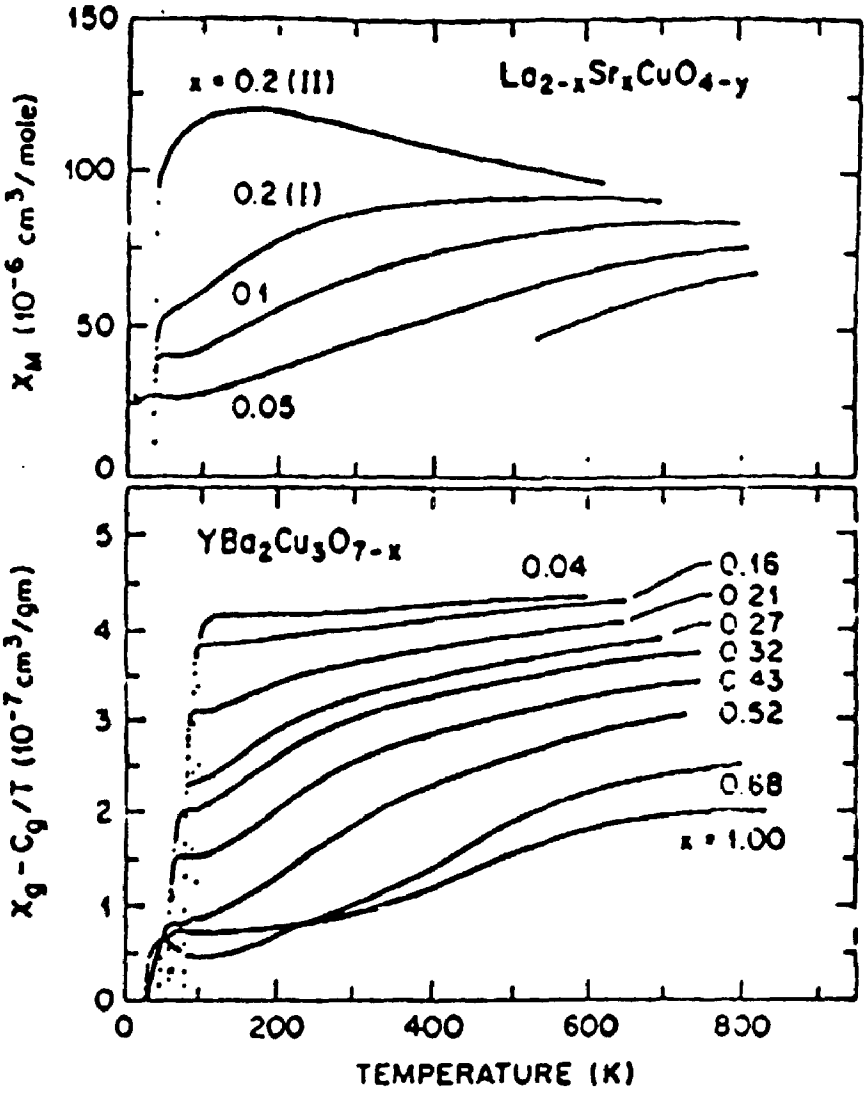

Figure 3.3: (a) Magnetic susceptibility χ vs. temperature for 2-1-4. (b) Corrected magnetic susceptibility χ_g - C/T vs. temperature for 1-2-3 compound.

formula unit. Now, since the chain sites have no magnetic moment in undoped compound, this suggests that 1-2-3 double layer has the same susceptibility as the single layer 2-1-4.

Lines [131] has also studied the susceptibility for K_2NiF_4 and has shown that the position of χ_{max} should occur at a temperature comparable to the intraplanar exchange parameter $J_{||}$. These results are also true for the layered copper oxides since the structure of undoped 2-1-4 is similar to the K_2NiF_4 system. We would discuss more about these susceptibility measurements and would compare some of these results when we calculate the magnetic susceptibility from the self-consistent theory in Chapter VI.

3.6 Magnetic Correlation Length

The two dimensional spin-correlations in 2-1-4 have been studied in some detail in a series of Neutron Scattering experiments [16, 15, 17]. In these experiments one integrates over the energy without changing the intraplanar momentum transfer by collecting all the outgoing neutrons in a direction parallel to the 2D plane. If the magnetic correlations are two dimensional in character, they shouldn't be affected by the momentum transfer perpendicular to the CuO_2 plane. The correlation length is then extracted from the static structure factor S(q) which has been approximated to have the form $S(q) \sim 1/q^2 + [1/\xi(T)]^2$ by Endoh et al. [17]. It is important to realize that experimentally this energy integration is carried out between -T and the incident neutron energy. The idea behind it is that a neutron can not, ofcourse, lose energy greater than it's incident energy. However, it can gain any amount of energy from the available excitations but the integration would be effectively cutoff

by the thermal occupation factor. Extraction of the correlation length from the structure factor like this has yielded a decreasing variation of correlation length with temperature. This was done for undoped samples of 2-1-4 compounds.

Recent experimental results of Keimer et al. on the magnetic correlation length show that it is greatly suppressed as a function of x. These experimental results have reached to the conclusion that the magnetic correlation length decreases as the doping of Strontium is increased in 2-1-4 compounds. We will discuss more about the magnetic correlation length when we calculate it by our self-consistent theory in Chapter VIII.

3.7 Conclusions

In conclusion, in this chapter we have reviewed some of the experiments which have given us an insight into the magnetic nature of these High-temperature superconductors, in their normal state. The results presented in this chapter will be explained on the basis of our theory that we will start building from the next chapter onwards.

Chapter 4

Self-Consistent calculation of the Neel Temperature *

In the last chapter, we surveyed the magnetic properties of 1-2-3 and 2-1-4 compounds in the normal state. The anomalous magnetic properties of these compounds can not be explained by the old theories and it has become essential to formulate a theory that could explain all the experimental results that we have presented in Chapter III. From this chapter onwards, we will develop a theory tailored especially to meet the requirements of these compounds. So far, there hasn't been any theoretical model for HTS that explains all the experimental results. Although, over the last couple of years, there have been a few attempts to explain some of the magnetic properties in the normal state. We will discuss these theoretical attempts and sometimes compare our theory with those that already exist.

*Results in this chapter are published in Physica Status Solidi (b), 169, 571, 1992 and in Physical Review, B46, 12277, 1992

4.1 Introduction

Various experimental techniques have been used to study the phase diagram and the variation of Neel temperature with the oxygen concentration in layered copper oxides such as 2-1-4 and 1-2-3 [36, 37, 54, 57, 35]. In Sec. 2.3 - 2.4 we have seen that these compounds have a highly anisotropic crystal structure and they undergo a phase transformation from Antiferromagnetic (AFM) insulator to orthorhombic superconductor [61, 48]. The copper spins are aligned antiferromagnetically in the planar CuO_2 plane at no doping but, as the oxygen concentration increases, they get aligned along the tetragonal axis also [36]. However, with increasing concentration of oxygen in 1-2-3 the Neel temperature falls rapidly and at x$\sim$0.4 the Neel temperature drops to zero. Different experimental techniques give very similar T_N vs. x results and give the maximum Neel temperature in 2-1-4 and 1-2-3 in the vicinity of 300K and 400K respectively [36, 37, 57, 35, 17]. In case of 2-1-4 compounds, the Neel temperature decreases tremendously as the Sr concentration increases from 0 to 0.02 [106, 35, 52, 107]. Undoped compound of ?-1-4 is an Antiferromagnetic insulator and it is orthorhombic. As x changes from 0.05 to 0.35 it undergoes an insulator to superconducting transition. Above 0.35 it undergoes a structural transformation from orthorhombic to tetragonal phase [see fig. (2.6)].

We have already seen in Chapter II that these oxide superconductors have a very strong antiferromagnetic correlation in the planar CuO_2 planes. The discovery of this strong antiferromagnetic correlation in these quasi-two dimensional magnetic systems has driven theorists for an extensive theoretical study on the two-dimensional quantum Heisenberg model. Among the approaches used to study such a model are the renormalization group treatment of the nonlinear σ model[67],

1/N expansion in the Schwinger-boson representation [68], modified spin-wave treatments [69, 70] etc. Linear spin-wave theory has been widely pursued to study the magnetic properties of anisotropic Heisenberg antiferromagnets [71, 72]. Most of the theories that have ventured to explain the magnetic properties are not able to explain all the experimental results of doping dependent Neel temperature.

In this chapter, we have developed a theory based on the quasi-2D Heisenberg model and Green's function method to explain the magnetic properties of 1-2-3 and 2-1-4 compounds. We have used the Equation of motion method for the Green's function. The chain of equations in the Green's function approach is decoupled by using the Random phase approximation. This theory is shown to give a self-consistent expression which is evaluated to explain the Neel temperature in layered cuprates. For this reason we call it the *Self-consistent theory.* We have for the first time, introduced a novel parameter which is dependent only on the ratios of inter to intraplanar couplings and provides us crucial information about the Neel temperature and it's dependence on doping. Before we started this study, there were limited reports about the use of Green's function approach to study these systems in the normal state [71]. However, recently, quite a few groups all over [73, 74, 75] have taken interest in such a study and as a result the Green's function approach for an antiferromagnet has developed into one of the forerunners in explaining the vast amount of experimental results.

4.1.1 Quasi - two dimensional Heisenberg Hamiltonian

Magnetism is a purely quantum mechanical phenomenon without any classical analog. It arises due to exchange interaction between spins which can be ordered either ferromagnetically, antiferromagnetically or in any of the different kinds of ordering

possible depending upon the electronic structure of the material and the nature and strength of the interaction between spins. To study a behaviour of this kind it almost becomes imperative to use a method which may explain such quantum phenomenon. In quantum field theory the Green's functions describe the propagation of particles and it seems appropriate to use them in a theory which could describe some normal state properties of HTS since they too are known to be insulators in normal state. In the 60-70s, a very popular theoretical approach to study three dimensional magnetic systems was based on these Green's functions which were introduced by Bogoliubov and Tyablikov. A direct evaluation of these Green's functions by diagrammatic techniques is not available, but, considerable progress has been made in decoupling the chain of equations of motion for the Green's function.

A simple valence counting leads us to the fact that in HTS like 1-2-3 and 2-1-4 Cu is present in the 2+ state. Accordingly, Cu[2+] ion should have a 3d hole. In the presence of a crystal field inside the material the five-fold degeneracy of the 3d orbital is lifted and the only remaining orbital of interest to us is the $3d_{x^2-y^2}$ orbital. We can imagine that the intervening oxygen atoms in the plane could mediate an antiferromagnetic coupling via the superexchange mechanism leading to a $S=\frac{1}{2}$ Heisenberg Model. We have here a lattice which has all the nearest neighbours of a site on sublattice 'f' present on a different sublattice 'g' which has opposite orientation of spins on it. This is called a two-sublattice picture for an Antiferromagnet. The crystal structure of these two antiferromagnets suggest to us that the copper spins are aligned antiferromagnetically within the planar CuO_2 layer and also in the c-direction within two such planes. The correlations within the planar layers are result of the exchange interaction between two copper spins and a coupling of this kind is called as the 'Intralayer Coupling'. The coupling

between two spins in the c-direction, as we have discussed before, is much weaker but is crucial for the long range antiferromagnetic order. This coupling is called the 'Interlayer Coupling'. Here, before going any further, we will discuss the origin of this interlayer coupling in case of 2-1-4 compounds.

In their ground state these high temperature superconductors such as 1-2-3 and 2-1-4 are quantum antiferromagnetic insulators for $x \leq 0.4$ and $x \leq 0.02$ respectively [56]. The parent compound of the La-Sr-Cu-O system is $La_2CuO_{4-\delta}$. The origin of the interlayer coupling can be understood by observing the spin structure of this parent compound. Fig.(4.1) shows the alignment of Cu spins in this compound since the magnetic moments are known to reside on the Cu spins [52]. The exchange interaction between the copper spins on the planar layer is mediated through the presence of oxygen atoms in between. Also, the bonding between the Cu-O atoms within the plane gives rise to an interaction which is much larger than the interaction between two such planar layers. Due to the presence of a highly anisotropic structure with 'c' substantially larger than either of 'a' and 'b' axes, this difference in the exchange interaction is highly amplified. Hence, the intralayer exchange coupling is much larger than the interlayer couplings. Also, it should be noted that each copper spin on the planar layer has four spins above and four spins below it at almost equal distance from each of these spins due to the fact that 'a' $\cong$ 'b'. The interactions between layers should cancel out and they in fact do for a system which is isotropic, for eg. K_2NiF_4. However, due to the orthorhombic distortion present in the 2-1-4 compounds this cancellation is incomplete and as a result the interlayer coupling is much less than the intralayer coupling. This anisotropy in the exchange coupling constant leads to strong correlations within the planar CuO_2 layers and

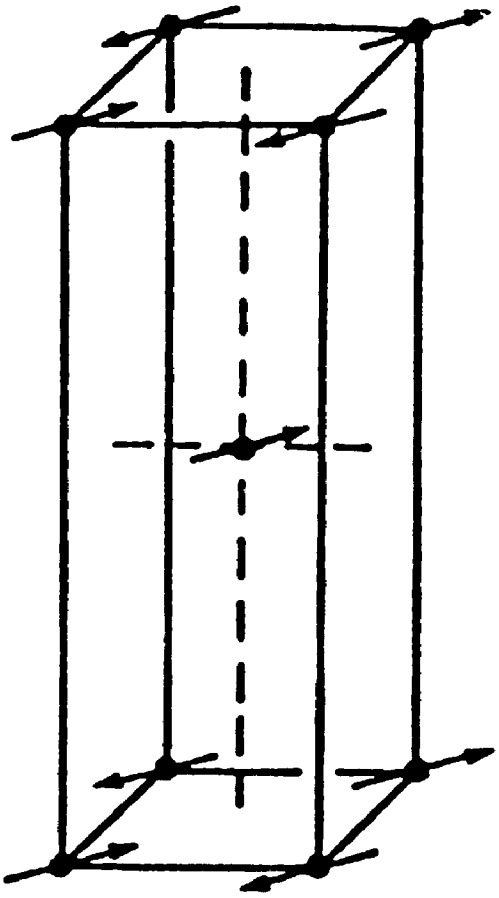

Figure 4.1: Antiferromagnetic alignment of spins in La_2CuO_{4-x}. The spins within the bc-plane are ferromagnetically aligned but they are antiferromagnetically aligned with adjacent planes

that's the reason why these compounds have strong 2-dimensional behaviour [16]. The three dimensional interlayer coupling is less than the intralayer coupling by a factor of $10^{-3} - 10^{-5}$ in both these oxides [15, 62, 36]. The interlayer coupling for 1-2-3 is even stronger than in 2-1-4 [16, 64, 36, 66]. So, theoretically these compounds can be described as spin - $\frac{1}{2}$ quasi-two dimensional quantum Heisenberg antiferromagnets [63]. Any theoretical model, which attempts to describe the magnetic properties of these compounds should hence take this interlayer coupling into account.

With these requirements in mind, we will hence consider a quasi - two dimensional Heisenberg Hamiltonian which is a true depiction of the system at hand. So, we will start with a Hamiltonian of the type

$$H = \sum_{ab} 2J_{||}\, \mathbf{S_i}\cdot\mathbf{S_j} + \sum_{c} 2J_{\perp}\, \mathbf{S_i}\cdot\mathbf{S_j} \tag{4.1}$$

where $J_{||}$ and $J_{\perp}$ are the AFM coupling constants in *ab*-plane and *c*-direction respectively. Similar situation arises in high temperature superconductors. For example, in 1-2-3 and 2-1-4 compounds $J_{||}$ will be the coupling constant between spins within the copper-oxygen planes and $J_{\perp}$ will be between the copper-oxygen planes. The sums are taken between nearest neighbours within the *ab*-plane and between planes in the c -direction. We will now make use of the thermodynamical Green's function method [See Appendix I] to investigate the Hamiltonian given in eqn.(4.1).

4.2 Self-consistent Green's function Method

We divide the simple cubic lattice into two sublattices denoted by 'f' and 'g' where the nearest neighbour of 'f' is on 'g' sublattice and vice-versa. We develop now the equation of motion for the Green's function given by $\ll S_f^+(t), S_g^-(t') \gg$ where $S^{\pm} = S^x \pm iS^y$ are the spin raising and lowering operators respectively. We have

used the expressions obtained in Appendix I. The corresponding equation of motion at $t = t'$ is written as:

$$E \ll S_f^+, S_g^- \gg = \frac{< [S_f^+, S_g^-] >}{2\pi} + \ll [S_f^+, H], S_g^- \gg \tag{4.2}$$

Rewriting the Hamiltonian given in eqn.(4.1) for the spin operators defined above we get

$$H = 2(\sum_{ab} J_{\|} + \sum_{c} J_{\perp})(\frac{1}{2} S_i^+ S_j^- + \frac{1}{2} S_i^- S_j^+ + S_i^z S_j^z) \tag{4.3}$$

Using the commutation relations for the components of spin operators and fixing i=j, we sum over all nearest neighbour sites, ie. over j and obtain,

$$[S_f^+, H] = 2(\sum_{ab} J_{\|} + \sum_{c} J_{\perp})(S_f^z S_j^+ - S_j^z S_f^+) \tag{4.4}$$

Using the results in eqn.(4.4) and putting them in eqn.(4.2), the equation of motion can be written as

$$E << S_f^+; S_g^- >> = \frac{2 < S_j^z >}{2\pi} \delta_{fg} + 2(\sum_{ab} J_{\|} + \sum_{c} J_{\perp}) << (S_f^z S_j^+ - S_f^+ S_j^z); S_g^- >> \tag{4.5}$$

where the first term is a consequence of the commutation relation between the components of the spin operator, viz. $< [S_f^+; S_g^-] >= 2 < S_j^z > \delta_{fg}$. We see that the Green's function appearing in the above equation on the right hand side of the equation is of an higher order than the original Green's function. We can now write the equation of motion for this new Green's function and we will then land up with an even more complicated Green's function of yet higher order. To go around the problem of evaluating this never ending chain of equations we will decouple using some approximation. The most obvious choice of approximation that has been successfully used in the past is **Random Phase Approximation** (RPA). In the RPA we write the Green's function approximately as

$$\ll S_f^z S_j^+, S_g^- \gg \approx < S_f^z > \ll S_j^+, S_g^- \gg$$

$$\ll S_f^+ S_j^z, S_g^- \gg \approx < S_j^z > \ll S_f^+, S_g^- \gg$$

The whole idea of making an approximation like this is to ignore the fluctuations in S_f^z and S_j^z and replace them by their average values. Incorporating these approximations and substituting for the higher order Green's function we obtain

$$E << S_f^+; S_g^- >> = \frac{2 < S_j^z >}{2\pi}\delta_{fg} + 2(\sum_{ab} J_{\parallel} + \sum_{c} J_{\perp})[< S_f^z ><< S_j^+; S_g^- >> - < S_j^z ><< S_f^+; S_g^- >>] \quad (4.6)$$

Now since we have a two sublattice model for an Antiferromagnet we have one sublattice with all spins 'up' and the average spin $\bar{S} =< S_f^z >$ while the other sublattice has all its spin oriented in the 'down' direction with an average spin of $-\bar{S}$. We now define the Green's function for these two sublattices as G_{1k} and G_{2k}.

- For both sites 'f' and 'g' on the same sublattice, we have

$$<< S_f^+; S_g^- >>= \frac{2}{N}\sum_k G_{1k}\, e^{ik\cdot(f-g)} \quad (4.7)$$

$$G_{1k} = \sum_{f-g} << S_f^+; S_g^- >> e^{-ik\cdot(f-g)} \quad (4.8)$$

- For both sites 'f' and 'g' on different sublattices, we have

$$<< S_f^+; S_g^- >>= \frac{2}{N}\sum_k G_{2k}\, e^{ik\cdot(f-g)} \quad (4.9)$$

$$G_{2k} = \sum_{f-g} << S_f^+; S_g^- >> e^{-ik\cdot(f-g)} \quad (4.10)$$

Here, N is the total no. of spins in the lattice and k is the reciprocal lattice vector which runs over the magnetic Brillouin zone, which incidentally is half of the crystallographic one. We consider an Antiferromagnet as a system with two atoms in the unit cell and hence the 'k' summation will run over N/2 values rather than N values in the first Brillouin zone. The kronecker delta can be written as

$$\delta_{fg} = \frac{2}{N} \sum_{k} e^{ik\cdot(f-g)} \tag{4.11}$$

Putting these expressions together we can obtain an expression such as

$$\begin{aligned} E\,G_{1k} &= \frac{< S_f^z >}{\pi} + 2 \sum_{ab} J_{||} \left\{ \bar{S} \sum_{k} G_{2k} e^{ik\cdot(j-f)} + \bar{S} G_{1k} \right\} \\ &\quad + 2 \sum_{c} J_{\perp} \left\{ \bar{S} \sum_{k} G_{2k} e^{ik\cdot(j-f)} + \bar{S} G_{1k} \right\} \end{aligned} \tag{4.12}$$

The above equation in a simpler form can be written as

$$EG_{1k} = \frac{< S_f^z >}{\pi} + < S_f^z > \; (\xi G_{2k} + \eta G_{1k}) \tag{4.13}$$

In the above equation, ξ and η are defined as

$$\xi = 2J_{||} \sum_{ab}^{j} e^{ik\cdot(j-f)} + 2J_{\perp} \sum_{c}^{j} e^{ik\cdot(j-f)}$$

and

$$\eta = 8J_{||} + 4J_{\perp}$$

The relation between the two Green's functions turns out to be

$$(E - \eta\bar{S})\, G_{1k} = \frac{< S_f^z >}{\pi} + \xi \bar{S} G_{2k} \tag{4.14}$$

when the sites 'f' and 'g' are on same sublattice. But, when they are on different sublattice a similar approach will yield

$$(E - \eta\bar{S})\, G_{2k} = -\xi \bar{S} G_{1k} \tag{4.15}$$

Finally, G_{1k} has the following form:

$$G_{1k} = \frac{(1-P) < S_f^z >}{2\pi(E+E_1)} + \frac{(1+P) < S_f^z >}{2\pi(E-E_1)} \tag{4.16}$$

where

$$P = \eta/\sqrt{(\eta^2 - \xi^2)}$$

and

$$E_1 = < S_f^z > \sqrt{(\eta^2 - \xi^2)}$$

The correlation functions are related to the Green's function by the following equation

$$< B(t')A(t) > = \lim_{n \to +0} i \int_{-\infty}^{+\infty} \frac{\ll A(t), B(t') \gg_{E=\omega+i\epsilon} - \ll A(t), B(t') \gg_{E=\omega-i\epsilon}}{e^{\omega/k_BT} - 1} \cdot e^{-i\omega(t-t')} d\omega \tag{4.17}$$

Using this equation with the fact that [see Appendix I, eqn.(I.23)]

$$\lim_{\epsilon \to +0} \left[\frac{1}{\omega + i\epsilon - E_k} - \frac{1}{\omega - i\epsilon - E_k} \right] = -2\pi i \delta(\omega - E_k) \tag{4.18}$$

we have for 'f' and 'g' on the same sublattice, at t=t'

$$< S_g^- S_f^+ > = \frac{2}{N} \lim_{\epsilon \to +0} \sum_k i \int_{-\infty}^{\infty} \frac{G_{(1k)_{(E=\omega+i\epsilon)}} - G_{(1k)_{(E=\omega-i\epsilon)}}}{e^{\omega/k_BT} - 1} e^{ik\cdot(f-g)} d\omega \tag{4.19}$$

Substituting expressions for G_{1k} into the above equation, we obtain

$$< S_g^- S_f^+ > = \frac{2}{N} < S_f^z > \sum_k \int_{-\infty}^{\infty} e^{ik\cdot(f-g)} d\omega \left[\frac{(1-P)\delta(\omega+E_1)}{e^{\omega/k_BT} - 1} + \frac{(1+P)\delta(\omega-E_1)}{e^{\omega/k_BT} - 1} \right] \tag{4.20}$$

Solving the integration we obtain for the correlation function,

$$< S_g^- S_f^+ > = \frac{2 < S_f^z >}{N} \sum_k \left[P \coth\left(\frac{E_1}{2k_BT} \right) - 1 \right] \tag{4.21}$$

4.2.1 Neel Temperature for quasi - 2d systems

To calculate the average value of spin in one of the sublattices in c-direction we use the following equation for spin $\frac{1}{2}$:

$$< S_l^z > \equiv \frac{1}{2} - < S_l^- S_l^+ > \tag{4.22}$$

where at $t = t'$, $< S_l^-, S_l^+ >$ is equal to $< S_l^-(t) S_l^+(t') >$. Putting the value of $< S_g^- S_f^+ >$ from eqn.(4.21) in the above equation we get:

$$\frac{1}{\bar{S}} = \frac{4}{N} \sum_k \left[P \coth \left(\frac{E_1}{2 k_B T} \right) - 1 \right] + 2 \tag{4.23}$$

Substituting the values of 'P' and 'E_1' from the values obtained previously we can get

$$1 = \frac{4}{N} \sum_k \left[\frac{\bar{S}\eta}{\sqrt{\eta^2 - \xi^2}} \coth \left[\frac{\bar{S}\sqrt{\eta^2 - \xi^2}}{2 k_B T} \right] - \bar{S} \right] + 2\bar{S} \tag{4.24}$$

Here we have represented $< S_l^z >$ by $\bar{S}$. The above equation will give us the variation of sublattice magnetization with temperature. It can however be reduced to give an explicit expression for the Neel temperature. We know that as $T \rightarrow T_N, \bar{S} \rightarrow 0$ and in the above expression we will have:

$$\coth \left[\frac{\bar{S}\sqrt{\eta^2 - \xi^2}}{2 k_B T} \right] \rightarrow \frac{2 k_B T_N}{\bar{S}\sqrt{\eta^2 - \xi^2}} \tag{4.25}$$

This expression gives us a compact form for the Neel temperature in Artiferromagnets as

$$T_N = \frac{1}{8 k_B} \left[\frac{1}{N} \sum_k \frac{\eta}{\eta^2 - \xi^2} \right]^{-1} \tag{4.26}$$

To calculate the Neel temperature explicitly, we need to put in the values for all the variables mentioned in the above equation to get an expression of the form

$$T_N = \frac{1}{8 k_B} \left[\frac{1}{N} \sum_k \frac{2J_{\parallel} + J_{\perp}}{4(2J_{\parallel} + J_{\perp})^2 - \left(J_{\parallel} \sum_{ab}^{j} e^{ik \cdot (j-f)} + J_{\perp} \sum_{c}^{j} e^{ik \cdot (j-f)} \right)^2} \right]^{-1} \tag{4.27}$$

A precise numerical estimate of Neel temperature can be obtained by integrating this expression. This is a general expression and it can be used to give us the variation of Neel temperature with the intralayer and more importantly the interlayer coupling in case of High Temperature Superconductors.

4.2.2 Neel temperature for undoped 1-2-3 and 2-1-4

We have calculated the Neel temperature of both 1-2-3 and 2-1-4 compounds by choosing the proper values of $J_{||}$ and $J_{\perp}$. Fig.(4.2) shows the results obtained for the Magnetization as a function of temperature for the undoped samples of 2-1-4 and 1-2-3. The evaluation of the Neel temperature is done by the self-consistent expression derived earlier ie. eqn.(4.24). By choosing a value of the intralayer exchange coupling $J_{||} = 98.0meV$ and the ratio of interlayer to intralayer exchange coupling strengths 'r'$(= J_{\perp}/J_{||})$ as $6x10^{-3}$ for 1-2-3 we obtained a Neel temperature of 420K. For $J_{||} = 120.0meV$ and $r=3.0x10^{-5}$ gives a Neel temperature of 320K for 2-1-4. These results for the undoped compounds are in excellent agreement with the results experimentally obtained [36, 37, 106, 35, 52, 107].

The parameters that we have used in the calculation above agree very well with their estimated values from various experiments. For the intraplanar coupling, Neutron scattering experiments have estimated a value of 0.138eV [66], 0.14eV

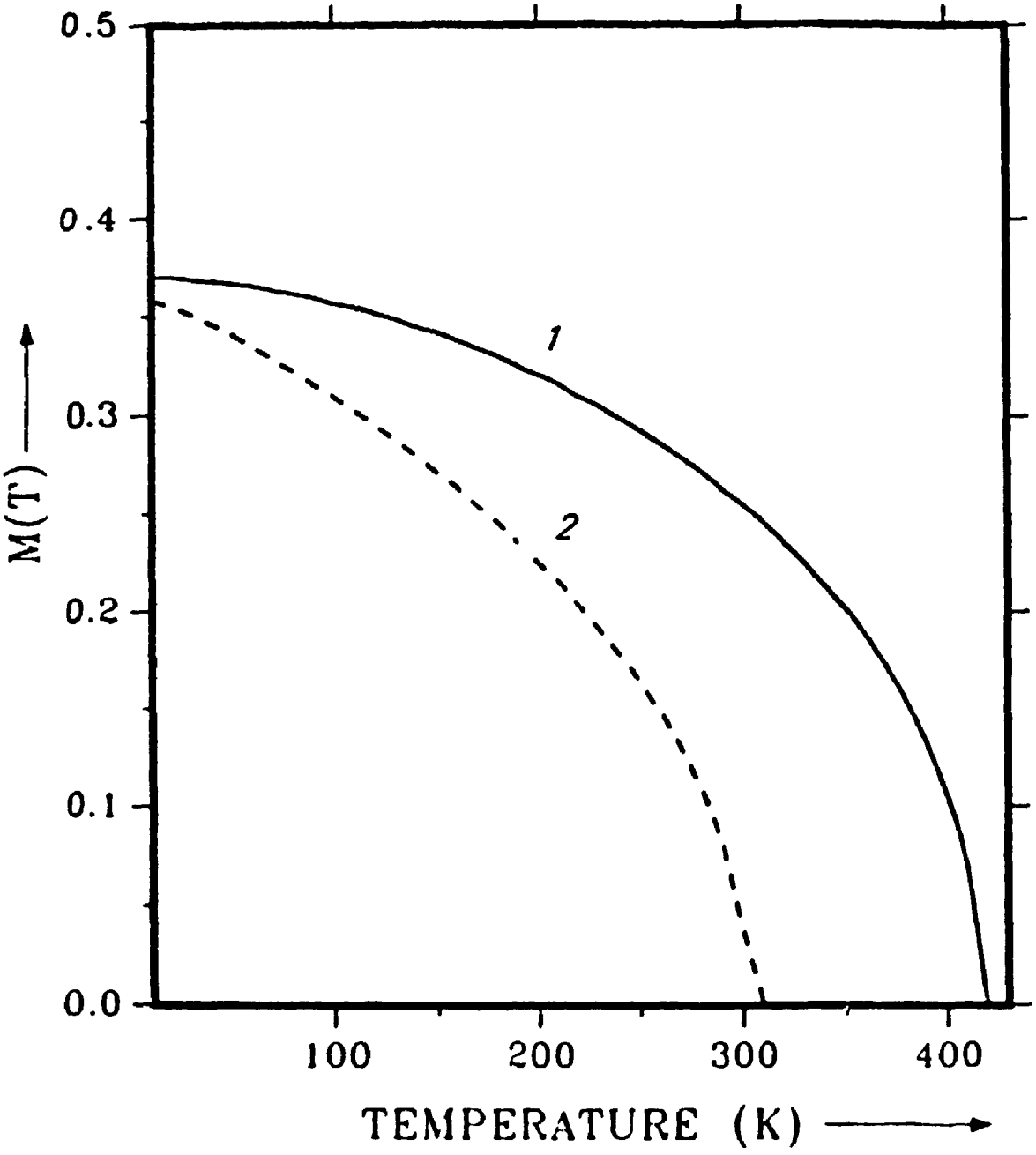

Figure 4.2: Neel temperature for 1-2-3 and 2-1-4

by Raman Scattering [64], 0.13eV by fitting the spin-correlation length within the nonlinear sigma model [67] and 1500K was obtained from optical studies on 2-1-4 compounds[79]. Inelastic light scattering measurements were done recently on various cuprates and the intralayer exchange was found to be 0.128eV for 2-1-4 and 0.098eV for 1-2-3 compounds [65]. Apart from these, an estimate of 1450K was obtained by fitting the spin-correlation length within a Monte Carlo simulation of spin-1/2 Heisenberg model[147]. We have already pointed earlier in Chapter II and sec. 4.1.1 that the magnitude of the interlayer coupling is at least 3-5 orders of magnitude less than the intralayer coupling. Numerical analysis of various experiments has given a net interplanar coupling of 0.002meV for undoped 2-1-4. It is also known that the interlayer coupling in case of 1-2-3 is at least two orders of magnitude larger than 2-1-4 [62].

Using the same parameters for undoped compounds of 1-2-3 and 2-1-4 we have compared our self-consistent calculation [cf. eqn. (4.24)] to the approximate evaluation of the Neel temperature from eqn. (4.27). The results obtained from such a direct evaluation are not very different from the earlier results. For the case of undoped 1-2-3 the Neel temperature comes out to be 419K while for undoped 2-1-4 it is 316K. The comparison with the earlier results suggest that the approximation used to obtain eqn. (4.27) is a very accurate one.

4.3 Doping dependent Neel Temperature

A lot of experimental evidence [81 - 104] has come up during the last couple of years suggesting the importance of interlayer coupling in the magnetic dynamics of layered superconductors which is related to the doping of oxygen in case of 1-2-3

[62]. We have already shown in Chapter II, that the Neel temperature decreases as the material is doped with oxygen. The neutron scattering experiments reported in Chapter III, have established that at a critical value of $x \sim 0.4$ in 1-2-3 the Neel temperature is found to reduce to zero [37]. The changing concentration of oxygen in $YBa_2Cu_3O_{6+x}$ makes the system undergo an antiferromagnetic to superconducting phase transition. Addition of oxygen into these layered compounds will destroy the AFM long range order along with the appearance of the metallic superconducting phase. This doping of oxygen is also crucial since a variety of interactions [105] come into play and they affect the dynamics of the system.

We have explained in Sec. 4.1.1, that the difference in the interplanar and intraplanar coupling strengths is a consequence of the layered structure of 1-2-3 and 2-1-4 compounds [see fig.(4.1)]. It is also observed that the Neel temperature depends crucially on the interplanar coupling in these materials [36, 37, 80]. In the temperature range $T < T_N$, when 2D ordering becomes sufficiently long ranged, quasi- 2D ordering sets in and the interlayer coupling plays a crucial role in determining the AFM correlation in these materials [62].

The experimental results for the Neel temperature reported in Chapter III combined with what we have learnt here, suggest to us that both the doping and the interlayer couplings should have some dependence over one another since both are known to affect the Neel temperature. We will find such a dependence, if any, in the study we are going to undertake in the next section. We will develop and use our theory to calculate the variation of Neel temperature with doping concentration. The comparison of the results thus obtained with the existing experimental results of Chapter III will also be discussed later in the chapter. For the sake of simplicity, we have taken intraplanar coupling as a constant independent of the doping con-

centration 'x' for our calculations. We discuss the behaviour of Neel temperature with the variation of the ratio of interplanar to intraplanar couplings and show that in the limiting case when $J_\perp/J_\parallel \rightarrow 0$, the 3D AFM ordering is lost. In the discussions to follow, we will show that the results thus achieved with the assumption that the ratio of interplanar to intraplanar exchange coupling strength is directly proportional to the doping concentration 'x', are in excellent agreement with the experimental results.

4.3.1 A New method to calculate the Neel temperature

We will now venture to study the expression for the Neel temperature obtained in sec. 4.2.1 in order to extract more information about the possible consequences of doping on the Neel temperature. Here, we have identified a function of the ratio of inter to intraplanar coupling ratios. The Neel temperature is found to be inversely proportional to this function. The advantage of identifying a function of this type in the expression of the Neel temperature is manyfold. It not only provides us with the dependence of Neel temperature on 'r' but can also be used for the study of doping.

We start by writing the equation for Neel temperature obtained in the earlier section, eqn.(4.27), as follows

$$T_N = \frac{J_\parallel}{2k_B\, I(r)} \tag{4.28}$$

where, I(r) is given as:

$$I(r) = \frac{2}{N}\sum_k \frac{2+r}{(2+r)^2 - [\cos k_x a + \cos k_y a + r\cos k_z c]^2} \tag{4.29}$$

Breaking the fraction in the above equation into two parts and changing the sum-

mation over 'k' into integration

$$I(r) = \frac{V}{2\pi^3}\int_0^{\pi/a}\int_0^{\pi/a}\int_0^{\pi/c}\frac{dk_x dk_y dk_z}{(2-\cos k_x a-\cos k_y a)+r(1-\cos k_z c)} + \frac{dk_x dk_y dk_z}{(2+\cos k_x a+\cos k_y a)+r(1+\cos k_z c)} \quad (4.30)$$

Here, V is the volume of the unit cell. In the above equations we have replaced the ratio of interplanar to intraplanar coupling strengths by $r(=J_\perp/J_\parallel)$. It can be proved that the last term gives the same contribution to I(r) as the first term. Therefore, the above expression of I(r) reduces to:

$$I(r) = \frac{V}{\pi^3}\int_0^{\pi/a}\int_0^{\pi/a}\int_0^{\pi/c}\frac{dk_x dk_y dk_z}{(2-\cos k_x a-\cos k_y a)+r(1-\cos k_z c)} \quad (4.31)$$

Making the substitution $u = k_x a, v = k_y a, w = k_z c$, and integrating over w we get

$$I(r) = \frac{1}{\pi^2}\int_0^{\pi}\int_0^{\pi}\frac{dudv}{\sqrt{(2-\cos u-\cos v)}\sqrt{(2-\cos u-\cos v)+2r}} \quad (4.32)$$

Now, performing the integration over v the above integral reduces to

$$I(r) = \int_0^{\pi} F(u,r)K(u,r)du \quad (4.33)$$

where F and K are given as:

$$F(u,r) = \frac{2}{\sqrt{(1-\cos u+2r)(3-\cos u)}} \quad (4.34)$$

and

$$K(u,r) = \int_0^{\pi/2}\frac{d\theta}{\sqrt{1-\alpha\sin^2\theta}} \quad (4.35)$$

where,

$$\alpha = \frac{4r}{(1-\cos u+r)(3-\cos u)} \quad (4.36)$$

For very small 'r', K becomes constant $\pi/2$ and the leading contribution to the integration comes from small u. With the help of numerical calculation, we found that I(r) is proportional to ln (1/r).

4.3.2 Mermin and Wagner Theorem

Mermin and Wagner [110] have proved through their ingenious paper that for a 2-D antiferromagnet, there cannot be a long range order at any finite temperature. It should however be noted that the Mermin and Wagner theorem does not exclude long range order for 2D systems at zero temperature. Over the decades that followed no one has come up with results that indicate otherwise.

In our expression for I(r) [c.f. eqn.(4.33)], it can be easily shown analytically that when $r = 0$, $I(r) = \infty$. Hence, the Neel temperature $T_N = J_{\|}/2k_B\, I(r) = 0$ for r=0. This establishes the consistency of our theory with the Mermin and Wagner theorem that there can not be long range order in 2D systems at finite temperature. Hence, our Self-consistent theory which is basically developed for quasi-2D systems does show agreement with the Mermin and Wagner theory in the limiting case when there is no interplanar coupling.

4.3.3 Comparison with Experiments

We have calculated numerically I(r) as a function of 'r' using eqn.(4.33). The numerical results are presented in fig.(4.3) by solid lines. It is shown that the value of I(r) decreases as 'r' increases. Fig. (4.3) which has the variation of I(r) with r was then fitted with an analytical expression of the type

$$I(r) = 0.1616 \ln(\frac{1}{r}) + 0.5055 \qquad (4.37)$$

for values of 'r' ranging from $1.0 \cdot 10^{-8}$ to 1. By using this analytical expression of I(r) given by eqn.(4.37) we have calculated I(r) as a function of 'r'. The results are shown in fig.(4.3) by dotted line. One can see from the figure that the above

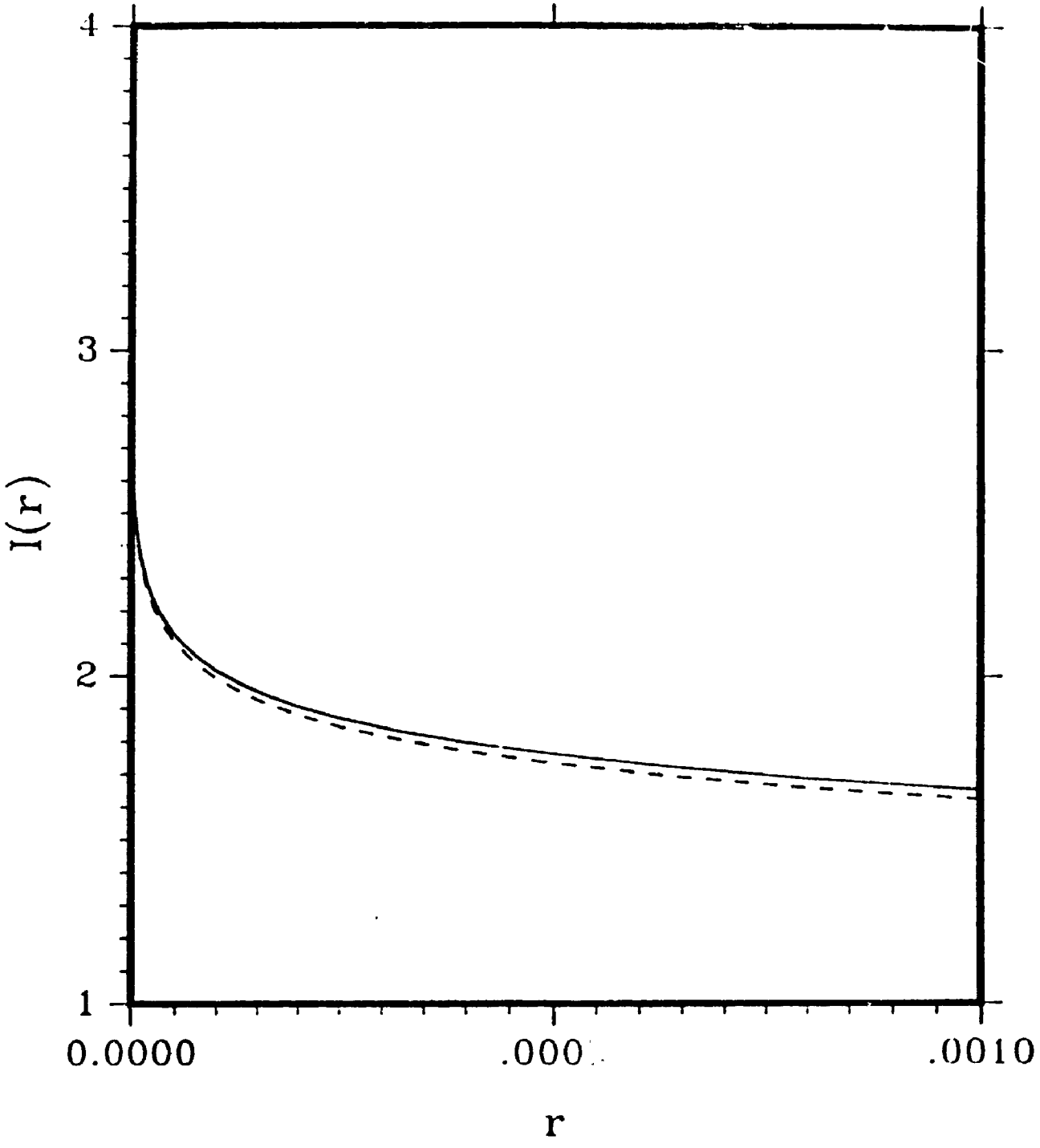

Figure 4.3: Variation of I(r) with 'r'. Solid curve is obtained from equation (4.33). The dotted curve is obtained from the analytical expression given in equation (4.37).

analytical expression [ie. eqn.(4.37)] is an excellent approximation for I(r) given by eqn.(4.33). On the basis of this analytical expression , the Neel temperature can be approximately written as

$$T_N = \frac{J_{||}}{2k_B\,[0.1616\ln(J_{||}/J_{\perp}) + 0.5055]} \tag{4.38}$$

This expression of the Neel temperature will come in handy when we compare our results with those of other theories in the next section. Also, this expression establishes that the Neel temperature is solely a function of the ratio of inter to intraplanar exchange couplings. We will discuss more about it at the end.

By explicitly calculating the Neel temperature from eqn. (4.28) at a constant value of the intraplanar exchange coupling we found that the Neel temperature depends crucially on the value of the ratio r. This suggests to us that there should be a direct relation between 'r' and 'x'. Let us for a moment assume, that the ratio of interplanar to intraplanar exchange interaction strength, 'r' is a linear function of the doping concentration. For example,

$$r(x) = c(1 - \frac{x}{x_0}) \tag{4.39}$$

where, $c = 6.0 \cdot 10^{-3}$ and $x_0 = 0.4$. Using this form for the ratio of interplanar to intraplanar exchange couplings we have calculated the Neel temperature as a function of doping ie. $T_N(x)$. The theoretical calculation is presented along with the experimental values in fig.(4.4). The experimental results are taken from Tranquada et al.[37]. In our calculation, for 1-2-3, we have taken the intraplanar exchange coupling interaction as a constant ($J_{||} = 98.0meV$) throughout the entire doping range. The experimental results of Tranquada et al. gives a different value of Neel temperature at different doping concentrations (x). We have now used these values of r(x) to find the Neel temperature by our theoretical expression [eqn. (4.28)], while

fixing the value of intraplanar coupling at 98.0 meV. The results are presented in fig.(4.5) along with the experimental results. In fig.(4.6), we plot the variation of 'r' with 'x'. The dotted curve in fig.(4.6) represents the values of r(x) vs. x that we obtained above while the solid line shows the linear dependence of 'r' on 'x'. As we discussed earlier, fig.(4.4) was obtained by assuming that 'r' is a linear function of 'x'. The solid curve in fig.(4.6) represents this linear dependence as given in eqn.(4.39). One can see from this figure that at 'x=0' and 'x=0.4' there is no difference between the two curves but other than these values there is some deviation. The dotted curve seems to give a quasilinear relation between 'x' and 'r' for $0.05 < x < 0.3$. The slope of dotted curve is slightly different than that of the solid curve. For $x < 0.0$ and $x > 0.3$ the dotted curve shows a large non-linearity. It can hence be concluded that, the linear dependence between 'x' and 'r' is a fairly good approximation for most values of 'x.

In Chapter III, we have shown that the experimental results for the doping dependence of Neel temperature for 2-1-4 is different from 1-2-3. For a very small value of Sr doping, the Neel temperature falls rapidly and is zero for $x \sim 0.02$. We have calculated the doping dependence for 2-1-4 employing the same techniques discussed earlier. The results achieved for 2-1-4 are shown in fig. (4.7). The open circles are the experimental points from Kumagai et al. [108]. The results thus obtained from our self-consistent theory are in very good agreement with the experimental results of Kumagai et al.

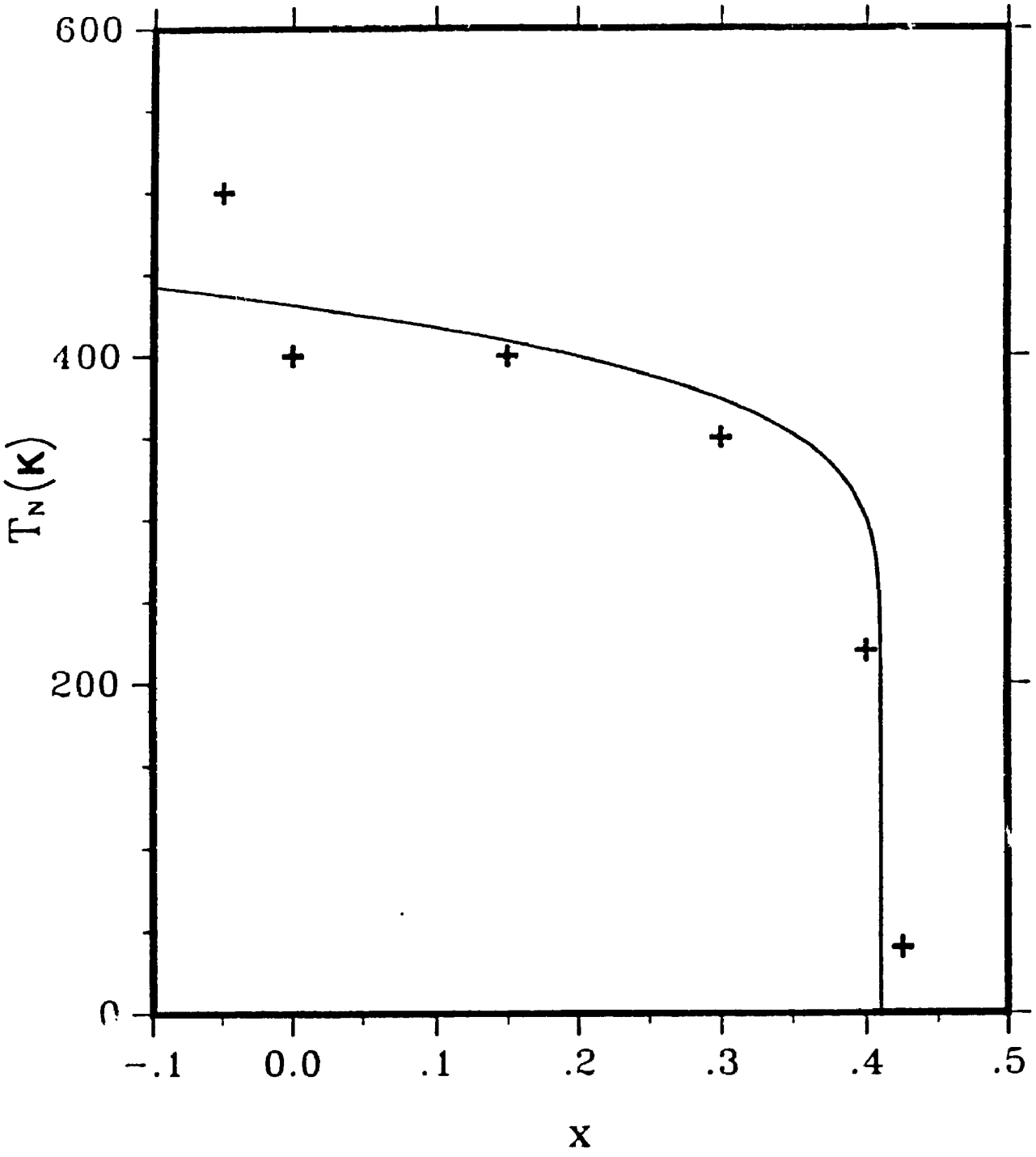

Figure 4.4: Variation of Neel temperature as a function of doping concentration 'x' in 1-2-3 compounds. Solid curve represents the theoretical results. Crosses represent the experimental points. Here, a linear relation between 'x' and 'r' is assumed

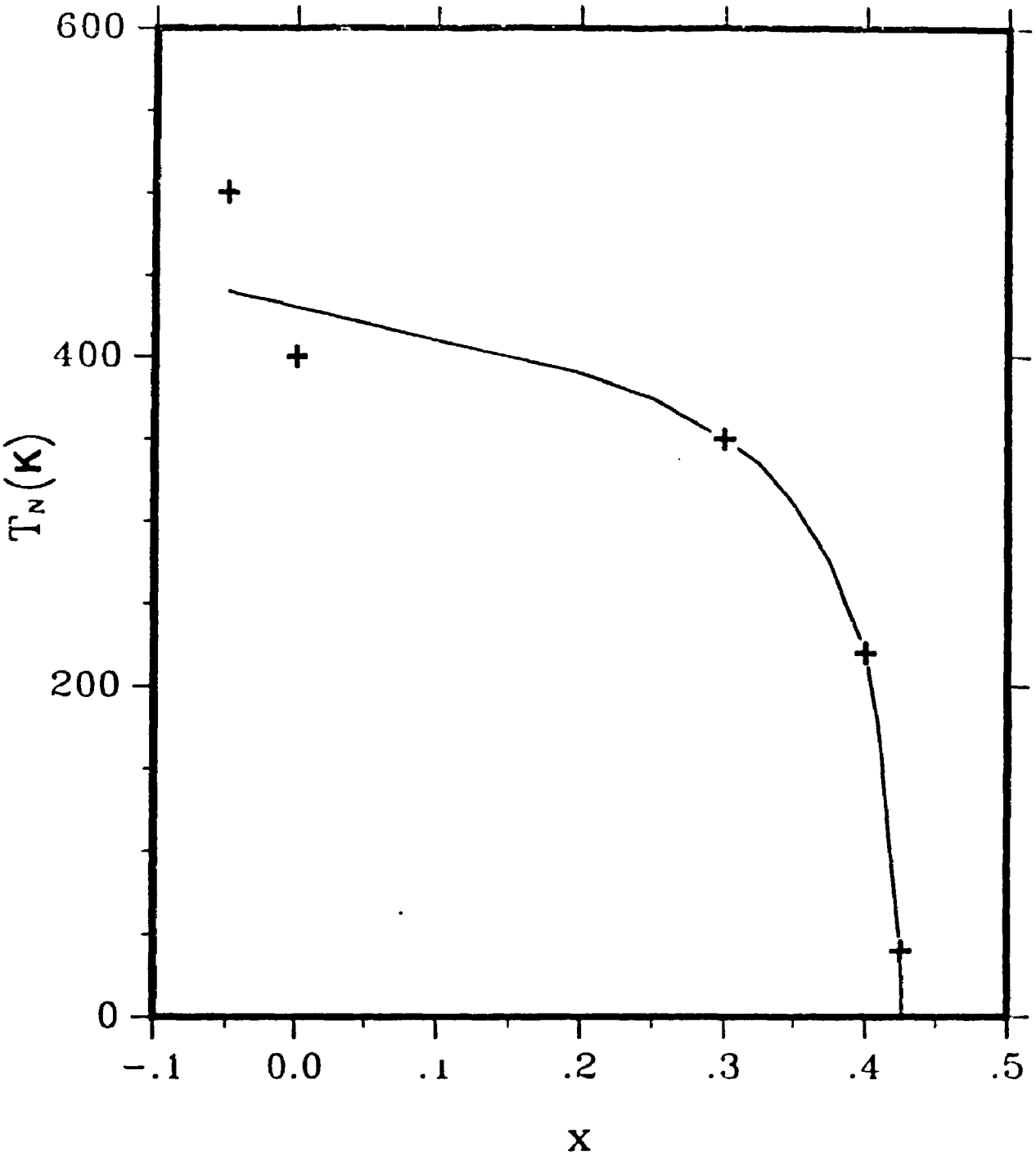

Figure 4.5: Variation of Neel temperature as a function of doping concentration 'x' in 1-2-3 compounds. Solid curve represents the theoretical results and crosses represent the experimental points. Solid curve is obtained by fitting equation (4.32) with experimental points choosing the proper value of 'r'

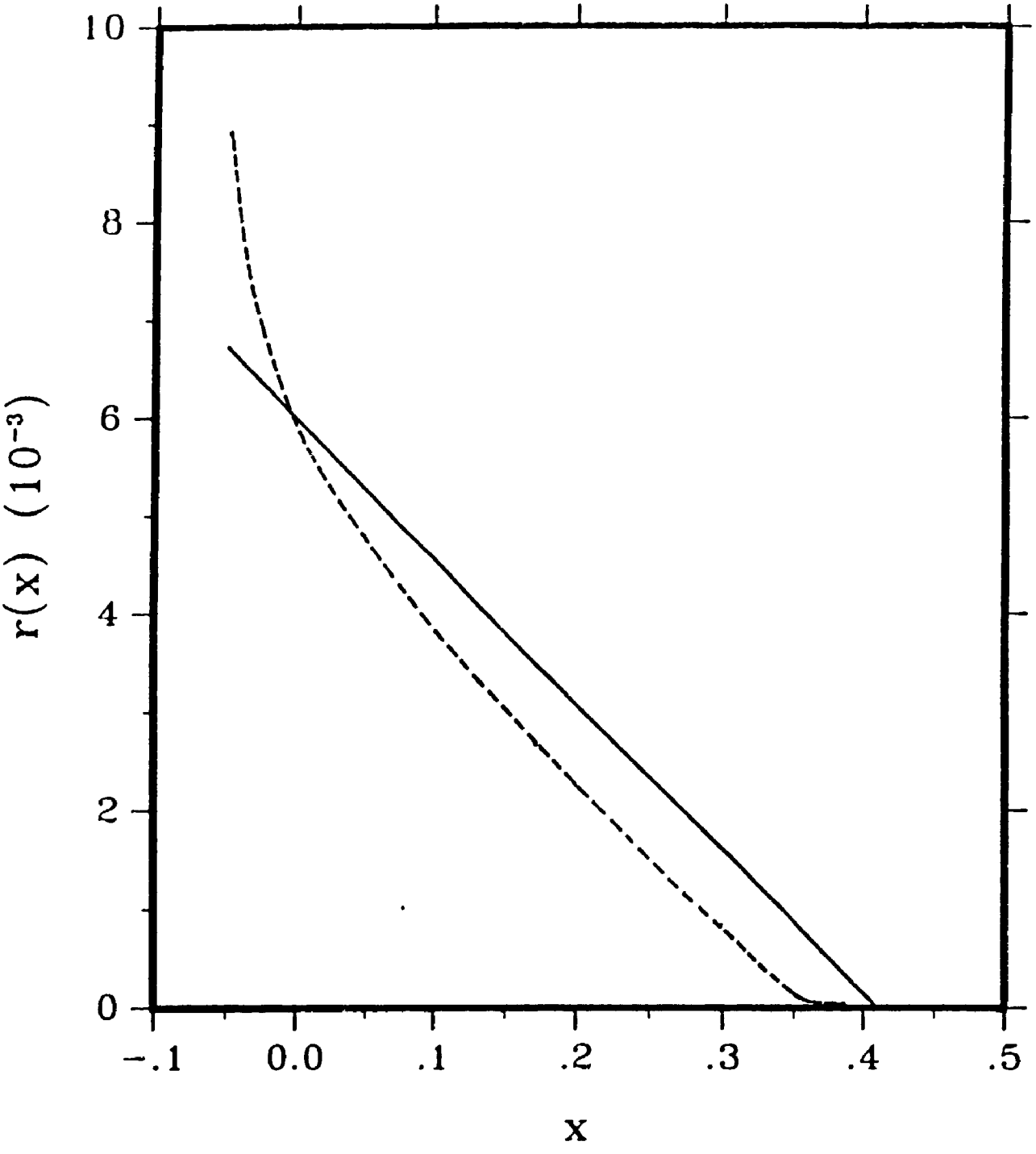

Figure 4.6: Variation of 'r' with 'x'. Dashed curve represents the value of 'r' obtained from fig.(4.5) as a function of 'x'. The solid line represents the linear dependence of 'r' with 'x'

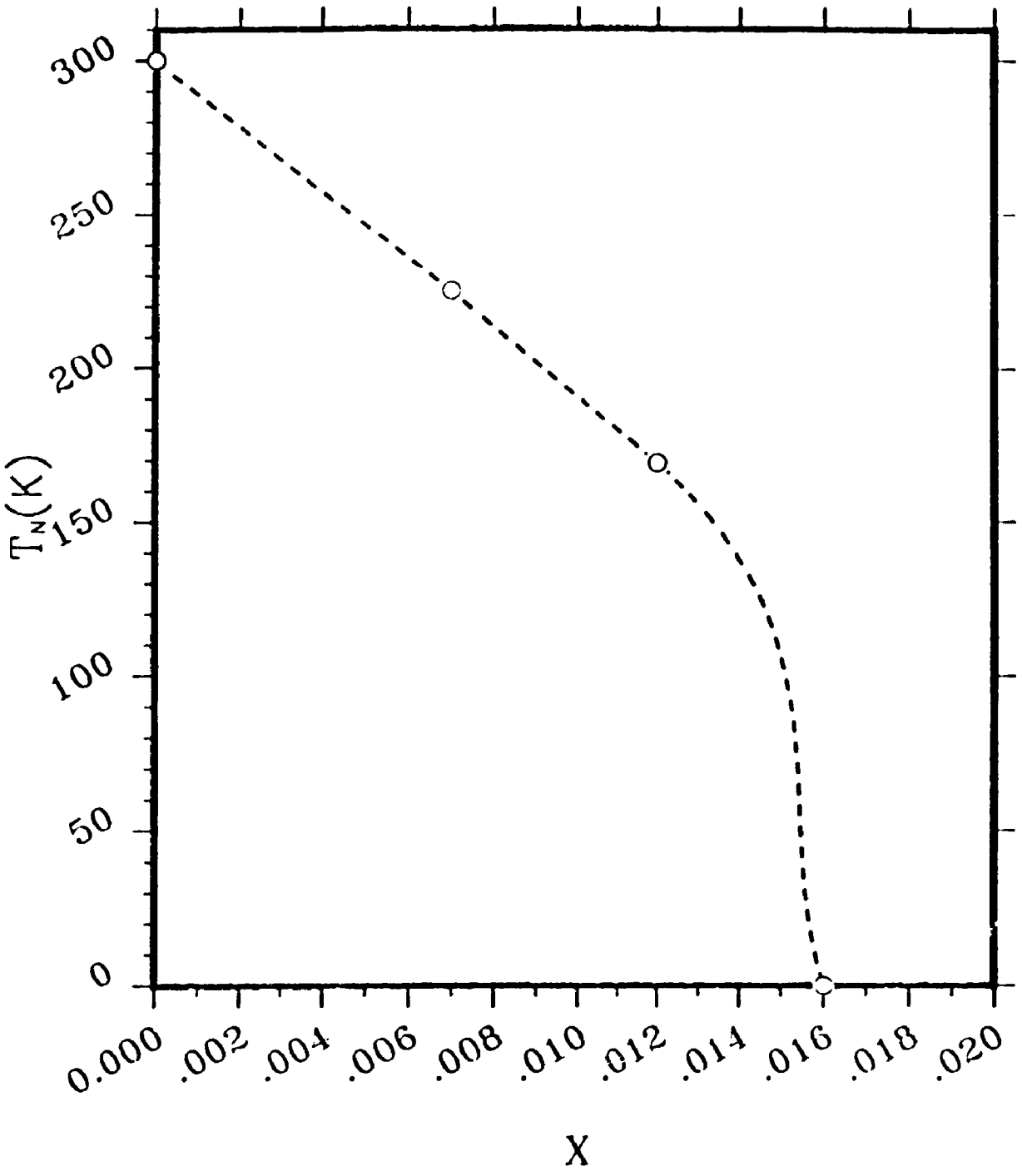

Figure 4.7: Variation of Neel temperature as a function of Sr doping in 2-1-4 compounds. The dashed curve represents the theoretical results while the open circles represent the experimental points.

4.4 Results and Discussion

As we have already pointed out earlier that the maximum Neel temperature observed experimentally is in the vicinity of 300K and 400K for 2-1-4 and 1-2-3 compounds. We have obtained a Neel temperature of 320K and 420K for 2-1-4 and 1-2-3 compounds in Sec.4.2.2. This is consistent with the experimental results reported sofar for 1-2-3 and 2-1-4 compounds [37, 62].

Our theory is consistent with the Mermin and Wagner theory which excludes any long range order at finite temperatures in 2-dimensional systems. The theory also gives a logarithmic dependence of the Neel temperature on the ratio of inter to intraplanar coupling. A logarithmic term was also obtained by Tesanovic group [76] by linear spin-wave theory. Other authors have also used the linear spin-wave theory to study the quasi- 2D quantum Heisenberg Antiferromagnet [71, 75]. Soukoulis et al. [71] have obtained an expression for the Neel temperature by using the linear spin wave theory as

$$T_N \simeq \frac{4\pi}{3}|J_{||}|/\ln(\frac{32}{\gamma}) \tag{4.40}$$

where γ is the anisotropy parameter or the ratio of inter to intraplanar couplings. This expression is different from the one we have obtained here. The above expression is valid only when the spin $S \rightarrow \infty$ ie. for classical spins. Infact, their results are equivalent to the classical limit of Tahir-Kheli and de Ter Haar's three dimensional ferromagnetic Curie temperature divided by S^2 [111]. It is inappropriate to use the classical limit when considering these layered compounds which are unambiguously known to be S=1/2 quantum antiferromagnets. They have obtained a value of $1.36J_{||}$ for the Neel temperature while ours is $0.987J_{||}$.

Modelling of the undoped copper oxides by the quasi-2D quantum Heisenberg

antiferromagnet has also been done by the linear spin-wave theory [75, 72]. Our results of the Neel temperature are quite consistent with these results rather than that of Soukalis et al. Results by Liu for the Neel temperature for 'r=1.0' gives $T_N = 0.989 J_{||}$ which is in excellent agreement to ours [75]. It is worth pointing out here that high temperature series expansion result $T_N = 0.951 J_{||}$ is also quite close to our results [112, 113].

A recent study on the quasi-two dimensional systems is done by Majlis et al. [74] on the basis of Green's function approach in the Random phase approximation (RPA), Callen Modified RPA (MRPA) and Free spin wave approximation. The Neel temperature according to their results in RPA is

$$\frac{k_B T_N^{(RPA)}}{J_{||}} = \frac{A}{B_\epsilon + \ln(1/\epsilon)}$$

where 'A' is a numerical constant and 'B' is a smooth function of ϵ. For the RPA, values of 'A' and 'B' are 6.0 and 3.0 respectively [74]. This expression is very similar to the analytical expression we have obtained in our theory. Comparing the analytical form for the Neel temperature in our theory [cf. eqn. (4.38)] with the expression by Majlis et al. given above shows that their value of 'A' is almost twice ours. According to our calculations, 'A' and 'B' are 3.09 and 3.13 respectively. We have already shown that our analytical expression gives very accurate results for the Neel temperature. It is worth reiterating here that our values of A and B again give us $k_B T_N = 0.987 J_{||}$, at r=1 consistent to the results we quoted above while Majlis's result won't.

A Schwinger Boson Mean Field Theory (SBMFT) calculations done by Keimer et al. [114] have obtained an expression for Neel temperature which too has an analogous logarithmic dependence. For describing the behaviours at higher temperatures

Keimer et al. have used the generalized version of SBMFT. They have found good agreement between their theory and experiments up to T$\sim 0.8T_N$.

Our comparisons to these results have shown us that SBMFT and spin-wave theory cover complementary temperature regimes. At high temperatures, the range of the intraplanar correlations is highly reduced and the harmonic spin wave theory fails. This has also been found from the neutron scattering data of 2-1-4 where it is evident that systematic departures from spin-wave results exist as the temperature is raised well above T=0. While the spin wave theory is good for regions where there is large staggered magnetization, the SBMFT should be applied to higher temperatures when the ordered moments are considerably reduced. In retrospect, the self-consistent theory can be applied to a wide temperature range and gives results consistent with the experiments for temperatures close to the Neel temperature where at least spin-wave theory clearly fails. In Chapter V, we will specifically show that the linear spin-wave theory is found to overestimate the value of the Neel temperature in these layered copper oxides.

We have compared our doping dependent results with experiments of Tranquada et al. [36]. Neutron diffraction results for 1-2-3 [see fig.(4.4) and fig.(4.5)] show that our theoretical results are in very good agreement. This indicates to us that the approximation where we have assumed doping parameter as a linear function of 'r' works reasonably well.

4.5 Conclusion

In this Chapter we have developed a theory for oxide superconductors by using the Green's function method. This theory gives us a self-consistent expression which

is evaluated to obtain the Neel temperature for 1-2-3 and 2-1-4 compounds. Thus, we call it the self-consistent theory. We have shown that the results obtained from this theory are consistent with the Mermin and Wagner theorem. Also, the analytical expression that comes out of this theory gives very accurate results for the Neel temperatures at different values of the anisotropy parameter 'r'. This has enabled us to explicitly evaluate the dependence of doping on the Neel temperature. The evaluation and the comparisons of this doping dependent Neel temperature for 1-2-3 with Neutron scattering results show that the doping parameter varies approximately linearly with the ratio of inter to intraplanar coupling. It also predicts a logarithmic dependence of 'r' on the Neel temperature which has been found independently within a linear spin-wave theory [72] and a Schwinger boson mean field approach [114]. The advantages of such a theory over the linear-spin wave theory will become apparent in the next Chapter when we compare the results of sublattice Magnetization from these two theories.

Chapter 5

Self-consistent calculation for Magnetization[†]

In the last chapter we developed a self-consistent theory for the magnetic properties of cuprates based on the quasi-two dimensional Heisenberg model. In the formulation of the theory we have included the effect of the planar CuO_2 layers and the interlayer coupling. We have also shown in the last chapter, by comparing our theoretical results to various experiments that our theory was able to explain the Neel temperature and it's doping dependence for 1-2-3 and 2-1-4 compounds. Now, we will extend this theory to account for the sublattice magnetization in these compounds. The sublattice magnetization will then be evaluated and compared with some of the experimental and theoretical results available on the subject.

5.1 Introduction

We have shown in Chapter III, that experimental studies of the temperature variation of sublattice magnetization in La_2CuO_4 has revealed a weak dependence at low

[†]The results in this section have been published in Physical Rev.B46, 14069, 1992

temperatures. However, as the temperature is increased this dependence increases to an almost linear falloff. This was inferred by Mossbauer spectroscopic studies of 2-1-4 doped with about half a percent of ^{57}Fe [116]. The doped Fe goes to the Cu sites in 2-1-4 and their spins become antiferromagnetically coupled with those of Copper. This process hence helps in determining some crucial information about the magnetic properties in copper oxides [117, 118].

Apart from this, Neutron studies have been done on L_2CuO_4 where L= Pr, Nd, Sm to investigate the magnetic structure of this class of compounds. By, analyzing the intensity of the magnetic $(\frac{1}{2}, \frac{1}{2}, 1)$ peak, it was inferred that the sublattice magnetization shows an approximately linear fall off with temperature. This was observed in a large temperature range from about 45K to just below the Neel temperature. This linear falloff is considered to be a signature of very weak magnetic interlayer coupling. Some reports have suggested that ordering transition in cuprates follows a mean-field type of behaviour [119]. This hasn't been confirmed experimentally because most of the experimental results are surrounded by controversies and are inconclusive. We have already discussed some of them in Chapter III.

The discovery of quasi-two dimensional behaviour of these magnetic systems have prompted extensive theoretical work on quantum Heisenberg antiferromagnet. These approaches include renormalization group treatment of the non-linear σ model [67], 1/N representations of the Schwinger boson representation [68], linear spin-wave theory [120, 75, 71], modified spin-wave treatments [69, 70], and Green's function approach [73]. Some of these methods have been used to study the magnetic properties of the normal state. For ex. linear spin wave theory has been used by various authors to calculate the sublattice magnetization [120, 75], specific heat [75] etc. Some of these theories that are used to explain the magnetic properties

have not been able to explain all the experimental results that we have mentioned in Chapter III.

In this chapter our aim is to extend the self-consistent theory, the foundations of which has already been laid in Chapter IV, and to obtain an expression for the sublattice magnetization. We will be using the equation of motion [see appendix I] method for Green's function on a quasi-two dimensional quantum Heisenberg antiferromagnet in the presence of a weak external magnetic field. We obtain a self-consistent expression for sublattice magnetization. We will show that in the absence of any external magnetic field the results obtained here correspond to the one we have obtained in Chapter IV. We have compared our results with the theoretical results of spin-wave theory and show that a simple approximation on our theory yields the spin-wave results. The self-consistent expression obtained for magnetization is evaluated numerically by a multi-dimensional Gaussian Quadrature method. Results so obtained are compared with numerous experimental and theoretical results.

5.2 Expression for Magnetization

We start again with a quasi-two dimensional system in the presence of a magnetic field 'B', the significance of which will become apparent later in the next chapter when we differentiate the magnetization obtained here with respect to 'B' to obtain the susceptibility. As we have already mentioned in earlier chapters, for copper oxides, the spins are arranged antiferromagnetically in the CuO_2 planes. The exchange interaction within the CuO_2 planes ($J_{\|}$) differs from that between the planes ($J_{\perp}$) by several orders of magnitude. Dividing the spin lattice into spin up (f) and

down (g) sublattices as before, one can write the Hamiltonian in the presence of an external magnetic field B, as the following

$$H = \sum_{ab} J_{\|} S_f \cdot S_{\cdot} + \sum_{c} J_{\perp} S_f \cdot S_g - \mu g B \sum_f S_f^z - \mu g B \sum_g S_g^z \ , \qquad (5.1)$$

where ab and c denote the nearest neighbor summation in the CuO_2 planes in the ab and the c directions respectively. f and g denote the lattice sites of two sublattices (f and g) with different spin orientations respectively. The magnetic field B is applied along the z direction which lies in the CuO_2 plane. μ is the Bohr magneton and g is the usual g-factor.

For antiferromagnets, there are two kinds of Green's functions, resulting from the correlation functions between spins on the same sublattice and on the different sublattices. We have calculated the Green's function $G_{ff}(=<< S_f^- S_f^+ >>)$ on the same sublattice in the momentum and frequency space which is given by

$$\begin{aligned} G_{ff}(q,E) &= < S_f^z > [(\frac{1}{E - E_{1q}} + \frac{1}{E - E_{2q}}) \\ &\quad + (< S_f^z > - < S_g^z >) \frac{J_{\|} Z}{E_{1q} - E_{2q}} (\frac{1}{E - E_{1q}} - \frac{1}{E - E_{2q}})] \ . \end{aligned} \qquad (5.2)$$

Here S^+ and S^- are the spin raising and lowering operators perpendicular to the CuO_2 plane. E_{1q} and E_{2q} are given as

$$\begin{aligned} E_{1,2q} &= \mu g B + J_{\|} Z (< S_f^z > + < S_g^z >)/2 \\ &\quad \pm J_{\|} Z \sqrt{[(< S_f^z > - < S_g^z >)/2]^2 + \gamma_q^2 \ < S_f^z >< S_g^z >} \ , \end{aligned} \qquad (5.3)$$

where

$$\gamma_q = [2cosq_x a + 2cosq_y a + 2rcosq_z c]/Z \ , \qquad (5.4)$$

with $Z = 4 + 2r$, and $r = J_{\perp}/J_{\|}$. $< S_f^z >$ and $< S_g^z >$ are the staggered spin momentum of the f and g sublattices respectively. The sublattice magnetization M_f

is related to $< S_f^z >$ by $M_f = \mu g < S_f^z >$. Now the magnetization for the sublattice 'f', using the identity for spin-$\frac{1}{2}$ particles can be written as

$$M_f = \frac{\mu g}{2} - \mu g < S_f^- S_f^+ > \tag{5.5}$$

and the relation between the correlation function and the Green's function

$$< S_f^- S_f^+ > = \frac{1}{N} \sum_q \int \frac{d\omega}{2\pi} n_B(\omega) \left[-2Im\, G_{ff}(q, E) \right] , \tag{5.6}$$

where $n_B(\omega)$ is the Bose distribution function. With the help of eqns.(5.5), (5.6), and (5.2), one finds the sublattice magnetization as a function of the magnetic field

$$\begin{aligned} M_f &= \frac{\mu g}{2} \frac{1}{1+W} \\ W &= \frac{1}{N} \sum_q \Big[\Big(\frac{1}{e^{\beta E_{1q}} - 1} + \frac{1}{e^{\beta E_{2q}} - 1} \Big) \\ &\quad + \frac{M_f - M_g}{\mu g} \frac{J_{\|} Z}{E_{1q} - E_{2q}} \Big(\frac{1}{e^{\beta E_{1q}} - 1} - \frac{1}{e^{\beta E_{2q}} - 1} \Big) \Big] . \end{aligned} \tag{5.7}$$

Similarly one can obtain an expression for M_g from the above expression by exchanging f and g in the right hand side. In the absence of an external magnetic field, ie. by putting B = 0, $M_f = -M_g = M$, and $E_{1q} = -E_{2q} = E_q$, the above expression takes a more compact form, which reduces to zero at and above the Neel temperature as one would expect.

$$M(T) = \frac{1}{2} \frac{\mu g}{\frac{1}{N} \sum_q (1 + 2n_B(E_q)) / \sqrt{1 - \gamma_q^2}} . \tag{5.8}$$

This expression is similar to the one we have already obtained in Chapter IV, on a quasi-two dimensional Heisenberg model in the absence of an external Magnetic field [cf. eqn.(4.21)-eqn.(4.22)]. At this point we will borrow the expression from Chapter IV. Eqn.(4.21) and eqn.(4.22) gives us the sublattice magnetization as

$$< S_f^z > = \frac{1}{2} - \frac{2 < S_f^z >}{N} \sum_k \left[P_k \coth \left[\frac{E_k}{2k_B T} \right] - 1 \right] \tag{5.9}$$

These two self-consistent expressions viz. eqn.(5.8) and eqn.(5.9) for magnetization are equivalent except for a constant multiplication factor in eqn.(5.9), since M(T)= $\mu g < S_f^z >$. We can easily see here that one of the interesting features of this theory for quantum Heisenberg antiferromagnets is the departure of the sublattice magnetization from the value S=1/2 which corresponds to the elementary classical picture of a saturated sublattice.

The expression for magnetic moment at zero temperature can be obtained from eqn.(5.9). At zero temperature, $\coth(E_k/2k_BT) = 1$ and hence eqn.(5.9) becomes:

$$< S_f^z >= \frac{1}{2} - 2 < S_f^z > \left[\frac{1}{N}(\sum_k \eta/\sqrt{(\eta^2 - \xi_k^2)} - 1)\right] \tag{5.10}$$

This value of $< S_f^z >$ gives us the effective magnetization by the relation $M_{eff} = 2\mu_B < S_f^z >$. To evaluate the value of $< S_f^z >$ from eqn.(5.9) and eqn.(5.10), the sum over 'k' can be converted to an integral over Brillouin zone whose volume corresponds to $N/2$ values of 'k'. This gives us:

$$\sum_k = \frac{1}{2}\frac{V}{(2\pi)^3}\int\int\int dk_x\, dk_y\, dk_z \tag{5.11}$$

Here, 'V' is the volume of the crystal and the integration limit for 'k' are taken within the first Brillouin zone. The above eqn.(5.10) reduces to Anderson's expression[121] if one replaces $J_{ab} = J_c = J$ and $< S_f^z >= S$ on the r.h.s of the equation. Eqn.(5.10) can also be reduced to the expression given in eqn. (4.24), if one replaces $< S_f^z >= \bar{S}$. To get around the problems of self-consistent calculation of magnetization one can simplify eqn.(5.9) by putting $< S_f^z >= 1/2$ on the r.h.s. In this approximation eqn.(5.9) reduces to the expression of 'Spin wave theory' which is written as:

$$< S_f^z >= 1 - \frac{1}{N}\sum_k P_k \coth\left[\frac{\sqrt{\eta^2 - \xi_k^2}}{4\,k_B\,T}\right] \tag{5.12}$$

We will compare the numerical results obtained from the two expressions given in eqn.(5.9) and eqn.(5.12) in the next section.

5.2.1 Comparison with Experiments

We have evaluated eqn.(5.9) numerically using multidimensional Gaussian Quadrature method. By using eqn.(5.9) we have calculated self consistently the magnetization as a function of temperature for La-Sr-Cu-O and Y-Ba-Cu-O. In our deliberations here, we will use M(T) and M(0) for the values of $< S_z >$ evaluated at any arbitrary temperature T and zero respectively. The parameters used in the calculation are $J_{||} = 120meV$ and r= $3x10^{-5}$. We get M(0)=0.359 and it is found that this value doesn't change much by changing the value of intraplanar coupling $J_{||}$. The dependence of M(0) on the interlayer coupling is rather large in comparison to intraplanar coupling as expected. If we substitute $< S_f^z >=1/2$ in the r.h.s of eqn.(5.10) we retrieve the equation of AS [†] [72] and Liu et al.[75]. Further, if we put r=1 we get back the Anderson's and Oguchi's result [121, 77]. They have shown that within linear spin-wave theory, for spin-1/2 system, the spin deviation ie. $\Delta S_f^z = \frac{1}{2} - < S_f^z >$, for 3-D and 2-D case are 0.078 and 0.197 respectively, in case of simple cubic lattices at zero temperature. In the limiting case of r=1 and 0, our theory also reproduces these results.

We have compared our theoretical results with the Mossbauer spectroscopic data of Tang et al. on 2-1-4 [116]. The results are presented in fig.(5.1). One can see from this fig. that there is a good agreement between theory and experiments. Our theoretical results agree very well with that of experimental data between temperatures zero till 200 K. Our Curve falls sharply as we approach the Neel temperature,

[†] AS signifies A. Singh et al.

as it should. For the above values of intraplanar and interlayer coupling we find a Neel temperature of 318K, which is consistent with the value of T_N reported for 2-1-4 compounds in the literature.

We have compared our theoretical results for 1-2-3 compounds with the experiments too. The experimental data is taken from Keimer et al. [114]. In fig.(5.2), we have shown the theoretical calculation along with the experimental data for undoped samples of 1-2-3 compounds. The parameters used for this calculation are $J_{||}$ = 98meV and r= 1.25 x 10^{-2}. Our results are in very good agreement with the results of Keimer et al. over the entire temperature range. As we approach the Neel temperature, however, there is a little deviation from the experiments and our theory seems to overestimate the Neel temperature.

We have also studied the variation of magnetization with r. We found that as r decreases the value of Neel temperature decreases which is consistent with the experimental results. In fig.(5.3) we have presented magnetization as a function of temperature for r=1, 0.01 and 1x10^{-5}. As the temperature increases the deviation between these three curves increases. It indicates that the nature of magnetization changes tremendously with the value of interlayer coupling as the temperature is increased.

Further, to stress on the role of interlayer coupling towards magnetization we have plotted the variation of magnetization with ln(1/r) in fig.(5.4). It can be seen from this figure that there is a drop between $r = 10^{-1}$ to 10^{-5}. This drop shows a strong dependence of magnetization on the value of 'r' as the system goes from strictly 3D to quasi-2D configuration. These calculations were done at a constant value of temperature (T= 280 K). This fig. also shows a comparative analysis of

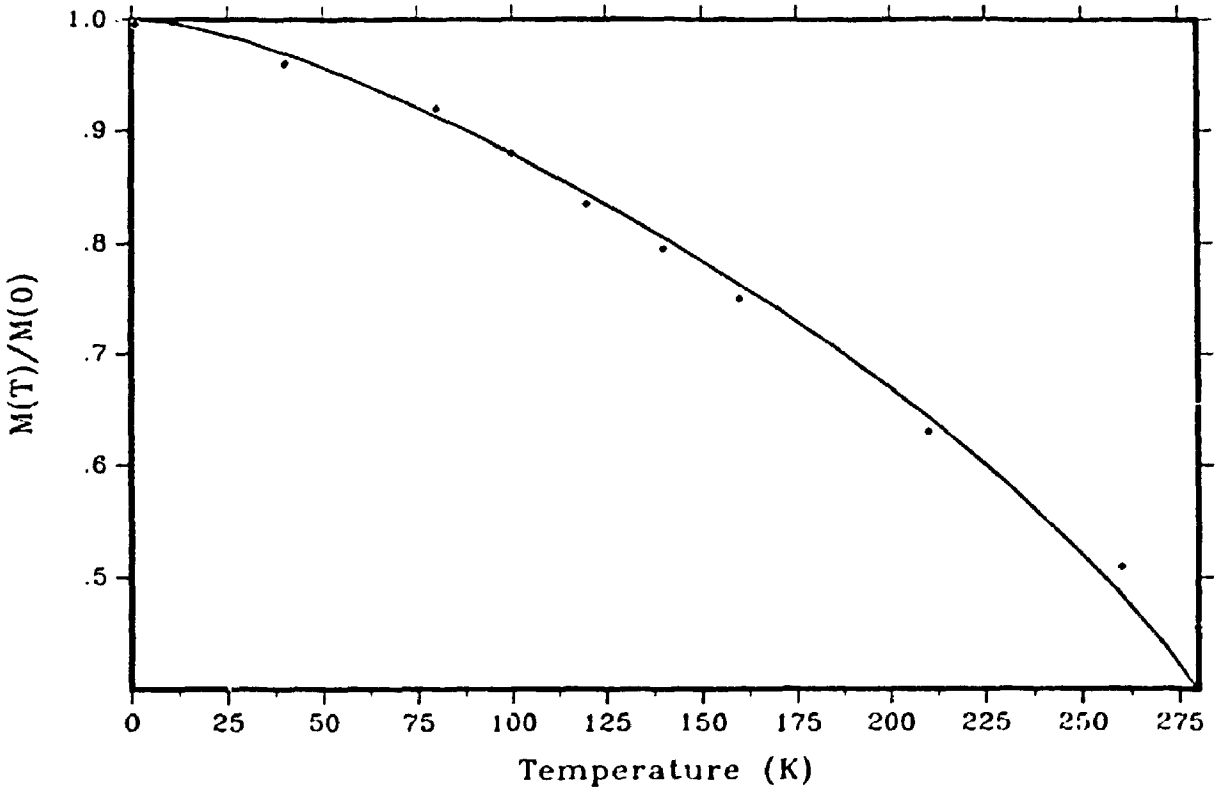

Figure 5.1: Variation of Normalized sublattice magnetization with temperature . Experimental points referred to as solid squares are from Tang et al. [116]. The solid line is obtained from self-consistent calculation with $J_{\|}$ = 120meV and r= $3x10^{-5}$

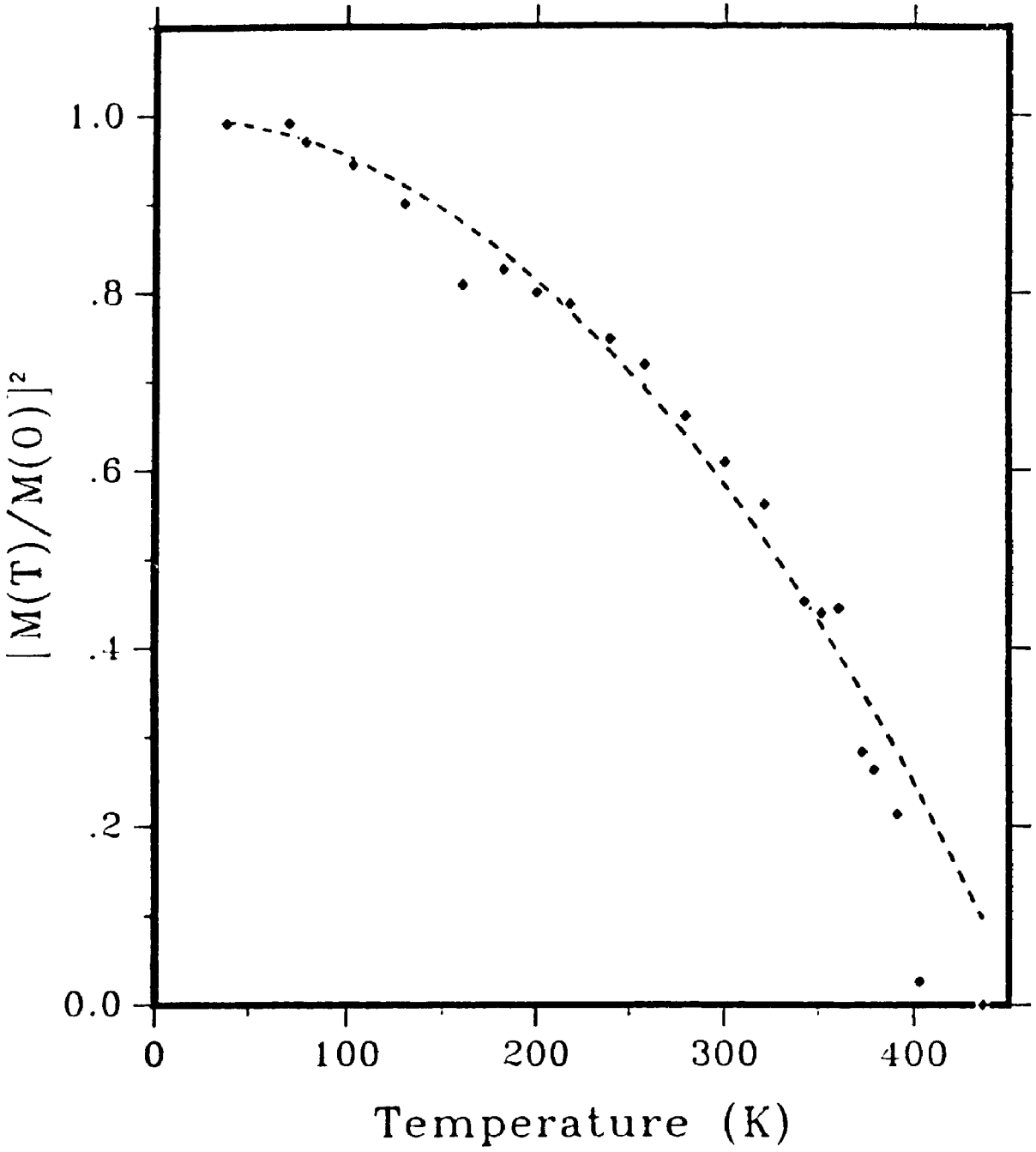

Figure 5.2: Variation of Normalized sublattice magnetization with temperature . Experimental points referred to as solid squares are from Keimer et al. [114]. The solid line is obtained from self-consistent calculation with J_1 = 98meV and τ= 1.25×10^{-2}

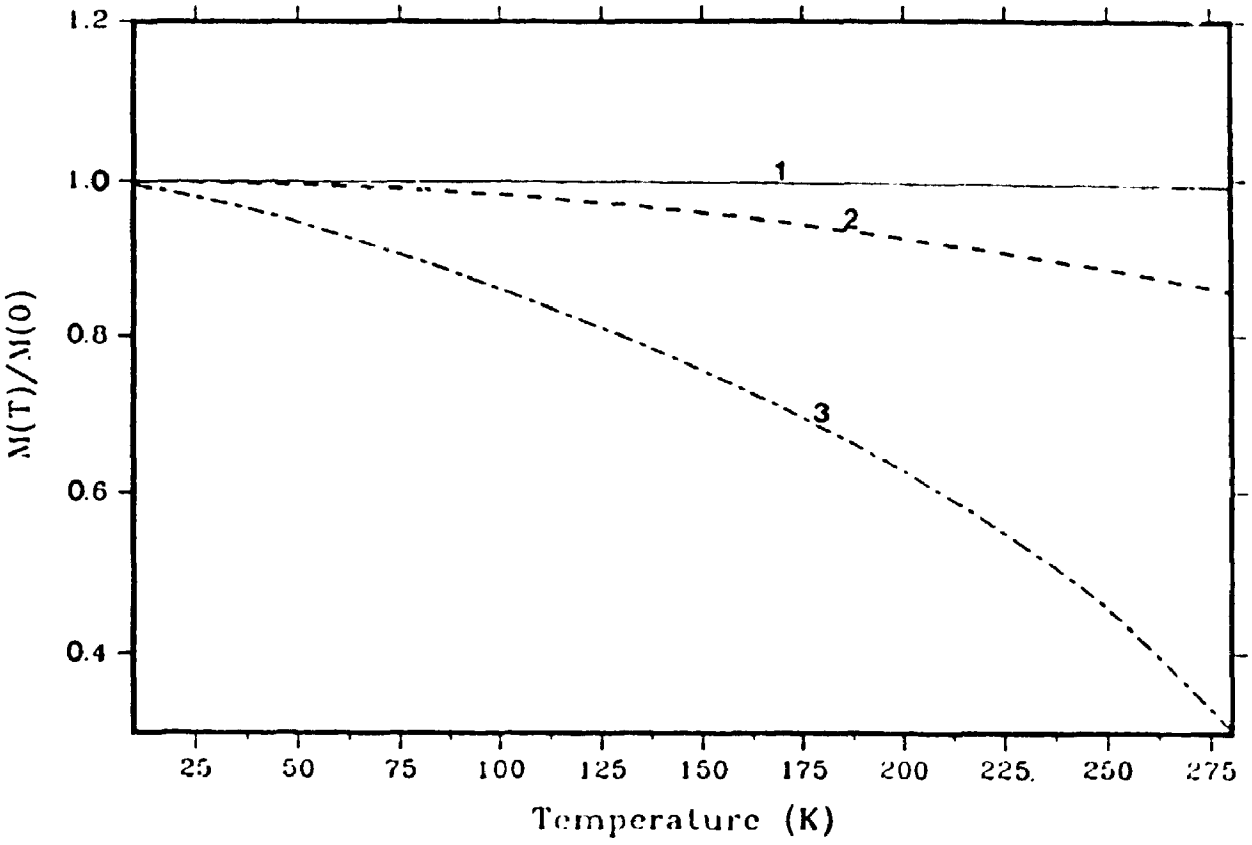

Figure 5.3: Variation of normalized sublattice magnetization with temperature at different values of ratio of interplanar to intraplanar coupling. Curves 1,2,3 represent values of 'r' as 1.0, 0.01, 1.00×10^{-5} respectively.

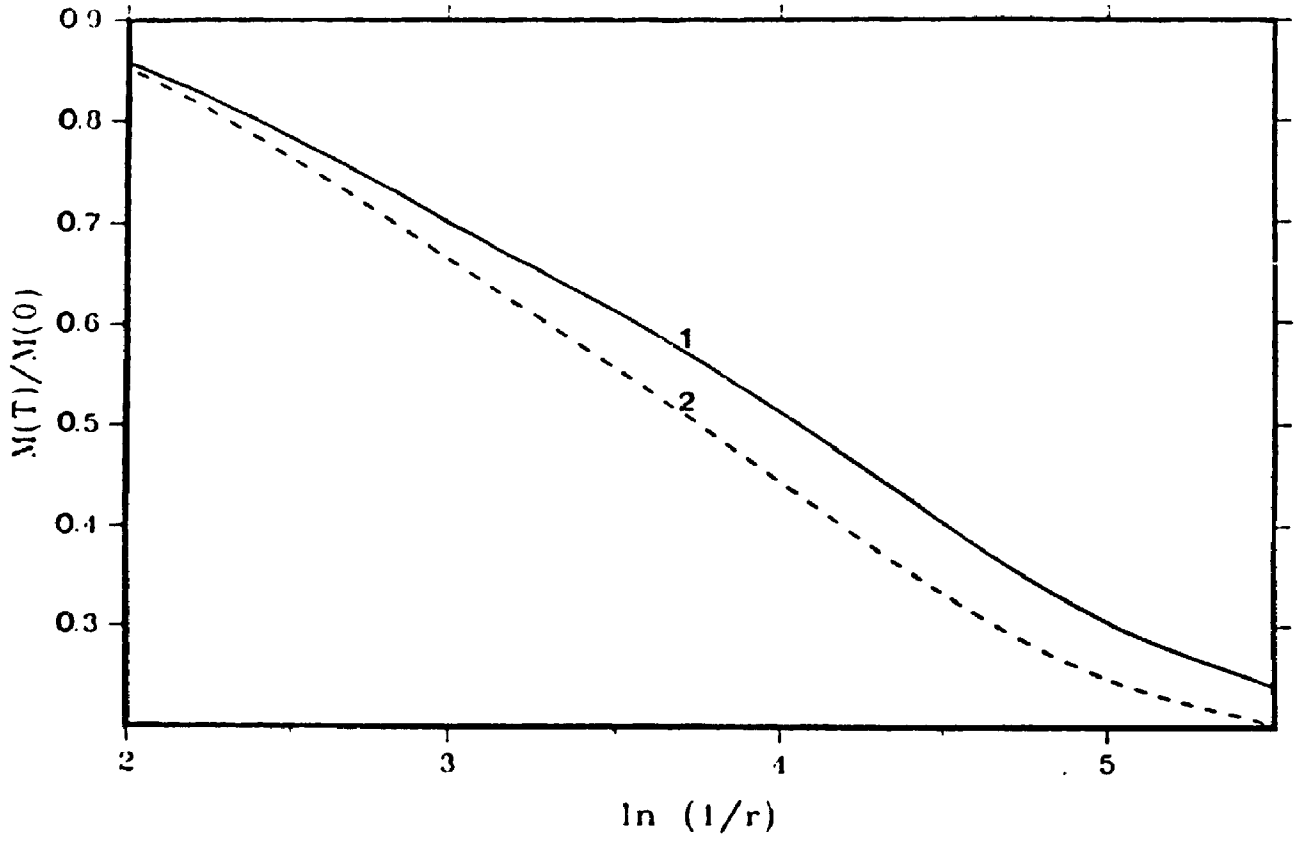

Figure 5.4: Variation of normalized sublattice magnetization with ln(1/r). Curve 1 represents the self-consistent calculation done by equation (5.9) while curve 2 is the spin-wave theory result.

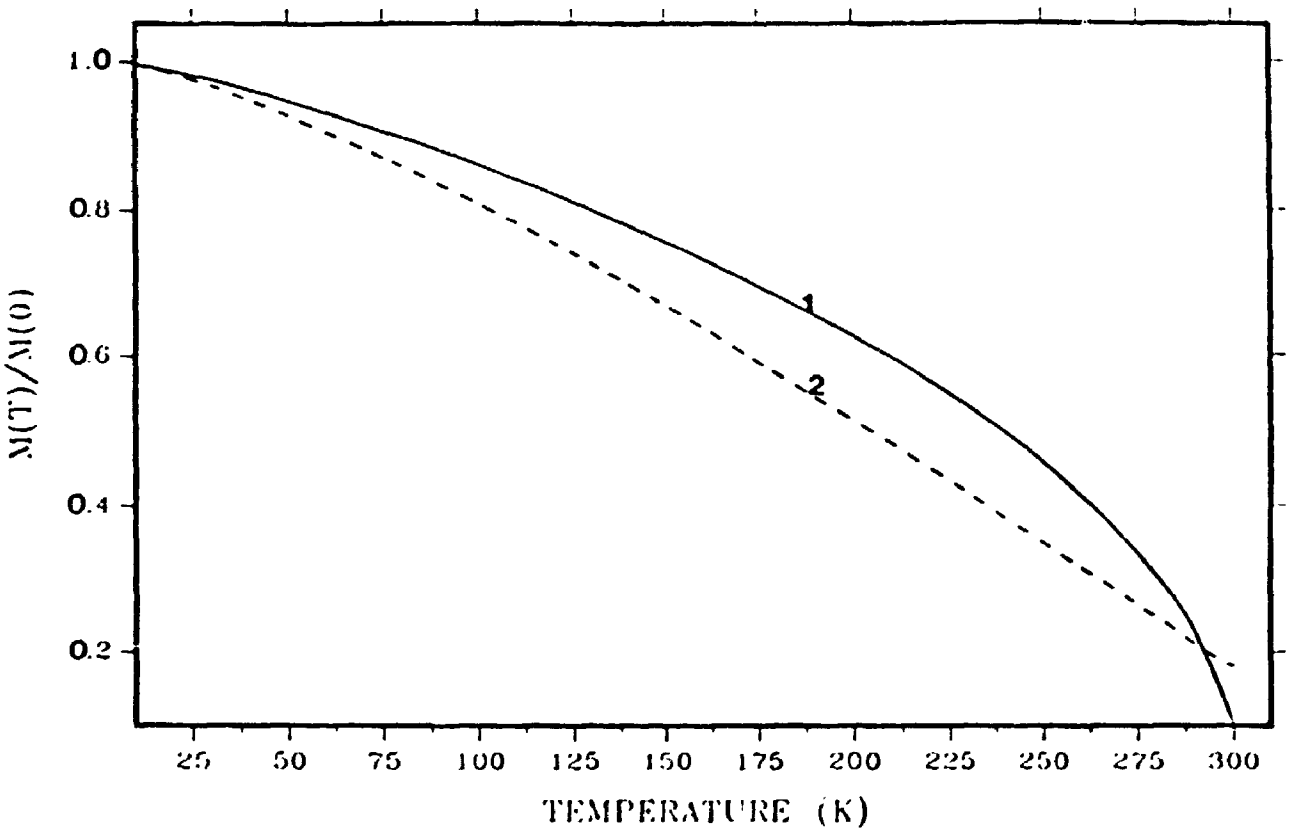

Figure 5.5: Variation of normalized sublattice magnetization with temperature at a value of r = 1.00x10^{-5}. Curve 1 shows the self-consistent calculation from eqn (5 9) while curve 2 is the spin-wave theory result.

our self-consistent calculations and those obtained by spin wave theory [cf. eqn.(5.12)]. It is shown that at low enough temperatures, there is almost no difference between the two results but as the temperature is increased the difference becomes more apparent. This could be easily comprehended by our next figure , fig.(5.5), where we plot the variation of magnetization with temperature for a fixed value of r= 1.00×10^{-5} and have compared our results with that obtained by spin-wave theory. As we approach the Neel temperature our curve starts falling sharply and cuts the curve obtained from spin-wave calculations at about 290 K.

5.3 Discussion of Results

In this chapter, we have studied the variation of magnetization with temperature and r. The temperature variation of sublattice magnetization is compared with Mossbauer spectroscopic results of Tang et al. [116] for 2-1-4 and those of Keimer et al. [114] for 1-2-3 compounds. We have obtained very good agreement between our theoretical results and these experiments [see fig.(5.1) and (5.2)]. The parameters are carefully chosen and are consistent with the experimentally determined values of $J_{||}$ and 'r' [62].

The calculations for the variation of magnetization with r has shown that with the decrease in the interlayer coupling the magnetization decreases. For theoretical calculations from our theory at a constant temperature of 280K, the magnetization decreases with r and eventually it begins to saturate at the quasi-2D value when r becomes considerably small. However, for the spin-wave theory the magnetization saturates at a 2-D value for almost the same value of r. These results are shown in fig. (5.4).

Linear spin wave theory has been used in the past to explain some of the magnetic properties [75, 76]. AS have derived M(T) on the basis of spin-wave theory and have compared the results with the MES data and muon-spin rotation experiments of Uemura et al.[54]. Although their results do not fit with the results obtained from the NS experiments but they get good agreement with the MES and muon-spin rotation results at temperatures below the Neel temperature. It has been argued by AS that the reduction in the staggered magnetization δM due to thermally excited spin waves follow a T ln T law [72], in apparent contradiction with accepted experimental results. Their calculation on 2-1-4 has yielded a Neel temperature of 350K.

We have compared our theoretical results for 2-1-4 compounds with the numerical evaluation within the spin-wave approximation [cf. eqn. (5.12)]. The comparisons of these two calculations have shown that for the same parameters while our calculation gives a Neel temperature of 318K close to the experimental value for 2-1-4, spin-wave expression overestimates it. AS results have also overestimated the Neel temperature for 2-1-4 [76]. These results indicate that while spin wave theory does overestimate the Neel temperature in these cuprates, our theory gives a much more accurate variation of sublattice magnetization with temperature. We have also shown that our theoretical predictions are consistent with the experimental results of Tang et al., which are incidentally the same results used by AS. Later on, other theoretical results of Majlis et al.[74] and Keimer et al [114] have concurred with our results and have shown independently that the spin-wave theory does break down in the vicinity of Neel temperature.

The reason for such a behaviour of spin-wave theory near the phase transition point could be the lack of self-consistency in this approach. We have already sho :n

that the expression in the spin-wave theory [viz. eqn. (5.12)] can be obtained in the limiting case in our theory [eqn.(5.9)] as $< S_f^z > \rightarrow \frac{1}{2}$. By doing so one avoids the self consistency in the equation and as a result the calculation becomes much simpler. Another reason that could be affecting the behaviour of magnetization near the Neel temperature could be the presence of quantum fluctuations. Near the phase transition point these fluctuations become important and should be included.

5.4 Conclusions

This chapter reports the study of sublattice magnetization and it's dependence over temperature and r The numerical calculations have established that our theory gives excellent results for the sublattice magnetization in case of both 1-2-3 and 2-1-4 compounds. The comparisons between the theoretical results and recent experimental results also suggest that the sublattice magnetization can be best explained by a self-consistent theory such as ours. We have established that the spin-wave theory overestimates the sublattice magnetization near the Neel temperature. The advantage of our theory over the linear spin-wave theory is the inherent self-consistency and it is shown that the spin-wave results can be retrieved from our theory with some simple approximations. In the next chapter, we will build on the theoretical framework and introduce the spectral function for spin waves to calculate the magnetic susceptibility.

Chapter 6

Magnetic Susceptibility §

So far in previous chapters, we have obtained, among other things, the Neel temperature, it's dependence on doping and the sublattice magnetization. The theoretical results obtained from the self-consistent theory have encouraged us to explore other magnetic properties and explain them. So now, in this chapter, we will calculate the magnetic susceptibility by using our self-consistent theory and by introducing the spectral function of spin waves. We will compare our theoretical results with the experiments

6.1 Introduction

We have already presented a brief review of some of the salient features of the experimental results of susceptibility on 1-2-3 and 2-1-4 in Chapter III. Some of the earliest results for the magnetic susceptibility came from the works of Johnston et al. [125]. They studied the dc magnetic susceptibility as a function of temperature even before the antiferromagnetic ordering was found in these layered copper oxides

§The results in this section have been published in Physica Status Solidi (b) 179, 539, 1993

by positive muon spin resonance [126] and neutron-diffraction studies [127]. They couldn't find any features which could reveal a 2-D to three dimensional phase transition in the susceptibility data. But since then, reexamination of these earlier results have clarified the problems which occurred in the susceptibility data.

For compounds like 1-2-3, a clear picture about the magnetic susceptibility can only be achieved by isolating some of the intrinsic impurities which contribute to the susceptibility. One such impurity is $BaCuO_2$, which is known to be paramagnetic from both susceptibility [128, 129] and electron- paramagnetic resonance studies [129]. The earlier susceptibility measurements of Johnston et al. contained this paramagnetic contribution which tends to dominate at low temperatures thus masking the phase transition [125]. Later, after identifying this problem Johnston [39] has reanalysed the experimental measurements of the magnetic susceptibility and after separating the contributions from ions and holes, he found that the spin lattice magnetic susceptibility scales universally with temperature normalized to the temperature where the magnetic susceptibility has a maximum. This temperature is called T_M.

In an effort to extract the correct susceptibility free from the paramagnetic impurities, a Curie-like contribution (C_g/T) was subtracted by Tranquada et al. from the susceptibility data [37]. It was assumed that the corrected susceptibility $\chi^{corr}(T)$ would have $d\chi/dT \geq 0$ above 100K. The shapes of the residual curves were found not to be sensitive to the precise value of the curie coefficient, C_g, or to the replacement of the Curie term by a Curie-Weiss form $C_g/(T-\theta)$. The corrected susceptibility hence is written as $\chi^{corr} = \chi_g - (C_g/T)$. For 1-2-3, such a corrected susceptibility data has been shown in Fig.(3.3b). Each curve is dominated by a broad maximum at temperature $\geq$ 800K and the susceptibility is found to decrease

with decreasing temperature [130].

It is believed that such a maxima can be explained in terms of a 2D Heisenberg model. From High temperature series expansion techniques, Lines [131] has shown that the position of χ_{max} should occur at a temperature comparable to the intraplanar exchange parameter $J_{||}$. Tranquada et al. [37] have shown that their T_M is very similar to the value of intraplanar exchange parameter estimated from the spin-wave dispersion measured in 2-1-4 by neutron-scattering experiments [43]. We will discuss some of these experiments in view of our theoretical results later in the chapter.

Here, we derive the expression of magnetic susceptibility by introducing the spectral function of spin waves in the theory that we have developed in the earlier chapters. This is a totally new approach, used by us for the first time to study the magnetic susceptibility and it's temperature dependence. We will extend the self-consistent theory developed in the earlier chapters and we will use the magnetization expression [cf. eqn.(5.8)] in the presence of an external magnetic field. The expressions for magnetic susceptibility are evaluated numerically and we will compare them with the experimental results.

6.2 Magnetic Susceptibility: A new method

We again use the quasi-two dimensional quantum Heisenberg antiferromagnet in the presence of an external magnetic field applied in the z-direction. We have the same hamiltonian as expressed in eqn.(5.1). We recall the expression for sublattice

magnetization given in Chapter V [cf. eqn.(5.7)], by

$$\begin{aligned} M_f &= \frac{\mu g}{2}\frac{1}{1+W} \\ W &= \frac{1}{N}\sum_q \left[\left(\frac{1}{e^{\beta E_{1q}}-1}+\frac{1}{e^{\beta E_{2q}}-1}\right) \right. \\ &\quad \left. + \frac{M_f - M_g}{\mu g}\frac{J_{\|}Z}{E_{1q}-E_{2q}}\left(\frac{1}{e^{\beta E_{1q}}-1}-\frac{1}{e^{\beta E_{2q}}-1}\right)\right] . \end{aligned} \tag{6.1}$$

The susceptibility is defined in the linear response theory as $\chi = \partial M/\partial B$ at B = 0. Differentiating eqn.(6.1) with respect to B, we get the following expression for the magnetic susceptibility

$$\chi = \frac{\beta(\mu g)^2 \frac{1}{N}\sum_q \frac{e^{\beta E_q}}{(e^{\beta E_q}-1)^2}}{(\mu g)^2/(2M(T))^2 + \beta J_{\|} Z \frac{1}{N}\sum_q \frac{e^{\beta E_q}}{(e^{\beta E_q}-1)^2}} , \tag{6.2}$$

for $T < T_N$, and

$$\chi = \frac{\beta}{4\frac{1}{N}\sum_q \frac{1}{(\mu g)^2 - \chi J_{\|} Z(1+\gamma_q)}} , \tag{6.3}$$

for $T > T_N$. For $T = T_N$, one finds from both equations that the magnetic susceptibility has the molecular field value, i.e.,

$$\chi = (\mu g)^2/(2J_{\|}Z) \tag{6.4}$$

These expressions for the sublattice magnetization and magnetic susceptibility, ie. eqns.(6.1-6.3), contain the summation over the momentum q. Now we would like to replace the q summation in terms of an integration over frequencies. We note that the expression inside the q summation is a function of γ_q^2 and E_q. Here E_q is given as a function of γ_q^2

$$\begin{aligned} E_q &= E_0\sqrt{1-\gamma_q^2} \\ E_0 &= M(T)J_{\|}Z/(\mu g) \end{aligned} \tag{6.5}$$

in the absence of the magnetic field. We denote the expression inside the q summation by $f(\gamma_q^2, E_q)$. Hence

$$\frac{1}{N}\sum_q f(\gamma_q^2, E_q) = \int_0^1 d\omega\ D(\omega) f(\omega^2, E_0\sqrt{1-\omega^2}) \tag{6.6}$$

where

$$D(\omega) = \frac{2}{N}\sum_q \delta(\omega - \gamma_q) = \frac{2}{\pi N}\sum_q\ Im\ \frac{1}{\omega - \gamma_q - i\delta} \tag{6.7}$$

We will discuss the properties of $D(\omega)$ at the end of this section. Now, if we change the integration variable in eqn.(6.6) from ω to $\sqrt{1-\omega^2}$, we have

$$\int_0^1 d\omega\ D(\omega) f(\omega^2, E(\omega)) = \int_0^1 d\omega\ \rho(\omega) f(1-\omega^2, E_0\omega) \tag{6.8}$$

where

$$\rho(\omega) = \omega\ D(\sqrt{1-\omega^2})/\sqrt{1-\omega^2}\ . \tag{6.9}$$

We call $\rho(\omega)$ as the spectral function of spin waves. In terms of this function, we can express the sublattice magnetization and magnetic susceptibility as follows

$$M(T) = \frac{\mu g/2}{\int_0^1 d\omega\ (\rho(\omega)/\omega)(1 + 2n_B(\omega E_0))} \tag{6.10}$$

- For $T < T_N$

$$\chi = \frac{\beta(\mu g)^2 \int_0^1 d\omega\ \rho(\omega)\frac{e^{\beta\omega E_0}}{(e^{\beta\omega E_0}-1)^2}}{(\mu g)^2/(2M(T))^2 + \beta J_{\|} Z \int_0^1 d\omega\ \rho(\omega)\frac{e^{\beta\omega E_0}}{(e^{\beta\omega E_0}-1)^2}} \tag{6.11}$$

- For $T > T_N$

$$\chi = \frac{\beta}{4(\mu g - \chi J_{\|} Z)[\int_0^1 d\omega\ \rho(\omega)/((\mu g)^2 - 2\chi\mu g J_{\|} Z + (\chi J_{\|} Z\omega)^2)\ ]} \tag{6.12}$$

Eqns.(6.10) and (6.12) constitute the nonlinear equations for M(T) and χ to be determined self-consistently. With M(T) the magnetic susceptibility in antiferromagnetic phase can be calculated from eqn.(6.11).

Evidently, for the first time, we have obtained relations for the magnetic susceptibility with the help of spectral function of spin waves. All our expressions for sublattice magnetization and magnetic susceptibility in the theoretical deliberations above, have $D(\omega)$ or $\rho(\omega)$. We will first discuss some of the properties of $D(\omega)$ and $\rho(\omega)$. The D function, which is given in eqn.(6.7) can be evaluated as following

$$D(\omega) = \frac{4(2+r)}{\pi^3} \int_0^{\pi/2} d\theta \;\; K(\sqrt{1-(\omega + r\omega/2 - r/2 + r\sin^2\theta)^2}) \,. \qquad (6.13)$$

by replacing summation over q by integration. Here K is the complete elliptic function of the first kind. D function is the diagonal element of the generalized Watson function. For the isotropic case (r=1), it has been studied in the context of lattice dynamics, ferromagnetism, and electron band in simple cubic lattice. D has been evaluated analytically by Joyce and Glasser[137]. For arbitrary value of r, the analytical expression for D is not known. But, it can be shown rather generally that D has two singularities at frequencies given by $r/(2+r)$ and $(2-r)/(2+r)$. These singularities are known as the Van Hove singularities.

The calculations have given us some insight into the behaviour of the D function. It is found that for r=0, ie for strictly 2D case, $D(\omega)$ diverges at $\omega = 0$. For values of ω below the first van Hove singularity ie. $\omega < r/(2+r)$, D is nearly a constant depending on r. But between these two van Hove singularities ie. $r/(2+r) < \omega < (2-r)/(2+r)$, it is a decreasing function of frequency. For $\omega \sim 1$, D behaves $\sqrt{1-\omega^2}$.

Now that we know the behaviour of the D function with the frequency ω, we can easily infer the spectral function of spin waves. We have already seen in eqn.(6.9) that the spectral function depends on the D function. For example, $\rho(\omega)$ is a quadratic function of frequency for very small frequency. It also suggests that $\rho(\omega)$ will have two singularities corresponding to the two van Hove singularities of the D function. These two singularities in the spectral function occur at frequencies given by $\omega_1 = \sqrt{1-(\frac{(2-r)}{(2+r)})^2}$ and $\omega_2 = \sqrt{1-(\frac{r}{(2+r)})^2}$. We have calculated the spectral function by eqn.(6.9) and eqn.(6.13) for the D function. We have indeed found that the two singularities do occur at the frequencies given above.

6.3 Comparison with Experiments

Let's first investigate the behaviour of the spectral function with frequency. In fig.(6.1), we have shown the weighted spectral function with the variation of frequency. Curves 1 and 2 correspond to $\rho(\omega)/\omega$ vs ω for $r = 1.0 \cdot 10^{-4}$ and $r = 1.0$ respectively. We find that the weighted spectral function is a linear function of frequency in both cases for relatively low frequencies. For the case of $r = 1.0 \cdot 10^{-4}$, the weighted spectral function is a linear function of frequency below ω_1. Above ω_1, it becomes nearly a constant over a wide range of frequency. However, as ω gets close to unity, $\rho(\omega)/\omega$ increases with frequency in the manner of $1/\sqrt{1-\omega^2}$.

We have calculated the magnetic susceptibility from eqns.(6.11) and (6.12) for $T < T_N$ and $T > T_N$ respectively. We found that the magnetic susceptibility normalized to the value at the Neel temperature as a function of temperature normalized to the Neel temperature depends only on r, independent of $J_{||}$. We have presented our calculations for $r = 1.0 \cdot 10^{-4}$ and $r = 1$ in figs.(6.2) and (6.3) respec-

tively. As can be seen from these figures, the magnetic susceptibility has a peak at the Neel temperature for both cases.

Our numerical calculations suggest to us that below the Neel temperature, the magnetic susceptibility is a linear function of temperature. Above the Neel temperature, the magnetic susceptibility decreases with the increment of temperature. The rate is lower for quasi-2D case than the 3D case. As a result, the peak for quasi-2D case is much broader than that for 3D case. At low temperature, the magnetic susceptibility is a T^2 function of temperature for 3D case. The magnetic susceptibility is a linear function of temperature for quasi-2D case. At very low temperature, there is a crossover to 3D behavior in the quasi-2D situation. But this happens at $\sim 2J_{||}\sqrt{2r}/k_B$, a very low temperature to be seen in fig.(6.2).

In fig.(6.4), we compare the magnetic susceptibility to the experimental measurements on La_2CuO_{4-y} compounds. The parameters used in the calculation for La_2CuO_{4-y}, $J_{||} = 780K$, $T_M = 1460K$, $\chi_M = 1.54 \cdot 10^{-4}\ cm^3/mole$, and the experimental data are taken from [39]. The ratio of the interplanar coupling to the intraplanar coupling is assumed to be $r = 1.0 \cdot 10^{-4}$. This gives $T_N = 195K$ and $\chi_N = 3.26 \cdot 10^{-4}\ cm^3/mole$. We have chosen $y = 2.3$ to fit the magnetic susceptibility data with our calculations in the high temperature limit. As can be seen, although our self-consistent calculation gives good results at high temperatures, there is considerable difference between our results and experiments near the temperature $2J_{||}/k_B$. At this temperature, the magnetic susceptibility is observed experimentally to have a maximum. The magnetic susceptibility peak is totally missed by our theoretical calculations.

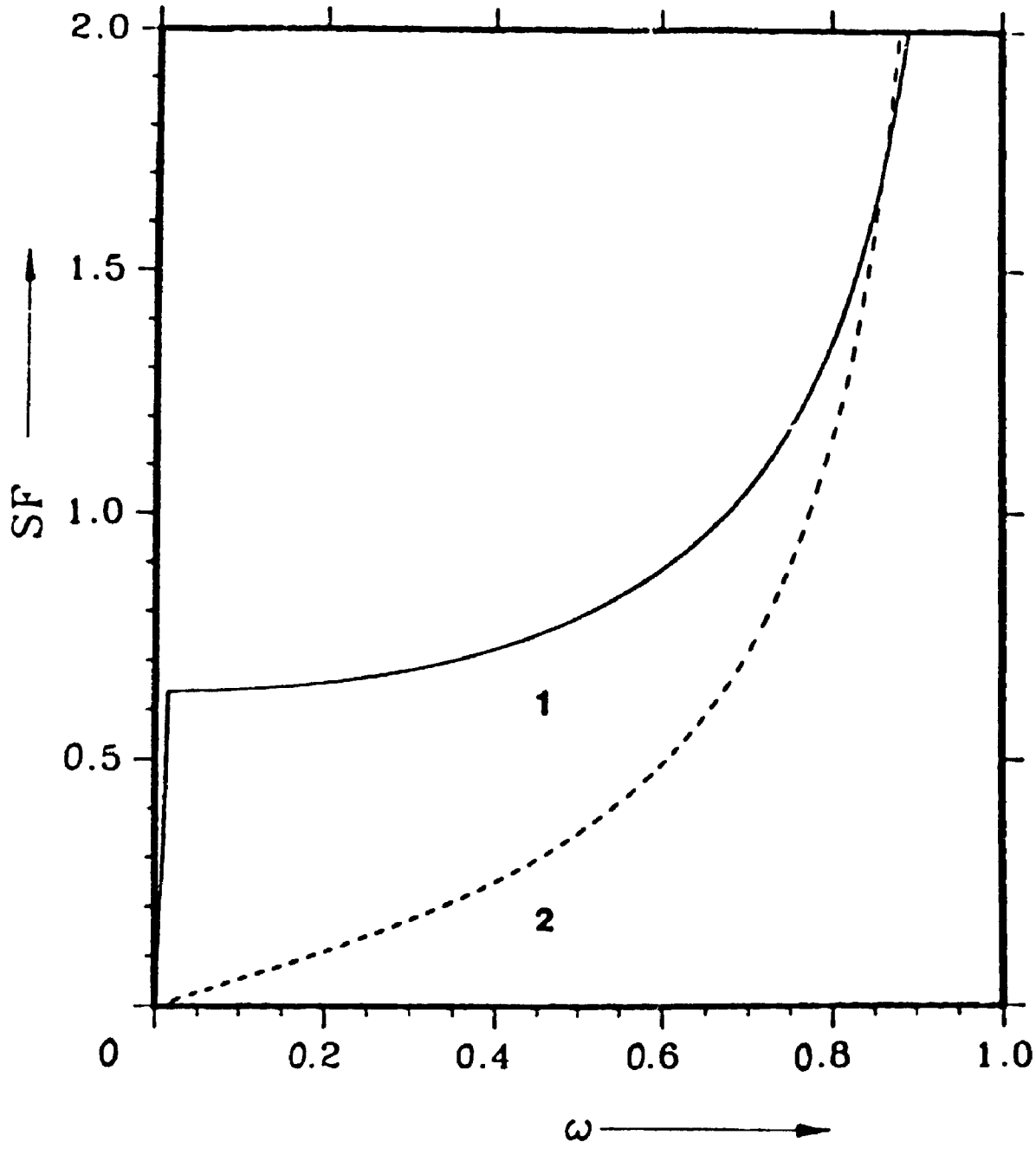

Figure 6.1: Variation of Weighted spectral function $\rho(\omega)/\omega$ as a function of frequency ω for quasi-2D and 3D antiferromagnets. Curve 1 and 2 are for 'r' = 1.00×10^{-4} and 'r' = 1.00 respectively.

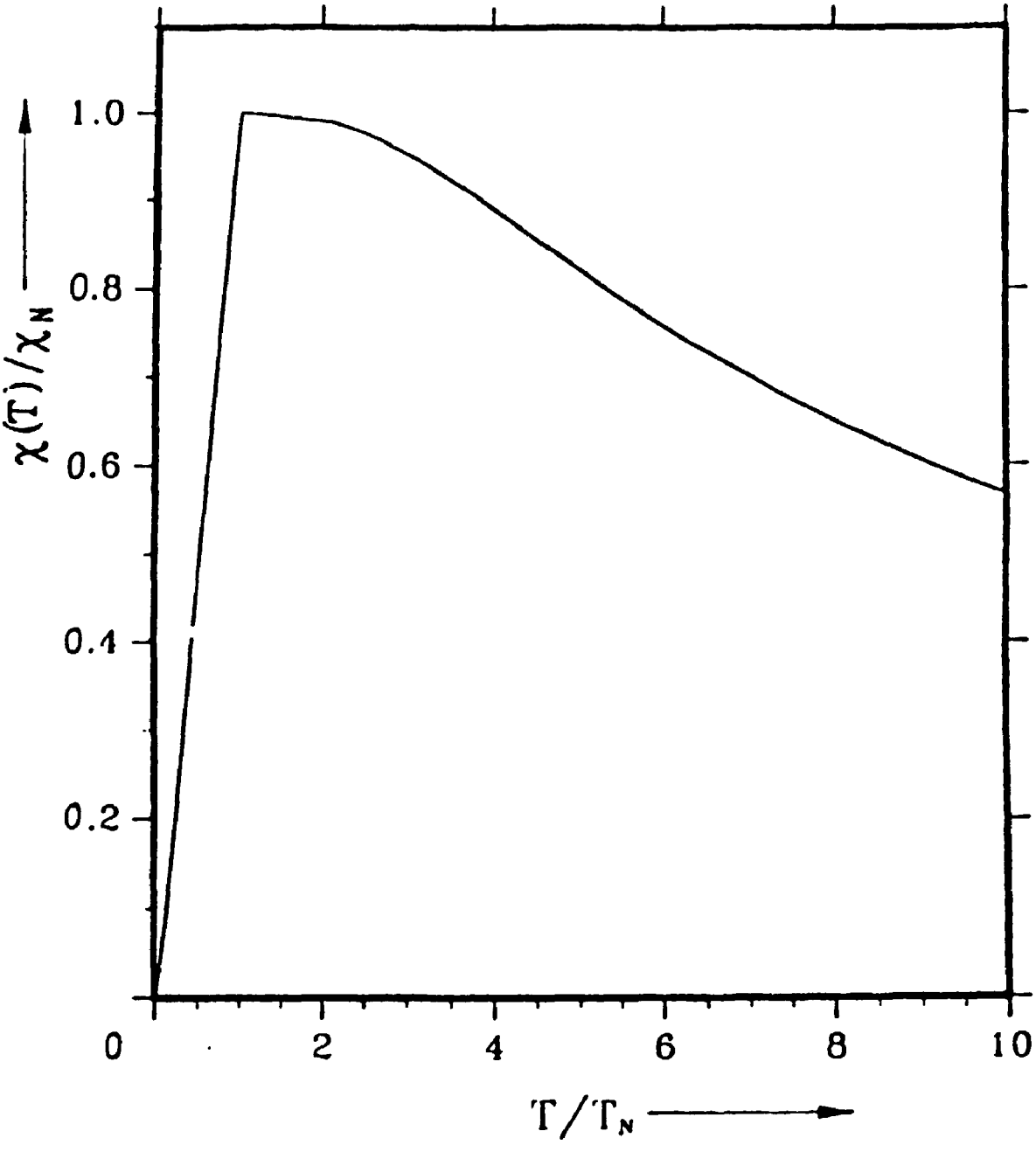

Figure 6.2: Variation ofχ/χ_N with T/T_N for quasi-2D antiferromagnet for 'r' = $1.00x10^{-4}$.

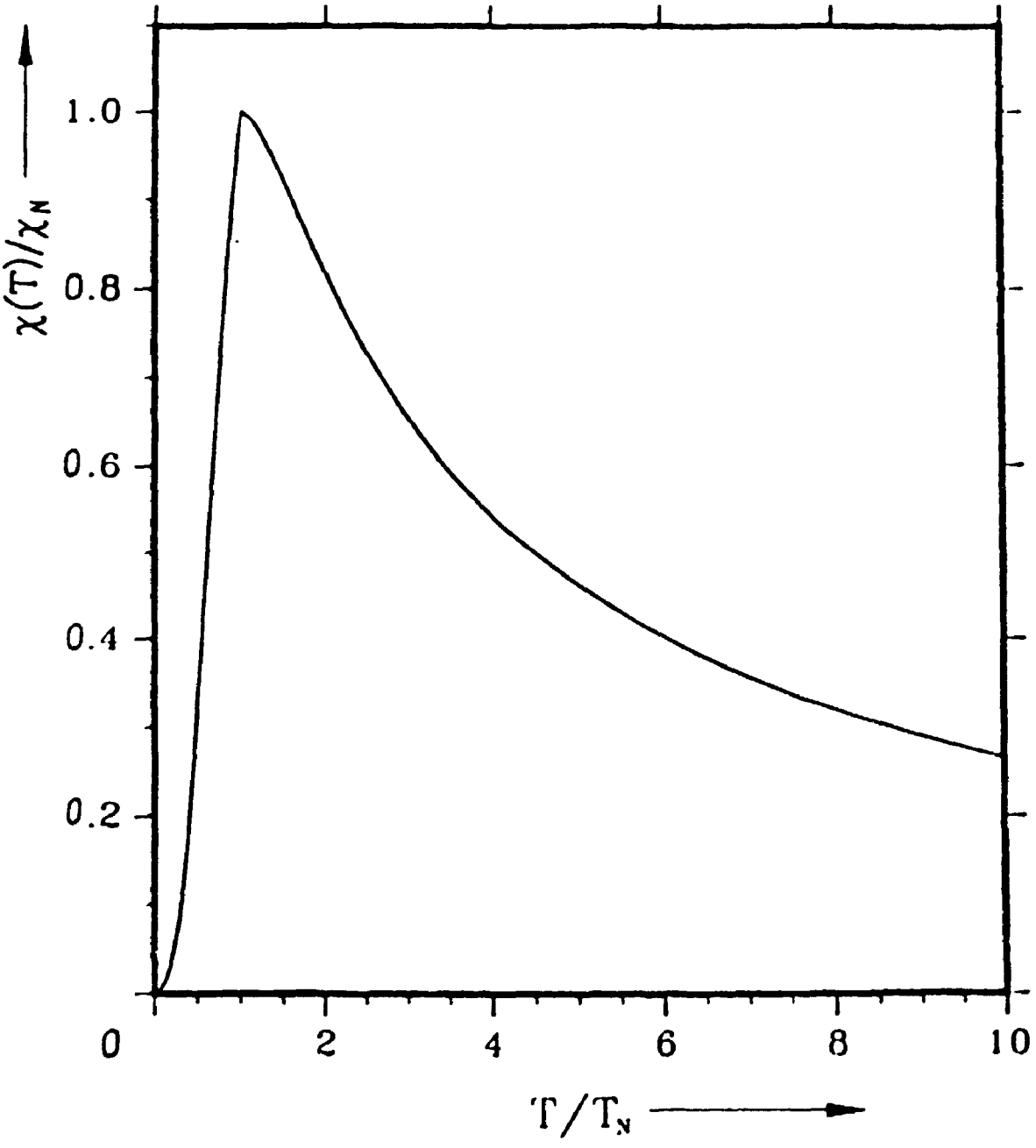

Figure 6.3: Variation ofχ/χ_N with T/T_N for 3D antiferromagnet for 'r' = 1.00

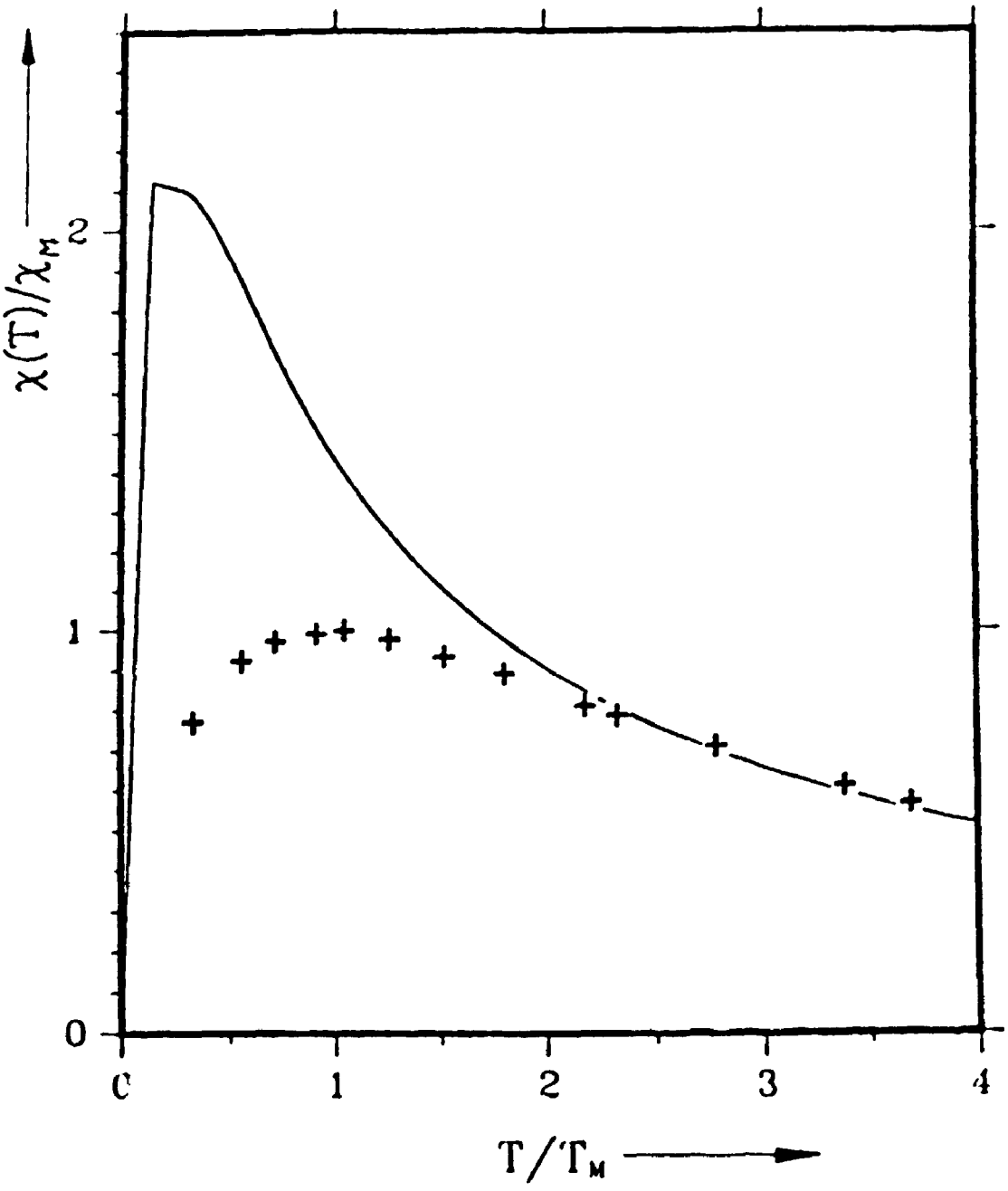

Figure 6.4: Variation ofχ/χ_M with T/T_M for quasi-2D antiferromagnet. The plus denotes the experimental data of Johnston[39] and the solid curve gives our calculation for 'r' = $1.00\text{x}10^{-4}$ and $J_{\|}$ = 780 K.

6.4 Results and Discussion

Our theoretical calculations show that the magnetic susceptibility has a maxima at the Neel temperature. These results are in agreement with those of Lines [131] who studied the temperature dependence of susceptibility in connection with K_2NiF_4. According to Lines, the maximum susceptibility should occur at a temperature comparable to the intraplanar coupling. Our results have shown that the magnetic susceptibility has a peak near the Neel temperature in case of both quasi-two dimensional and 3D cases. We recall, that the Neel temperature in the 3D case according to our theory is $T_N \sim 0.987 J_{\|}$. The startling similarities between our results and those of Lines arise due to similarity in K_2NiF_4 structure with copper oxides. The difference being, the localized spins have spin momentum 1 instead of 1/2 as is the case with copper oxides. For K_2NiF_4, Lines introduced an anisotropic field to stabilize the antiferromagnetic phase from thermal spin-wave fluctuations. Lines studied the sublattice magnetization and magnetic susceptibility as a function of temperature. The correspondence of the anisotropic field in the Lines approach can be made with the interplanar exchange coupling that we have used in our formulation.

We have obtained that the magnetic susceptibility in the direction perpendicular to the CuO_2 planes is independent of the temperature [cf. eqn.(6.4)]. This result is consistent with the results of Hewson et al.[133]. At the Neel temperature we have recovered the correct expression for the susceptibility ie. $\chi = (\mu g)^2/(2J_{\|}Z)$. This is the same expression which was obtained by Hewson et al. in RPA.

The theoretical results are then compared with the experimental results of Johnston [39] on $La_{1.8}Sr_{0.2}CuO_{4-y}$. Our theoretical results are shown to be in good agreement with the experimental results of Johnston [39] at high temperatures. At

low temperatures, however, our theory misses the susceptibility peak as found in 2-1-4 compounds. The reason for this apparent disagreement at low temperatures could be due to the presence of impurity contributions in the magnetic susceptibility data. We already know that the paramagnetic impurities that are present in the copper oxide superconductors affect the susceptibility at low temperatures. A susceptibility analysis of a impurity free sample has become a necessity to put to rest some of these disagreements. Another reason that could be affecting our theoretical results at low temperatures can be associated with the random phase approximation we have used. This approximation replaces the fluctuations in the z-component of spin by it's average value. But, in case of 1D and 2D systems these fluctuations near the phase transition can play very important role. Any future theory which includes these quantum fluctuations near the Neel temperature could improve upon the results we have achieved here.

6.5 Conclusions

In conclusion, we have shown in this chapter, that by using our self-consistent theory we were able to explain the magnetic susceptibility at high temperatures. We have found good agreement between our theory and experimental results of Johnston [39]. We should reiterate that the use of spectral function to calculate the magnetic susceptibility is a novel approach which hasn't been tried before. We have found that the magnetic susceptibility is a function of the ratio of inter to intraplanar couplings only. We have also found an apparent disagreement between our theoretical results and the experimental results at low temperatures. This disagreement can be resolved if susceptibility data on impurity free sample is made available. Our theory calls for such an experimental study.

Chapter 7

Study of crossover in Oxide Superconductors *

In the last chapter we studied the susceptibility of oxide superconductors in the antiferromagnetic phase. In this chapter we will study the crossover behaviour. The magnetic properties in these HTS show crossover both with the variation of temperature and the ratio of inter to intraplanar couplings. We will deal with both of these crossover properties in this chapter. We will call these as T-dependent and r-dependent crossover respectively.

7.1 Introduction

The study of dimensional crossover has received much attention recently [74, 119, 142, 143, 144, 140]. It was found that when the interlayer coupling is weak the physical properties in the normal state undergo a dimensional crossover (r-dependent) at low enough temperatures.

The quasi-two dimensional picture of layered antiferromagnets has been the

*The results of this chapter has been published in Physica Status Solidi (b) 179, 187, 1993

subject of some interest recently. An anisotropic quantum Heisenberg model has been used to describe the magnetic dynamics of these systems. Even most of the experimental results are explained on the basis of such a model, for ex. Neutron scattering experiments are usually explained by taking the free-spin wave approximation on an anisotropic Heisenberg model. Such deliberations have resulted in estimation of the anisotropy parameter of 10^{-5}- 10^{-4} in case of 2-1-4 [76]. Pure two dimensional character of magnetic excitation were used to find a scaling relation of Neel temperature with the anisotropy parameter [36]. An estimate of $r = J_{\perp}/J_{||} = 10^{-5}$ was obtained. Free spin wave results estimate a value of 10^{-4} for the anisotropy parameter, however, the approximation is not valid for T$\cong T_N$. Recently, efforts have been made to explain the magnetic properties of 2-1-4 including a weak XY anisotropy and the interlayer coupling. The predictions are quite consistent with the experimental results up to a temperature where the critical fluctuations become important. For 2-1-4, above 270K the results from such a study overshoots [114]. Some of these results have suggested that the magnetic properties in the normal state have a very crucial dependence over the anisotropy ratio and as it changes the magnetic properties show a crossover from quasi-two dimensional to three dimensional behaviour.

The magnetic properties also depend crucially on the temperature. We have already seen in chapter VI that at low enough temperatures the magnetic susceptibility undergoes change in temperature behaviour from T^2 to linear dependence which is a signature of crossover from 3D to quasi-2D behaviour. There are reports that the behaviour of sublattice magnetization too changes from T^2 to T ln T[119] and the specific heat from T^3 to T^2 with the increase of temperature which corresponds to 3-dimensional and quasi-2D behaviour respectively. It has also been found

that the critical exponent of sublattice magnetization near the Neel temperature is somewhere near 1/2[142]. Most of these results have found experimental approval too[143, 144, 140]. We will show in this chapter that our theoretical results of sublattice magnetization also show a crossover behaviour at a critical temperature.

Here, we will study the T-dependent and dimensional crossover from 3D to quasi-2D character in magnetic properties of Layered Antiferromagnets such as La_2CuO_4 (2-1-4). We have used the self-consistent theory for quasi-two dimensional antiferromagnets to study the effect of changing anisotropy on the magnetic properties. We show with the help of this self-consistent theory that the crossover occurs as the value of dimensional anisotropy parameter ($\frac{J_c}{J_{ab}}$) changes from $\sim 10^{-3}$, where J_{ab} and J_c are defined as $2J_{||}$ and $2J_{\perp}$ respectively. For the T-dependent case we have shown that the magnetization shows a crossover near the temperature ($\sim 2J_{||}\sqrt{2r}/k_B$). We have obtained numerical results for sublattice magnetization and it's crossover properties and have compared it with other theoretical results.

7.2 Numerical results

We have used the expressions obtained in the earlier chapters to study the crossover behaviour in 2-1-4 compounds. The expressions for magnetization are taken from eqn. (5.9) and (5.12) from Chapter V and eqn. (6.10) from Chapter VI. Eqn.(5.12) is the magnetization expression in the spin-wave approximation. We will use this equation to compare the self-consistent results with the spin-wave theory. Here, we have defined the anisotropy parameter (δ) as J_c/J_{ab}.

Fig.(7.1) shows the numerical evaluation of eqn.(5.9) for 2-1-4 (r =2.0 x 10^{-4}; J_{ab}=0.130eV). We have plotted the variation of normalized sublattice magnetization

with temperature along with the experimental results. We have fitted the experimental results[114] by choosing proper values of the anisotropy constant and the intralayer exchange coupling constant for 2-1-4. Same parameters are used for both self-consistent evaluation and FSW approximation. We find very good agreement between the theoretical predictions and the experimental data for $T \sim T_N$. As we approach T_N, both the self-consistent and FSW approximations overshoot. It is interesting to see that self-consistent calculations are still quite good as compared to FSW. Hereafter, it should be noted, that we have represented the z-component of the spin at an arbitrary temperature 'T' by the notation M(T) while at zero temperature as M(0).

In fig.(7.2), we show the crossover from 3D to quasi-2D behaviour by calculating the variation of the magnetic moment vs. ratio of inter to intraplanar coupling constant. It is shown that there is appreciable difference between the ordered moment for 3D and 2D limits in self-consistent and FSW theory at $T\sim 0$. The ordered moment for the self-consistent theory saturates at a quasi-2D value of ~ 0.718 while in case of FSW it saturates at 0.606. The crossover region appears to be near 'ln(1/r) = 6.0' which would correspond to a critical anisotropy ratio $\delta = 10^{-3}$. Above this critical value of anisotropy constant there is negligible change in the ordered moment. The difference in these two approximations can be attributed to the inherent self-consistency in our theory. It is worth noting that the ratio of inter to intraplanar coupling constants that we have used in this paper is different from the anisotropy ratio used by others[†]

Fig.(7.3) shows that for a quasi two dimensional system $0 < r < 1$ at $T\sim 0$

[†]It should be borne in mind that the ratio of interplanar to intraplanar coupling 'r' that we have used here is approximately equal to r^2 used by other authors viz. Ref.[76]. This is due to the fact that in our formulation $J_{ab} = 2J_{\parallel}$ and $J_c = 2J_{\perp}$.

the difference in the ordered moment is quite pronounced for RPA and FSW. We show the variation of ordered moment 2 M(T) vs. T for self-consistent and FSW theory near the crossover anisotropy value of 10^{-3} and J_{ab}= 0.120eV. Again, near the Neel temperature, the FSW theory falls apart.

For the T-dependent crossover characteristics of magnetization, we have used the spectral function of spin waves to calculate the sublattice magnetization as a function of temperature from eqn.(6.10). To appreciate the role of the interplanar coupling on the sublattice magnetization, we show that the sublattice magnetization as a function of temperature for $r = 1.0 \cdot 10^{-4}$ and $r = 1$ in Figs.(7.4) and (7.5) respectively. We have calculated sublattice magnetization as a function of temperature and found that it depends only on r, independent of the absolute value of $J_{||}$.

We have studied the crossover behaviour of the magnetic properties as a function of temperature. In figs.(7.4) and (7.5), the shape of the magnetization vs. temperature curve changes drastically from 3D behaviour to quasi-two dimensional behaviour. This was found to occur near the temperature $J_{||}Z\omega_1/2k_B \sim 2J_{||}\sqrt{2r}/k_B$, where $J_{||}$ is the intraplanar coupling constant and 'r' is the anisotropy ratio ($=J_\perp/J_{||}$). This is in agreement with AS results [76] who have on the basis of a perturbative calculation shown that the sublattice magnetization has a crossover from 3D (T^2) behaviour to quasi-2D behaviour (TlnT) at a temperature close to $2Jr/k_B$.

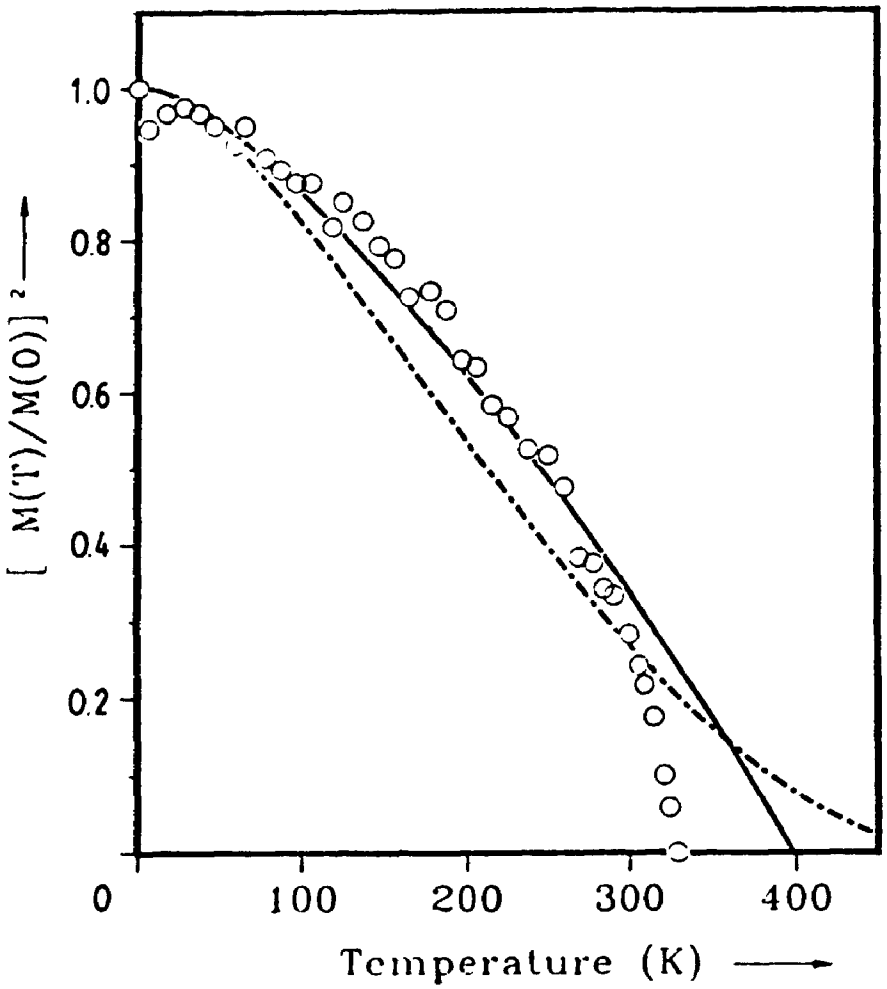

Figure 7.1: Variation of normalized sublattice magnetization with temperature for La_2CuO_4 with J_{ab}=0.130 eV and r=2.0 x 10^{-4} for both self-consistent RPA (solid line) and FSW (dashed) and experimental results on 2-1-4 shown by open circles.

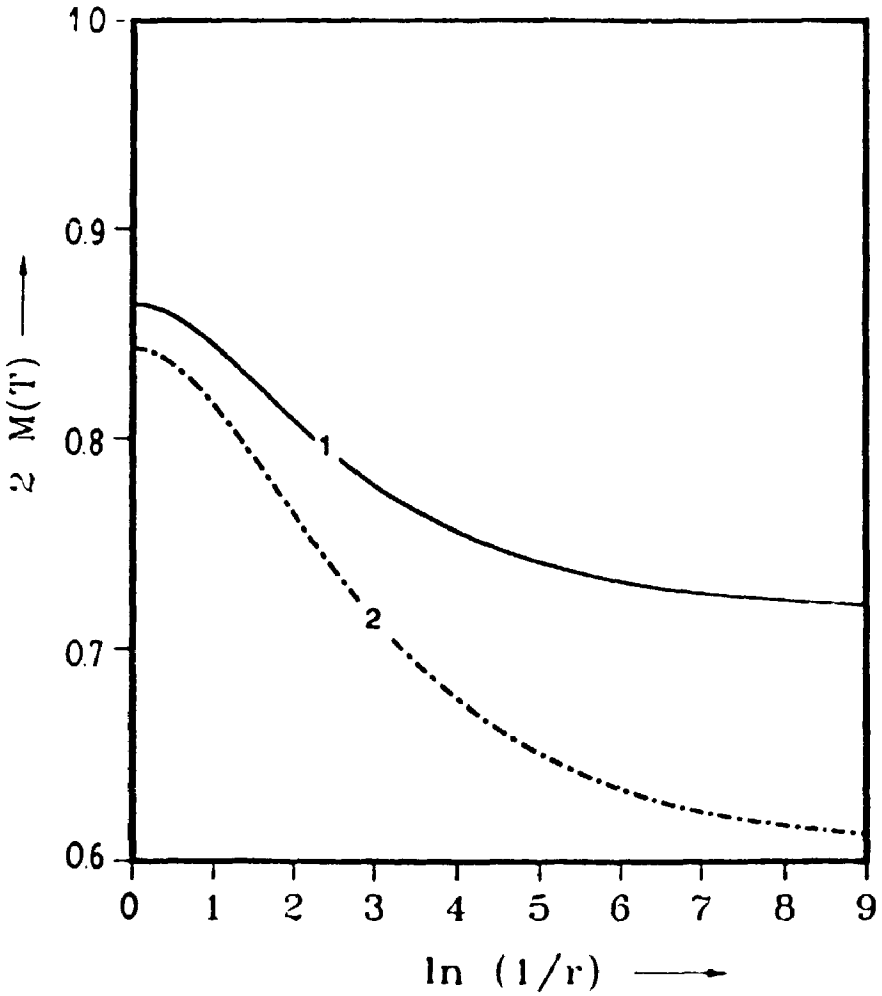

Figure 7.2: Variation of Local Magnetic moment 2M(T) vs. ln(1/r) for both self-consistent RPA (solid line) and FSW approximations (dashed).

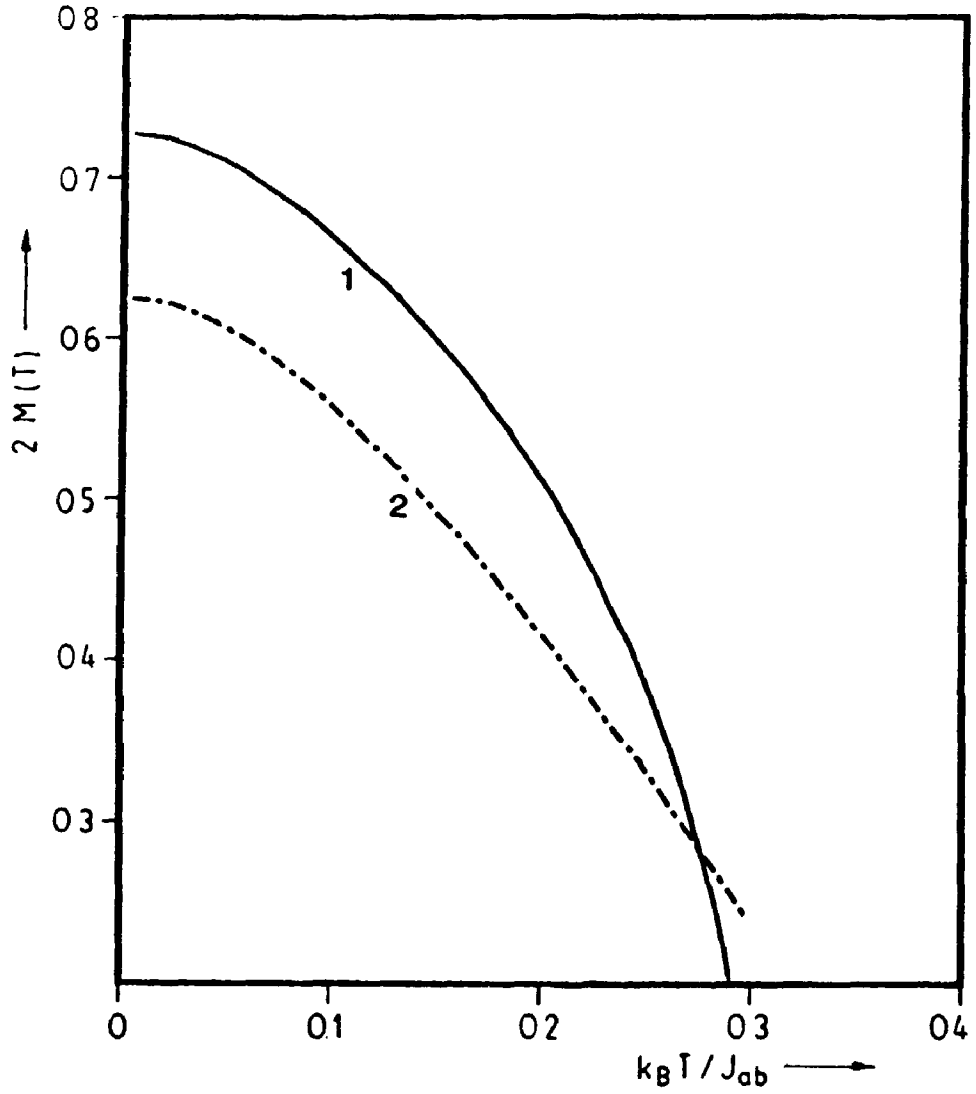

Figure 7.3: Variation of ordered moment 2M(T) vs. temperature for both self-consistent RPA (solid line) and FSW approximations (dashed).

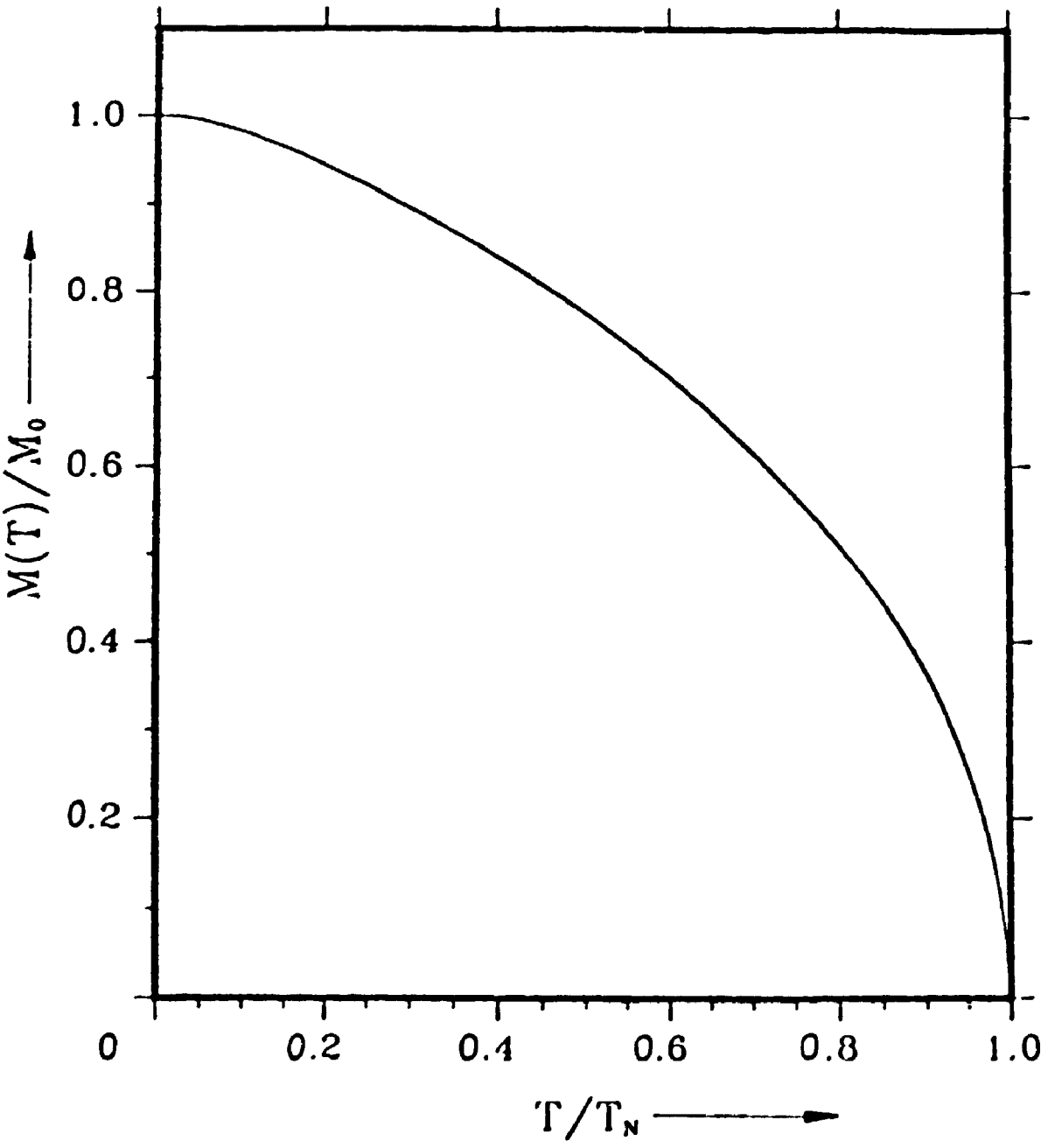

Figure 7.4: Variation of M(T)/M(0) with T/T_N for quasi-2D antiferromagnet for 'r' = 1.00×10^{-4}.

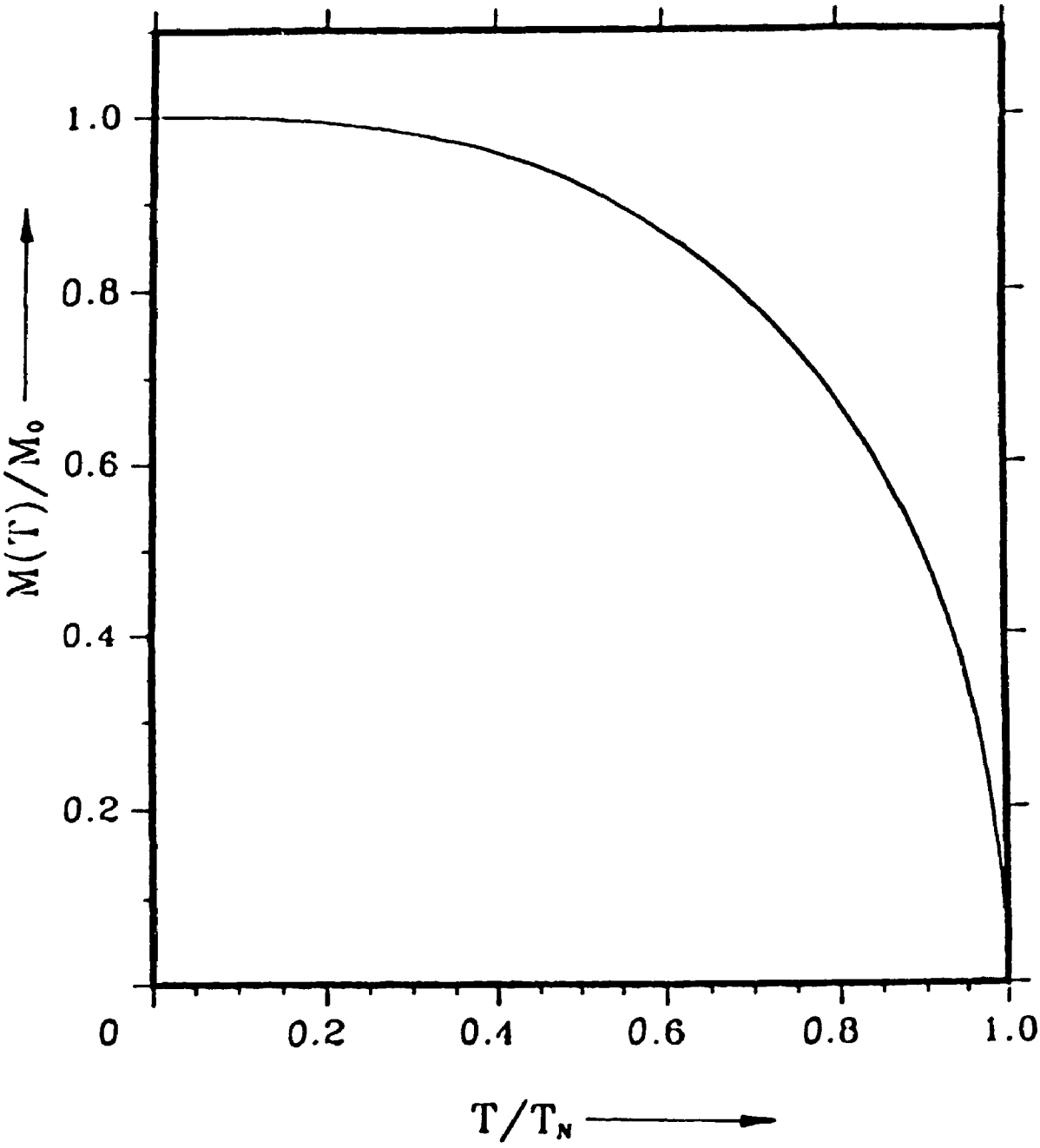

Figure 7.5: Variation of M(T)/M(0) with T/T_N for 3D antiferromagnet for 'r' = 1.00

As the value of r decreases, the shape of $M(T)/M(0) - T/T_N$ changes drastically from 3D behavior to quasi-2D behavior. The behavior of the sublattice magnetization as a function of temperature near the Neel temperature, however, is the same for 3D case and for 2D case. In both cases, near the Neel temperature, the sublattice magnetization exhibits a square root of temperature behavior. These results agree with the numerical calculations performed in Chapter V. Also, such a temperature behaviour has been observed by ^{111}In PAC experiment of Hohenemser et al. [140] and the recent Schwinger boson analysis of Kopietz [119].

7.3 Results and Discussion

We have shown the variation of the magnetic moment [2M(T)] with the anisotropy parameter in fig.(7.2). It clearly indicates the crossover from 3D to 2D behaviour. It demonstrates that in the self-consistent theory the crossover has been exhausted at r= 10^{-6}, which corresponds to an anisotropy parameter of $\delta = 10^{-3}$. Further increase in the value of the anisotropy parameter doesn't affect the moment. The same behaviour was found in the FSW theory, although the value of the moment is much less. Majlis et al. [74] have shown that in RPA, MRPA and FSW the value of moment is indeed different. They also found that the sublattice magnetic moment converges to it's two dimensional value for $\epsilon \cong 10^{-3}$ in both RPA and MRPA, while that same value is obtained in FSW theory for $\epsilon \cong 10^{-1}$ [74]. These results are consistent with our results of anisotropy parameter. The crossover from 3D to quasi-2D behaviour for sublattice magnetization suggests that the critical anisotropy ratio is indeed $\sim 10^{-3}$. We have also shown that the estimate for the Neel temperature obtained from such a calculation agrees very well with the experimental results while those obtained from the FSW theory overestimates.

We have shown in fig.(7.3) that as the temperature is increased or when the system is between the 2-D and three dimensional extremes, differences show up in the values of magnetic moment obtained from both the self-consistent theory and the free-spin wave theory. However, once the anisotropy parameter becomes sufficiently small the magnetic moment doesn't change much.

These theoretical results suggest to us that apart from the Neel temperature that has to scale to zero as r $\rightarrow$ 0, other magnetic properties like the magnetic moment saturate to their two dimensional values at a critical anisotropy parameter. It is also found that the value of these magnetic properties depend crucially on the approximation chosen. Our study thus concludes that in order to extract crucial information about the values of some of the macroscopic parameters of anisotropic antiferromagnets, simple minded use of the linear spin wave theory is inadequate. The comparisons of our theoretical results with experiments have shown that this self-consistent theory gives much better results for anisotropic antiferromagnets like 1-2-3 and 2-1-4.

AS [76] have demonstrated that the temperature dependence of sublattice magnetization contains crucial information about the thermal excitations of spin waves in anisotropic antiferromagnets. They identified two energy scales viz. 'J' and 'Jr' where 'J' and 'Jr^2' are the intraplanar and interplanar exchange coupling respectively. This temperature dependence of sublattice magnetization revealed that there is a crossover from 3D to quasi-2D with temperature characteristics of T^2 (3D) to T ln T (quasi-2D) near the transition temperature $\sim 2Jr/k_B$. However, such perturbative calculations that are used by AS are only valid at low temperatures. We also found this crossover in the magnetic properties but the temperature dependence was found to be square root of temperature.

In a recent letter Kopietz [119] has shown that if the magnetization is close to its zero temperature value M_0, T ln T is a fairly accurate approximation, however, as one moves towards the Neel temperature, this law clearly breaks down. By means of a Schwinger-Boson approach they have shown that for temperatures close to the Neel temperature, the staggered magnetization is proportional to $(1 - T/T_N)^{1/2}$. Our theory also gives a similar square root behaviour.

According to Kopietz, the value of β is a manifestation of the dimensional crossover between two and three dimensionality and should be observed in the temperature regime $1 \gg 1 - T/T_N \gg$ r. The parameter r is the ratio of the interplanar to intraplanar exchange coupling constant. They have reiterated that a value of 0.5 for β would give an affirmation to the notion that the Heisenberg model is the realistic model for La_2CuO_4. These results were initially supported experimentally by Perturbed Angular correlation measurements (PAC).

Very recently, even this observation has come under severe scrutiny with different results. Peter Imbert et al. [122] have concluded from their ^{57}Fe Mossbauer measurements that the value of mean-field exponent $\beta = \frac{1}{2}$ is in fact fictitious and is much bigger than the real local value. A different set of PAC measurements [123] do not support the dependence put forth by Kopietz either. The results of Imbert et al. though do not challenge the correctness of Kopietz theoretical model but at the same time give birth to the notion that the inhomogeneities in the sample of 2-1-4 make them a bad example of quasi-two dimensional Heisenberg model with nearest neighbour interactions [119].

In spite of all this controversy surrounding the dependence of magnetization over temperature, a definitive and conclusive experimental determination of the

mean-field exponent is still not available. It has to be noted here that even the ^{57}Fe Mossbauer results of Imbert et al. are not considered totally reliable. Arguments have been put forward against Mossbauer spectroscopic data by Rosov [124] and the scientific community has yet to come up to a consensus regarding the experimental procedure that gives the most accurate information. In light of the information now available on 2-1-4 like the reduced zero temperature moment M(0) compared to the mean-field value the criticisms of Rosov will have to wait for more experimental results to clarify these apparent discrepancies. The relative merits of local probes like MES and μSR versus the neutron diffraction in determining M(T) is an old debate and the scientific community is still waiting for the last word about this subject.

We have shown here with the general use of the spectral function of spin waves that the variation of sublattice magnetization versus temperature is a function of the ratio of the interplanar to the intraplanar coupling constant. We have deduced from the characteristics of the figs.(7.4) and (7.5) that the sublattice magnetization has a square root of temperature dependence near the Neel temperature. As already mentioned in Chapter III, this result is quite consistent with the recent PAC experiments and theoretical predictions of Kopietz that we have discussed above [119, 140]. In light of the recent controversies involving the authenticity of the ^{111}In PAC experiments of Hohenemser et al. it is difficult to pass judgements about the criticisms of Imbert et al[122]. However, the results obtained from this self-consistent theory are in agreement with the Schwinger-Boson Mean field approach. It will take some time and some careful experiments for a clear picture to emerge.

Our analysis here, suggests that for sublattice magnetization close to the

saturation value of M(0), Tln T could be a good approximation but as the value of M(T)/M(0) deviates significantly from unity, the ordering transition has to be described by a Mean-field nature and the dependence should be square root of temperature. We have also deduced from our results that the sublattice magnetization, at a low temperature shows a crossover from 3D behaviour to quasi-2D behaviour. The temperature at which this crossover happens is found to be in the vicinity of $J_{\|} Z\omega_1/2k_B \sim 2J_{\|}\sqrt{2r}/k_B$.

7.4 Conclusions

In conclusion, we have shown here that the ordered moment for 2-1-4 systems are well described within a framework of self-consistent theory rather in FSW. We have also shown that there is a dimensional crossover from 3D to quasi-2D behaviour in the magnetic properties of 2-1-4 compounds at a critical value of anisotropy parameter $\sim 10^{-3}$. We have also shown that our theoretical results are in good agreement with the experimental results. The T-dependent crossover has been a subject of recent controversies discussed above. However, our square root of temperature behaviour for the sublattice magnetization has been observed experimentally and the crossover temperature of $\sim J_{\|} Z\omega_1/2k_B \sim 2J_{\|}\sqrt{2r}/k_B$ has also been evaluated within the spin-wave approximation. In the next chapter, we will study the magnetic correlation length and will study the variation of it with the ratio of inter to intralayer couplings.

Chapter 8

Magnetic Correlation Length

In the previous chapter we saw that the magnetic properties undergo a dimensional and T-dependent crossover from 3-dimensional behaviour to quasi-two dimensional behaviour. Sofar, we have evaluated some important magnetic properties on the basis of our self-consistent approach and have shown that these results are in good agreement with the experimental results. Lately, magnetic correlation length has been the subject of much attention. The theoretical efforts to explain these experimental results for correlation length in the 2-1-4 compounds has only met with partial success. In this chapter, therefore, we will use our self-consistent theory to calculate the magnetic correlation length and will compare our theoretical results with the experimental results.

8.1 Introduction

We have already explained in Chapter III, about the manner in which the information about the magnetic correlation length can be obtained from the Neutron scattering. We have also mentioned about some of the experiments that have been

performed to extract information about the magnetic correlation length. Neutron scattering experiments have shown that the magnetic correlation length decreases as the temperature is increased [17, 15, 114, 61]. Keimer et al.[114] have studied the correlation length or 2-1-4 in the doping range $0 \leq x \leq 0.04$ [114]. They have also found identical results.

Ever since these experiments were performed various groups have tried to fit these experimental results with their theoretical models[63, 74, 67]. Chakravarty et al. [67] have calculated the temperature dependence of the magnetic correlation length of spin-1/2 Heisenberg antiferromagnet by the renormalized group analysis of the Quantum non-linear sigma model. Their theory gives good fit for the experimental data in case of undoped compounds. They have used two fitting parameters. Birgeneau et al. [61] have shown that the correlation length is limited by the average hole distance, namely, $\xi(x) \cong 3.8\mathring{A}/\sqrt{(x)}$. They have shown that a tiny amount of hole concentration is enough to limit the correlation length [61].

It was soon confirmed that even a small amount of excess holes in 2-1-4 can alter the magnetic correlation length to a large extent [61]. Hence, the theory of Chakravarty et al. could not explain the experiments for doped cuprates. This theory was later modified by doing an exact analytic calculation including the first order corrections in temperature by Hasenfratz and Neidermayer and others [148, 149, 150].

Manousakis [63] has obtained the magnetic correlation length by a direct simulation of the quantum nonlinear σ model. The fitting to the experimental results is achieved by varying the values of both the interplanar and intraplanar couplings separately. The experimental results of Endoh et al. is fitted by choosing

different values of J for different samples of 2-1-4. Manousakis has also pointed out that samples with higher Neel temperature give different values of correlation length [63].

Numerical simulations of the nearest neighbour spin-1/2 quantum Heisenberg antiferromagnet at low temperatures, has been considerably improved by the work of Ding and Makivic. They have obtained the correlation length via a large scale Monte Carlo simulation on latices up to 128x128. They have, in their simulations, reached temperatures as low as J/4. Their fits to the neutron scattering data has provided an estimate of J = 1450± 30 K [147]. Green's function methods are used by Majlis et al. recently to fit the experimental results of magnetic correlation length for doped and undoped samples of 2-1-4.

We have calculated the magnetic correlation length for 2-1-4 samples using our self-consistent theory, in this chapter. We have followed the method used by Majlis et al. to obtain expression the magnetic correlation length. Our expression has the advantage of being more accurate than the mean-field expression and also it is a sole function of the ratio of inter to intraplanar coupling. This expression, hence, can be used to provide us with crucial dependence of magnetic correlation length with doping. an expression for the magnetic correlation length and will then compare our numerical results with the available experiments.

8.2 Theoretical formulation

We have borrowed some of the expressions already derived under the premises of self-consistent theory in Chapter IV to find an expression for the magnetic correlation length. The correlation length is achieved by the asymptotic form of the

instantaneous spin correlation function $< S_i^+(t)S_j^-(t') >$. We have already calculated the correlation function in the absence and in the presence of the magnetic field in Chapters IV and V respectively. We will follow the method of Majlis et al.[74] and Yablonskiy [73] to derive the expression for the magnetic correlation length. The Fourier transform of the spin correlation function at t=t' is written as

$$< S_i^+ S_j^- >= \frac{T}{T_N}\frac{1}{N}\sum_q{}' \frac{e^{iq\cdot(R_i-R_j)}}{1-\delta_r(q)^2} \tag{8.1}$$

where

$$\delta_r(q) = \frac{z_{||}\delta_{||}(q) + rz_\perp\delta_\perp(q)}{z_{||}+rz_\perp} \tag{8.2}$$

$$\begin{aligned}\delta_{||}(q) &= \frac{1}{z_{||}}\sum_{\delta_{||}} e^{iq\cdot\delta_{||}} \\ \delta_\perp(q) &= \frac{1}{z_\perp}\sum_{\delta_\perp} e^{iq\cdot\delta_\perp}\end{aligned}$$

The dominant contribution to this correlation function comes from the $|R_i - R_j| \rightarrow \infty$ and in the neighbourhood of q=0. We can hence write

$$\begin{aligned}< S_i^+ S_j^- > \;\cong\; & \frac{T}{T_N}\frac{\delta_{||}^2\delta_\perp}{\pi^2}\int_0^{r_{ab}} q_{||}J_0(q_{||}R_{||})dq_{||} \\ & \int_0^{r_c}\left[\frac{A}{2}q_{||}^2\delta_{||}^2 + Bq_\perp^2\delta_\perp^2\right]^{-1} dq_\perp\end{aligned} \tag{8.3}$$

where, $J_0(z)$ is the Bessel function of zero order r_{ab} and r_c are the cutoff parameters. $R_{||} = |R_i - R_j|$ for i and j belonging to the same basal plane. The constants A and B are defined as $A = z_{||}/(z_{||}+rz_\perp)$ and $B = rz_\perp/(z_{||}+rz_\perp)$. We can change the integration variables by introducing at this point $\xi = \sqrt{A/2}q_{||}\delta_{||}$ and $\zeta = \sqrt{B}q_\perp\delta_\perp$. By doing this the above expression comes out to be [74]

$$< S_i^+ S_j^- > \cong \frac{T}{T_N}\frac{2}{\pi^2}\frac{1}{A\sqrt{B}}\int_0^{r'_{ab}} \frac{\xi J_0(\sqrt{2/A}\xi R_{||}/\delta_{||})}{\xi}\tan^{-1}\left[\frac{\sqrt{B}\delta_\perp r_c}{\xi}\right]d\xi \tag{8.4}$$

There can only be two extreme cases when the argument of $\tan^{-1}$ is either (a) very large or (b) very small. In conditions like this one gets

$$< S_i^+ S_j^- > \cong \frac{T}{T_N}\frac{2}{\pi^2}\frac{1}{A\sqrt{B}} \begin{cases} \frac{\pi}{2}\left[\frac{A}{2}\right]^{1/2}\frac{\delta_\parallel}{R_\parallel}e^{-R_\parallel/\xi_c} & \text{(a)} \\ \sqrt{B}\delta_\perp r_c K_0(R_\parallel/\xi_c) & \text{(b)} \end{cases} \tag{8.5}$$

here, $K_0(z)$ is the modified Bessel function of zero order which for large argument z behaves as $K_0(z) \sim \sqrt{\pi/2z}e^{-z}$. We can see that we have obtained the same exponential decay of the correlation function in both the extremities and hence can identify ξ_c as the *correlation length* for all values of T and r. Hence, the correlation length in the self-consistent theory is given by

$$\xi_c \cong C \exp\left[\frac{D\,T_N(r)}{T}\right] \tag{8.6}$$

where C = $r_{ab}/4\sqrt{2}$ and D = $\gamma\,\pi/2$. Here, γ is a constant. The expression for the Neel temperature is given by eqn.(4.28) and it is a function of the doping parameter. Once the value of Neel temperature is obtained at a specific value of the interplanar to intraplanar coupling ratio we can easily find the correlation length by choosing proper values for the parameters C and D. This equation also suggests a novel way to calculate the dependence of doping on the magnetic correlation length. Once we have obtained the values of constants C and D we can plot the variation of correlation length by varying the Neel temperature with r.

8.3 Results and Discussion

We have calculated the magnetic correlation length for the undoped and doped samples of 2-1-4 compounds. Fig.(8.1) shows the variation of the inverse magnetic correlation length for doped and undoped samples of 2-1-4. The stars and solid

squares represent the experimental results of undoped ($T_N = 325K$) and doped ($T_N = 190K$) samples of 2-1-4 obtained from neutron scattering experiments of Keimer et al[114].

The curves in fig.(8.1) show the theoretical results obtained from the self-consistent theory. We have chosen C such that it is close to the value calculated above ie. $r_{ab}/4\sqrt{2}$ and have varied D to obtain good agreement with experimental results. For the doped sample, reasonable agreement with the experimental results have given a value for C=1.27 and D=8.909 while for the undoped sample C=1.67 and D=5.62. It is obvious from the figure that the self-consistent theory gives excellent fitting to the experimental data of Keimer et al. Our parameters are very close to the ones obtained from Monte Carlo studies of Ding and Makivic [147].

In fig. (8.2), we have shown the variation of the inverse magnetic correlation length with the ratio of interplanar to intraplanar couplings. We have, for the same values of C and D obtained in fig.(8.1), varied the Neel temperature with the ratio of inter to intraplanar couplings. This gives us an indication that the magnetic correlation length increases with the increase of the interlayer couplings between the two dimensional planes in 2-1-4 compounds. It has to be kept in mind, that a doping dependent correlation length can be obtained from this expression since we have already established in Chapter IV that this ratio depends almost linearly with the doping. We couldn't find the experimental results of the correlation length measurements for 1-2-3 compounds to compare with our theoretical results.

Recently, various groups have used different methods to find the magnetic correlation length. Chakravarty et al. have found in the renormalization group approach on a quantum non-linear sigma model, that to the first order the magnetic

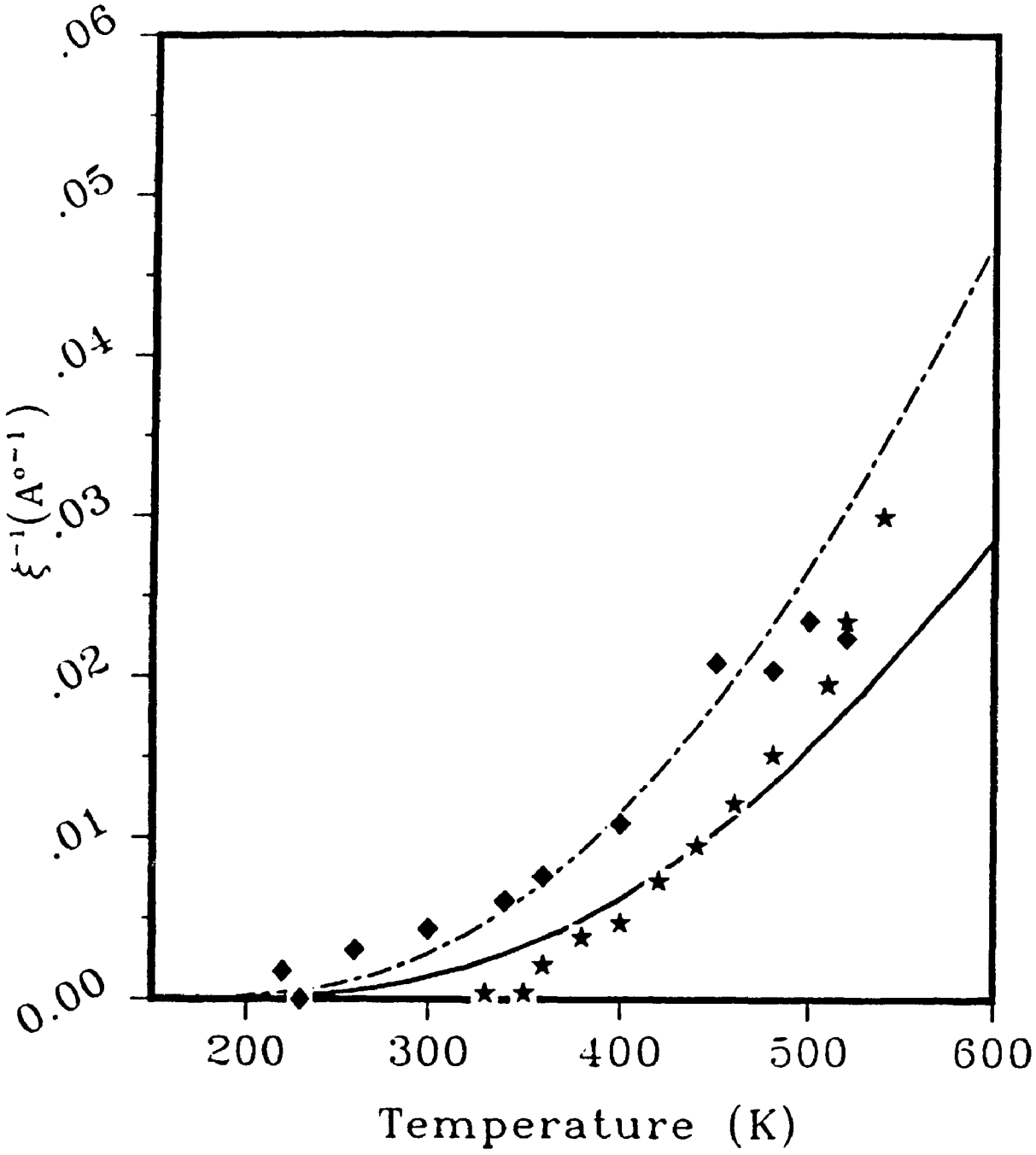

Figure 8.1: Variation of Magnetic Correlation length with temperature stars and squares are the experimental points from Keimer et. al [114] and solid and dashed lines are the self-consistent results for T_N = 325K and 190K respectively.

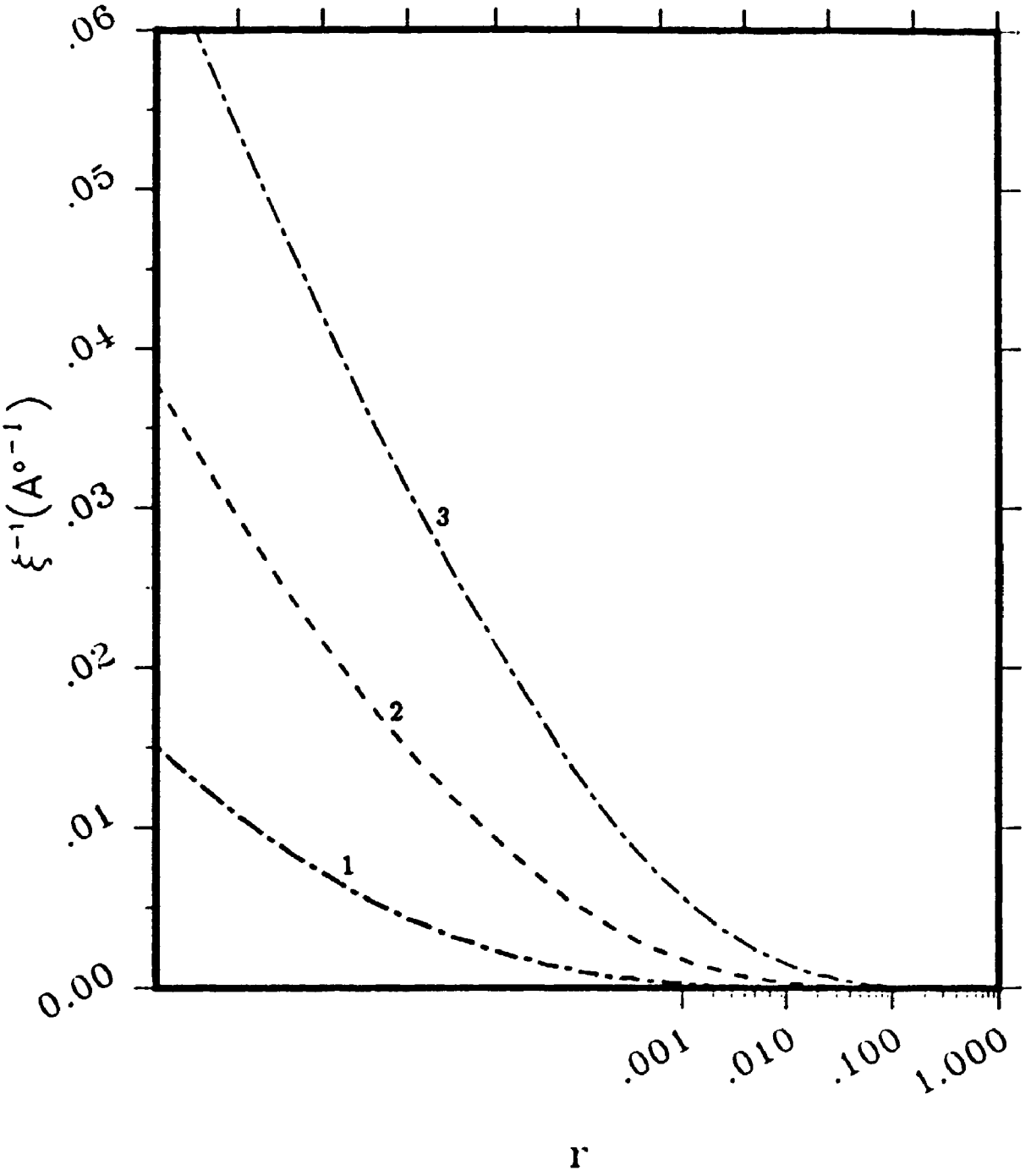

Figure 8.2: Variation of Magnetic Correlation length with ratio of inter to intra-planar couplings. Curves 1, 2, 3 are the self-consistent results for $\frac{J_\perp}{J_\parallel}$ from 10^{-8} to 1.0 at temperatures 300K, 400K and 500K respectively. The fitting parameters are C=1.67 and D=5.62.

correlation length can be suitably represented by

$$\xi = 0.24\frac{c}{2\pi\rho_s}\, e^{\frac{2\pi\rho_s}{T}} \tag{8.7}$$

where, c is the spin-wave velocity and $2\pi\rho_s$ is the spin-stiffness constant. The pre exponential factor was calculated by approximately matching the renormalization group analysis with a Monte-Carlo simulation of the 2D Heisenberg model. The above expression can only be applied to the undoped samples and can't be applied to the doped samples. Once it was realized that the doping greatly suppresses the magnetic correlation length, the above theory was modified by others [148, 149, 150]. Higher order terms were included to find an exact analytic expression for the magnetic correlation length.

So far, one of the most accurate simulation studies performed on the spin-1/2 quantum Heisenberg antiferromagnet, by Ding and Makivic [147] have found that their numerical data can be best fitted by an expression of the kind

$$\xi = 0.27a \exp[\frac{1.25J}{T}] \tag{8.8}$$

We have compared our theoretical results with these simulation results. According to our theory [cf. eqn.(8.6)], 0.27a in the expression above is replaced by a constant C while 1.25J is replaced by DT_N. The numerical results have shown that C=1.62 while simulation results have a value of 1.03 ($\sim$ 0.27 a). Our estimates give a value of D T_N=1826.5K while the simulation results are 1812.5K (1.25J). Hence, the results obtained from our self-consistent theory are in excellent agreement with the Monte Carlo simulation results of Ding and Makivic.

Keimer et al. have used the XY Heisenberg model to explain their neutron

scattering experiments. They have used a generic mean-field expression

$$\xi(\alpha_{eff}, T) = \frac{\xi_0(T)}{\sqrt{1 - \alpha_{eff}\xi_0(T)^2}} \tag{8.9}$$

where $\xi_0(T)$ is the correlation length for the unperturbed Heisenberg system. They have varied both stiffness constant and α in the above equation to obtain fitting to the experimental curves for carrier free 2-1-4. A best fit was obtained for $\alpha = 6.5 \cdot 10^{-4}$ and $2\pi\rho_s$= 140 meV for pure samples of 2-1-4. Majlis et al. have calculated the magnetic correlation length using RPA and MRPA. They have chosen a parameter, the ratio of interplanar to intraplanar couplings to fit the experimental curves. However, their approach takes the mean field theory to calculate the Neel temperature [74].

Some of other calculations [68, 69, 70, 148] although based on different methods have all arrived at the following form for the magnetic correlation length in two-dimensions:

$$\xi_c^{(2D)}(T \to 0) = \frac{Bc}{k_B T} \exp\left[\frac{2\pi\rho_s}{k_B T}\right] \tag{8.10}$$

where B is a numerical coefficient, c is the spin-wave velocity and ρ_s is the spin stiffness constant. These results are similar to the results of Chakravarty et al. which we have described above. Our values for C and D T_N are very close to the values obtained by all these methods.

The elaborate methods such as Quantum non-linear σ model, Monte Carlo studies etc. have still not yielded in a perfect fit of the experimental results. Our method requires just two constants as the fitting parameter and can be used for both undoped and doped samples of 2-1-4. It's a simple method not as elaborate as the QNLσ model but yet it gives very good fitting to the neutron scattering results of Keimer et al. The evaluation of magnetic correlation has given us an exponential

dependence of ξ, which agrees with the results of non-linear σ model and also the Monte Carlo simulation studies. So, in essence, we have found a simple analytical expression for the magnetic correlation length by using the self-consistent theory derived in Chapters IV and V. Our expression gives very good results both for the variation of magnetic correlation length with temperature and also with the doping concentration in 2-1-4 compounds.

Chapter 9

SUMMARY AND CONCLUSIONS

Antiferromagnetism and Superconductivity are so intimately connected with each other that a study of one without the other is incomplete. The subject has developed so much during the past seven years that a complete study of all the aspects has become a virtual impossibility. We have in this study chosen to focus our attention to the Normal state magnetic properties since it provides us with the knowledge that eventually would prove to be the building block for any future theory for High temperature Superconductivity.

In case of these High temperature superconductors, study of the normal state has given very important clues. It was Anderson [13] who first pointed out that the superexchange interactions between nearest neighbour copper within a CuO_2 plane would be unusually strong, and the magnetism would essentially be two-dimensional in character. Some of these speculations have now been confirmed in 2-1-4 [16]. It is however, still not confirmed if these strong antiferromagnetic correlations are in some way related to the pairing mechanism. Several theories have assumed that significant fluctuations of a magnetic type persist from the insulating phase to the

metallic and superconducting phase.

There has been few efforts which took these antiferromagnetic correlations to explain the pairing mechanism but still a lot is to be desired for a complete understanding. Fortunately, there are compelling evidences pointing to the fact that antiferromagnetic correlations do sustain in the Superconducting phase too. In quasi-one dimensional organic superconductors as well as in some two-dimensional layered superconductors, it has been reported that the antiferromagnetic ordering pertains in the metallic superconducting state. Without a tinge of doubt, it has now been established that these correlations are one of the strongest in the normal state and they do play a very important role in the onset of superconductivity. Precisely, what role do they play and how far are they responsible for the High temperature superconductivity in layered antiferromagnets is still anybody's guess.

Amidst this confusion and chaos, we have presented here a comprehensive study with our own tools to explain some of the interesting magnetic properties of HTS in the Normal state. The theory is built for quasi-two dimensional antiferromagnets and is shown to work well in explaining the magnetic properties of HTS. We have used the quasi-two dimensional Heisenberg model to encompass the layered structure of 1-2-3 and 2-1-4 type of compounds with weak but finite interlayer coupling. We have used the equation of motion method for the Green's function on a quasi-two dimensional Heisenberg Hamiltonian to obtain the correlation function between spins. Decoupling of the series of equations is obtained via the Random Phase Approximation which ignores the fluctuations in the z-component of spin and replaces it with corresponding average value. A variety of magnetic properties in the normal state are calculated using this self-consistent theory and the results are compared with the available experiments. We have established with the help of our

deliberations that:

- **The self-consistent theory is consistent with the Mermin-Wagner theory for Antiferromagnets.**

According to Mermin and Wagner (1960) there cannot be long range order at any finite temperature in 2-D antiferromagnets. We have shown that our theory also comes to the same conclusion when r, the interlayer coupling, becomes zero. The Neel temperature for strictly 2-D antiferromagnets is zero.

- **The theory gives a good estimate for the Neel temperature.**

The expression for Neel temperature given in Chapter IV was tested for 1-2-3 and 2-1-4 compounds. With known values for intralayer coupling and the ratio for interlayer to intralayer coupling, reasonably good approximation for the Neel temperature was obtained in both these cases. By assuming a linear dependence of 'r', the ratio of interlayer to intralayer coupling, on the doping parameter 'x' we get reasonable values for the doping dependent Neel temperature.

- **An analytical expression for the Neel temperature is proposed and its dependence on the ratio of inter to intraplanar coupling and temperature is studied.**

From our numerical calculations we have found that the Neel temperature is inversely proportional to logarithmic dependence on 'r', the ratio of interlayer to

intralayer coupling. The analytical expression which gives this dependence is:

$$T_N = \frac{J_{||}}{2k_B\,[0.1616\ ln(J_{||}/J_{\perp}) + 0.5055]}$$

Similar logarithmic term has been reported by various groups in the premises of a spin-wave theory. We have compared the variation of 'r' as a function of 'x' with the linear dependence of 'r' and 'x' and the fitting is pretty good. The analytical expression can be used for all practical purposes to evaluate the Neel temperature for layered antiferromagnets.

- **Self-consistent expression for the sublattice Magnetization is obtained and it is shown that the estimates obtained are in full agreement with the results of Anderson's spin-wave theory and others.**

The theory is used to find a self-consistent expression for the sublattice magnetization. The expression is numerically evaluated and the dependence of magnetization on the ratio of interlayer to intralayer coupling is studied. The temperature variation of sublattice magnetization is also studied. It is shown that the sublattice magnetization depends heavily on the interlayer coupling and the effect of the intralayer coupling is minimal. The theoretical predictions are quite consistent with the experimental observations and it is observed that the theory gives very good values for the fractional spin as observed by Anderson. The theoretical results are also compared with the spin-wave results and exceptional consistency at low temperatures is observed. Towards the Neel temperature it is established that our theory gives better estimate for the magnetization than the spin-wave theory.

- **Spectral function of spin waves is used to explain the magnetic susceptibility at high temperatures.**

We have introduced the spectral function of spin waves to calculate the magnetic Susceptibility in the presence of an external magnetic field. The Susceptibility is evaluated numerically and the results thus obtained are compared with other experimental results. At high enough temperatures, our results are quite consistent with the experiments. At low temperatures $\sim 2J_{\|}/K_B$ there is a maximum observed experimentally which is totally missed by our results. It is also shown that for 3D case the magnetic susceptibility is a T^2 function of the temperature while for quasi-2D case it has a linear temperature dependence.

- **Use of self-consistent theory to study dimensional crossover and determination of a critical anisotropy ratio in layered antiferromagnets**

It is shown from the study of magnetization that the magnetic properties undergo a dimensional crossover as the ratio of inter to intraplanar coupling approaches a value 'r$\sim 10^{-3}$. Most of the magnetic properties in the normal state are solely a function of 'r' and thus the determination of this critical ratio is a crucial one. Most of the recent experimental results and other theoretical approaches give an estimate which is exactly like ours.

- **Use of spectral function of spin waves to demonstrate that the magnetic properties have a T-dependent crossover from 3D to quasi-2D behaviour.**

It is shown rather generally by use of the spectral function that most of the magnetic properties in HTS have a crossover from 3D to quasi-2D behaviour near the temperature ($\sim 2J_{||}\sqrt{2r}/K_B$). We show that the sublattice magnetization normalized to its value at zero temperature ie. M(T)/M(0) as a function of temperature normalized to the Neel temperature ie. T/T_N is a sole function of r, the ratio between the interlayer to intralayer coupling. The variation of M(T)/M(0) vs. T/T_N is independent of the value of $J_{||}$. As the value of 'r' decreases, the shape of M(T)/M(0) - T/T_N changes drastically from the 3D behaviour to 2D behaviour. Identical crossover behaviour is also observed in the magnetic susceptibility calculations.

- **Magnetic correlation length is explained and it's variation with temperature and doping is studied.**

We have obtained an expression for the magnetic correlation length for doped and undoped 2-1-4 compounds. We have numerically evaluated the expression using two independent fitting parameters and found good agreement with the experimental results on 2-1-4. We have also compared our fitting parameters with other theoretical results and have found good agreement with results published to date. Our expression gives a correlation length which has a dependence over 'r' hidden in the expression for the Neel temperature. We have hence calculated the variation of correlation length with 'r' and show that near and above the Neel temperature the magnetic correlation increases drastically as 'r' increases.

Appendix I

Equation of Motion method

In what follows, we would briefly outline the Equation of motion method for the Green's function that has been used in our formulation for the normal state properties of layered antiferromagnets. This method was initially proposed by Bogoliubov to study ferromagnetism [145]. Later it was used by Hewson to study the magnetic properties of the antiferromagnet $CuCl_2 \cdot H_2O$ [146]. Over the years, Green's function has been extensively used in the study of isotropic ferromagnets and antiferromagnets [77, 132, 133, 134, 135, 131, 136]. Although recently, after the emergence of HTSc, a successful application of the equation of motion method for the Green's function to layered antiferromagnets have made it possible for us to understand lot of normal state properties in these compounds. We present here a very brief outline, however, interested researchers can find the details about this method in standard texts.

I.1 Green's function

We can define the double-time temperature dependent retarded Green's function $<< A(t); B(t') >>$ involving two Heisenberg operators A(t) and B(t') by :

$$G(t,t') =<< A(t); B(t') >>= -i\theta(t-t') < [A(t); B(t')] > \tag{I.1}$$

where the square brackets represent the commutator; single pointed brackets denote a thermal average over a canonical ensemble and $\theta(t-t')$ is a step function with the value unity when $t > t'$ and zero when $t < t'$. We shall obtain a set of equations for the Green's function in equationI.1. The operators A(t) and B(t') satisfy equations of motion of the form

$$i\frac{dA}{dt} = AH - HA \tag{I.2}$$

Differentiating the Green's function given in equation (I.1) with respect to 't' we get

$$i\frac{dG}{dt} = i\frac{d}{dt} << A; B >>= \frac{d\theta(t-t')}{dt} < [A(t), B(t')] > + << i\frac{dA(t)}{dt}; B(t') >> \tag{I.3}$$

This equation is called the **Equation of motion** for the Green's function. Also, it should be noted that the relation between the step function$\theta(t)$ and the δ function of 't' is given by

$$\theta(t) = \int_0^\infty \delta(t)dt \tag{I.4}$$

Using this identity we can now write the equation for the Green's function G in the form

$$i\frac{dG}{dt} = \delta(t-t') < [A(t), B(t')] > + << \{A(t)H(t) - H(t)A(t)\}; B(t') >> \tag{I.5}$$

The double time Green's function on the right hand side of above equation are, generally speaking, of higher order than the initial one. We now can construct equations

of the kind (I.3) and thus can obtain a system of coupled equations for different Green's functions. These chains should be supplemented with actual boundary conditions which would be done with the help of 'Spectral theorems'. These coupled chain of equations are exact and the solution of these are extremely complicated. One chooses to use some approximations to decouple this chain and reduce it to finite set of equations which can then be solved. This however, can be done in limiting cases of model Hamiltonians and as it turns out we would be using some of these approximations in case of Heisenberg Hamiltonian to solve for Antiferromagnetic materials.

I.1.1 Correlation functions

Particles in quantum system either follow Fermi or Bose statistics. They interact with each other. If there were no correlation between the probabilities of finding a particle at 'r' and other at 'r'' we should have

$$< \rho(r)\rho(r') >=< \rho(r) >< \rho(r') > \tag{I.6}$$

If 'A' and 'B' are two commuting operators then the correlation function can be defined as $< AB >$. However, if they do not commute then the simultaneous measurement is impossible and it's not possible to talk about correlation in such a situation. Yet, measurement of one may not affect the other and so it can be written and it is in fact written. The correlation between two commuting operators is defined as

$$< \rho(r)\rho(r') > - < \rho(r) >< \rho(r') > \tag{I.7}$$

Correlation functions can be either spatial or temporal. The Green's function depends on the correlation functions. There is a basic difference between the two

though. The Green's function or its time derivatives are discontinuous at ' t=t' but the correlation functions aren't.

Time correlation functions are the averages of the product of operators in the Heisenberg representation over a statistical ensemble. They are represented by

$$F_{BA}(t-t') =< B(t')A(t) >;\ F_{AB} =< A(t)B(t') >> \tag{I.8}$$

In case of statistical equilibrium the functions F_{BA} and F_{AB} depend, as do the Green's functions, on (t-t'). The difference with Green's functions is that they do not contain any discontinuous function and can also be defined when the times are same. At t=t' they give the average values of the product of operators. Hence these correlation functions or the distribution functions of statistical mechanics would enable us to evaluate the average values of some dynamical properties of the system.

I.1.2 Spectral Representation

For solving the equations for the Green's function it is important to have the spectral representations that supplement the set of equations with the necessary boundary conditions. We obtain these spectral relations for the Green's functions and for the corresponding correlation functions. The required spectral representations for the time correlation functions are defined as

$$F_{BA}(t-t') =< B(t')A(t) >= \int_{-\infty}^{\infty} J(\omega)e^{-i\omega(t-t')}d\omega \tag{I.9}$$

$$F_{AB}(t-t') =< A(t)B(t') >= \int_{-\infty}^{\infty} J(\omega)e^{\frac{\omega}{\theta}}e^{-i\omega(t-t')}d\omega \tag{I.10}$$

These are the required spectral representations for the time correlation functions where $J(\omega)$ is called the spectral intensity of the function $F_{BA}(t)$ [136].

Spectral Representation for the Green's function

If G(E) is the Fourier component of the Green's function G(t-t') then

$$G(t-t') = \int_{-\infty}^{\infty} G(E) e^{-iE(t-t')} dE \tag{I.11}$$

$$G(E) = \frac{1}{2\pi} \int_{-\infty}^{\infty} G(t) e^{iEt} dt \tag{I.12}$$

Putting the value of G(t) from eqn.(I.1) into the above equation we obtain

$$G(E) = \frac{1}{2\pi i} \int_{-\infty}^{\infty} dt e^{iE(t-t')} \theta(t-t') < A(t)B(t') - B(t')A(t) > \tag{I.13}$$

Under the above integral we have the time correlation functions. Introducing the spectral representation for them we get

$$G(E) = \int_{-\infty}^{\infty} d\omega J(\omega)(e^{\frac{\omega}{\tau}} - 1) \frac{1}{2\pi i} \int_{-\infty}^{\infty} dt e^{i(E-\omega)t} \theta(t) \tag{I.14}$$

We can write the discontinuous step function $\theta(t)$ in the form

$$\theta(t) = \int_{-\infty}^{t} e^{\epsilon t} \delta(t) dt \tag{I.15}$$

Now since

$$\delta(t) = \frac{1}{2\pi} \int_{-\infty}^{\infty} e^{-ixt} dx \tag{I.16}$$

or in the integral form we can write for the step function

$$\theta(t) = \frac{i}{2\pi} \int_{-\infty}^{\infty} \frac{e^{-ixt}}{x + i\epsilon} dx \tag{I.17}$$

Using the above two equations we get

$$\frac{1}{2\pi} \int_{-\infty}^{\infty} dt e^{i(E-\omega)t} \theta(t) = \frac{i}{2\pi} \frac{1}{E - \omega + i\epsilon} \tag{I.18}$$

The Fourier component G(E) of the Green's function G(t) is thus equal to

$$G(E) = \frac{1}{2\pi} \int_{-\infty}^{\infty} (e^{\frac{\omega}{\tau}} - 1) J(\omega) \frac{d\omega}{E - \omega + i\epsilon} \tag{I.19}$$

Sofar, we have considered E to be a real quantity. The above function can be analytically continued in the complex E plane. Assuming, E to be complex, we have

$$\frac{1}{2\pi}\int_{-\infty}^{\infty}(e^{\frac{\omega}{\theta}}-1)J(\omega)\frac{d\omega}{E-\omega}=G(E)\ ImE>0 \tag{I.20}$$

The above function can be considered to be analytical function in the complex plane with a singularity on the real axis. It can be shown that the function G(E) can be analytically continued in the region of complex E. If we know the function G(E), we can also find the spectral intensity J(ω) from the relation

$$G(\omega+i\epsilon)-G(\omega-i\epsilon)=-i(e^{\frac{\omega}{\theta}}-1)J(\omega) \tag{I.21}$$

where ω is real. Taking the difference of the two expressions we get

$$G(\omega+i\epsilon)-G(\omega-i\epsilon)=\frac{1}{2\pi}\int_{-\infty}^{\infty}(e^{\frac{\omega}{\theta}}-1)J(E)\left\{\frac{1}{\omega-E+i\epsilon}-\frac{1}{\omega-E-i\epsilon}\right\}dE \tag{I.22}$$

and then using the δ function representation

$$\delta(x)=\frac{1}{2\pi i}\left\{\frac{1}{x-i\epsilon}-\frac{1}{x+i\epsilon}\right\} \tag{I.23}$$

we arrive at equation (I.21). If we could decouple the chain of equations for the Green's function we can easily construct from G(E) the spectral intensity J(ω) and then find the time correlation functions. We'll then have

$$F_{BA}(t-t')=<B(t-t')A(t)>=i\int_{-\infty}^{\infty}\frac{G(\omega+i\epsilon)-G(\omega-i\epsilon)}{e^{\frac{\omega}{\theta}}-1)}e^{-i\omega(t-t')}d\omega \tag{I.24}$$

The above formula has been used in earlier chapters for the formulation of the theory for antiferromagnets and also to find the correlation function for two spin operators.

Appendix II

Second Quantization

Second quantization allows one to deal with variable number of particles as conveniently as with numbers. The particles can be electrons, phonons magnons depending upon the nature of the problem at hand. Here, we would use it in terms of electrons to find a correspondence between this notation and the spin operators that we have used throughout this study.

If we have an electron at site 'm' with spin 'σ'' and another electron at site 'l' with spin 'σ', the electron part of the hamiltonian can be written as

$$H = H_o + H_{ex} + H_{corr} + H_{tr} \tag{II.1}$$

where

$$H_o = \sum_{l,\sigma} \epsilon_l C^{\dagger}_{l,\sigma} C_{l,\sigma} + \frac{1}{2} \sum_{lm\sigma\sigma'} K_{lm} C^{\dagger}_{l\sigma} C_{l\sigma} C^{\dagger}_{m\sigma'} C_{m\sigma'} \tag{II.2}$$

Here, the ϵ_l is the one-electron orbital energy term and the first term is the kinetic energy term of the individual electrons while the second part is the coulomb repulsion energy between the two electrons. The K_{lm} is defined as the two-body Coulomb integral given as

$$K_{lm} = < \phi_l(r_1)\phi_m(r_2)|\frac{e^2}{r_{12}}|\phi_l(r_1)\phi_m(r_2) > \tag{II.3}$$

The second term in equation (II.1) is the 'Exchange Energy' while the third and the fourth terms are 'Correlation term' and 'Transfer term' which we won't be dealing with here. The Exchange energy term on the other hand can be written as

$$H_{ex} = \frac{1}{2} \sum_{l \neq m \sigma \sigma'} J_{lm} C^{\dagger}_{l\sigma'} C^{\dagger}_{m\sigma} C_{l\sigma} C_{m\sigma'} \tag{II.4}$$

where the exchange coupling constant J_{lm} is denoted as

$$J_{lm} = < \phi_l(r_1)\phi_m(r_2)|\frac{e^2}{r_{12}}|\phi_m(r_1)\phi_l(r_2) > \tag{II.5}$$

The exchange hamiltonian describes the annihilation of two fermions at sites 'm' and 'l' with spins 'σ' and 'σ'' and creation of two fermions at sites 'l' and 'm' with spins interchanged. These fermion creation and annihilation operators follow the anticommutation relation

$$\begin{aligned} \{C_{i\uparrow}, C_{j\downarrow}\} &= \{C^{-}_{i\uparrow}, C^{-}_{j\downarrow}\} = 0 \\ \{C_{i\uparrow}, C^{-}_{j\downarrow}\} &= \delta_{i,j}\delta_{\uparrow,\downarrow} \end{aligned}$$

For spin $\frac{1}{2}$ we have :

$$C^{\dagger}_{i\uparrow}C_{i\uparrow} + C^{\dagger}_{i\downarrow}C_{i\downarrow} = 1 = N_{i\uparrow} + N_{i\downarrow} \tag{II.6}$$

where N is the 'Number operator'.

$$C^{\dagger}_{i\uparrow}C_{i\uparrow} - C^{\dagger}_{i\downarrow}C_{i\downarrow} = 2S^z_i \tag{II.7}$$

$$C^{\dagger}_{i\uparrow}C_{i\downarrow} = S^+_i = S^x_i + iS^y_i \tag{II.8}$$

$$C^{\dagger}_{i\downarrow}C_{i\uparrow} = S^-_i = S^x_i - iS^y_i \tag{II.9}$$

Now,

$$\begin{aligned} \sum_{\sigma,\sigma'} C^{\dagger}_{l,\sigma'} C^{\dagger}_{m,\sigma} C_{l,\sigma} C_{m,\sigma'} &= C^{\dagger}_{l\uparrow}C^{\dagger}_{m\uparrow}C_{l\uparrow}C_{m\uparrow} + C^{\dagger}_{l\uparrow}C^{\dagger}_{m\downarrow}C_{l\downarrow}C_{m\uparrow} \\ &\quad + C^{\dagger}_{l\downarrow}C_{m\uparrow}C_{l\uparrow}C_{m\downarrow} + C^{\dagger}_{l\downarrow}C^{\dagger}_{m\downarrow}C_{l\downarrow}C_{m\downarrow} \end{aligned} \tag{II.10}$$

Here, we have replaced σ and σ' with the two possible orientations of spins in these states ie 'up ($\uparrow$)' and 'down ($\downarrow$)' Solving the right hand side (RHS) of the above equation we obtain

$$\begin{aligned}
RHS &= -\frac{1}{2}[-2C^{\dagger}_{l\uparrow}C^{\dagger}_{m\uparrow}C_{l\uparrow}C_{m\uparrow} - 2C^{\dagger}_{l\downarrow}C^{\dagger}_{m\downarrow}C_{l\downarrow}C_{m\downarrow} \\
&\quad \underbrace{-2C^{\dagger}_{l\uparrow}C^{\dagger}_{m\downarrow}C_{l\downarrow}C_{m\uparrow} - 2C^{\dagger}_{l\downarrow}C_{m\uparrow}C_{l\uparrow}C_{m\downarrow}}_{X}] \\
&= -\frac{1}{2}[X - 2\underbrace{(C^{\dagger}_{l\uparrow}C^{\dagger}_{m\uparrow}C_{l\uparrow}C_{m\uparrow} + C^{\dagger}_{l\downarrow}C^{\dagger}_{m\downarrow}C_{l\downarrow}C_{m\downarrow})}_{Y}] \\
&= -\frac{1}{2}[X - Y - C^{\dagger}_{l\uparrow}C^{\dagger}_{m\uparrow}C_{l\uparrow}C_{m\uparrow} - C^{\dagger}_{l\downarrow}C^{\dagger}_{m\downarrow}C_{l\downarrow}C_{m\downarrow}] \\
&= -\frac{1}{2}[X - Y + C^{\dagger}_{l\uparrow}C_{l\uparrow}C^{\dagger}_{m\uparrow}C_{m\uparrow} + C^{\dagger}_{l\downarrow}C_{l\downarrow}C^{\dagger}_{m\downarrow}C_{m\downarrow}] \\
&= -\frac{1}{2}[X - Y + C^{\dagger}_{l\uparrow}C_{l\uparrow}(1 - C^{\dagger}_{m\downarrow}C_{m\downarrow}) + C^{\dagger}_{l\downarrow}C_{l\downarrow}(1 - C^{\dagger}_{m\uparrow}C_{m\uparrow})] \\
&= -\frac{1}{2}[X - Y + 1 + C^{\dagger}_{l\uparrow}C^{\dagger}_{m\downarrow}C_{l\uparrow}C_{m\downarrow} + C^{\dagger}_{l\downarrow}C^{\dagger}_{m\uparrow}C_{l\downarrow}C_{m\uparrow}] \\
&= -\frac{1}{2}[1 - 2C^{\dagger}_{l\uparrow}C^{\dagger}_{m\downarrow}C_{l\downarrow}C_{m\uparrow} - 2C^{\dagger}_{l\downarrow}C^{\dagger}_{m\uparrow}C_{l\uparrow}C_{m\downarrow} \\
&\quad -C^{\dagger}_{l\uparrow}C^{\dagger}_{m\uparrow}C_{l\uparrow}C_{m\uparrow} - C^{\dagger}_{l\downarrow}C^{\dagger}_{m\downarrow}C_{l\downarrow}C_{m\downarrow} + C^{\dagger}_{l\uparrow}C^{\dagger}_{m\downarrow}C_{l\uparrow}C_{m\downarrow} + C^{\dagger}_{l\downarrow}C^{\dagger}_{m\uparrow}C_{l\downarrow}C_{m\uparrow}] \\
&= -\frac{1}{2}[1 + 2C^{\dagger}_{l\uparrow}C_{l\downarrow}C^{\dagger}_{m\downarrow}C_{m\uparrow} + 2C^{\dagger}_{l\downarrow}C_{l\uparrow}C^{\dagger}_{m\uparrow}C_{m\downarrow} \\
&\quad +(C^{\dagger}_{l\uparrow}C_{l\uparrow} - C^{\dagger}_{l\downarrow}C_{l\downarrow})(C^{\dagger}_{m\uparrow}C_{m\uparrow} - C^{\dagger}_{m\downarrow}C_{m\downarrow})] \\
&= [-\frac{1}{2} - S^{+}_{l}S^{-}_{m} - S^{-}_{l}S^{+}_{m} - \frac{1}{2}2S^{z}_{l}2S^{z}_{m}] \\
&= [-\frac{1}{2} - 2\{\frac{1}{2}(S^{+}_{l}S^{-}_{m} + S^{-}_{l}S^{+}_{m}) + S^{z}_{l}S^{z}_{m}\}] \\
&= -[\frac{1}{2} + 2S_{l}\cdot S_{m}]
\end{aligned}$$

So now, we have for the exchange hamiltonian :

$$H_{ex} = -\frac{1}{2}\sum_{l\neq m} J_{lm}[\frac{1}{2} + 2S_{l}\cdot S_{m}] \qquad (II.11)$$

$$H_{ex} = -\frac{1}{4}\sum_{l\neq m} J_{lm} - \sum_{l\neq m} J_{lm}S_{l}\cdot S_{m} \qquad (II.12)$$

The first term is a constant energy term and the exchange term in terms of spin operators can be written as

$$H_{ex} = -\sum_{l \neq m} J_{lm} S_l \cdot S_m \qquad \text{(II.13)}$$

This is infact the Heisenberg hamiltonian which plays an important role in studying Ferro and Antiferromagnetic materials.

Bibliography

[1] **Kammerling Onnes, H.** : 'Report on the Researches made in the Leiden Cryogenic Laboratory between the Second and Third International Co. gress of Refrigeration', Suppl. No. 34b.
(See *Superconductivity - Selected Reprints*, American Institute of Physics, New York, 1964, pp 8-23).

[2] **Meissner, W and R. Oschenfeld,** *Ein neuer Effekt bei Eintritt der Supraleitfahigkeit. Naturwiss.* **21**, 787-788 (1933).

[3] **Gorter, C.J and H. Casimir,** *Physica* **1**, 306-320 (1934).

[4] **London, H.** *Proc. Roy. Soc. (London)* **A 155** , 102 (1936).

[5] **Ginzburg, V.L and L.D. Landau** *Zh. Eksp. Teor. Fiz.* **20**, 1064 (1950).
See Collected papers of L. D. Landau. ed by D. Ter Haar. Gordan & Breach, nr 73 (1967).

[6] **Bardeen, J, L.N. Cooper and J.R. Schrieffer,** *Phys. Rev* **108**, 1175 (1957).

[7] **Bednorz, J.G and Muller, K.A,** *Z. Phys. B - Condensed matter* **64**, 189-193 (1986).

[8] **Wu, M.K, J.R. Ashburn, C.J. Torng, P.H. Hor, R L. Meng, L. Gao, Z.J. Huang, Y.Q. Wang and C.W. Chu** *Phys. Rev. Lett* **58**, 908 (1987).

[9] **Maeda, H. et al.** *Jpn. J. Appl. Phys. Lett.* **27**, 209 (1988).

[10] **Sheng, Z. and Hermann, A.** *Nature* **332**, 55 (1988).

[11] **Schilling, A. et al.** *Nature* **363**, 56 (1993).

[12] **Chu, C. W. et al.** *Nature* **365**, 323 (1993)

[13] **Anderson, P.W.** *Science* **235**, 1196 (1987).

[14] **Anderson, P.W. et al.** *Phys. Rev. Lett.* **58**, 2790 (1987).

[15] **Yamada, K. et al.** *Solid Stat. Comm.* **64**, 753 (1987).

[16] **Shirane, G. et al.** *Phys. Rev Lett.* **59**, 1613 (1987).

[17] **Endoh, Y. et al.** *Phys. Rev* **B37**, 7443 (1988).

[18] **Burns, Gerald** *High-Temperature Superconductivity, An Introduction*, Academic Press Inc., CA, USA (1992).

[19] **Friedman, T.A. et al** *Phys. Rev.* **B42**, 6217 (1990).

[20] **Marten, S. et. al** *Phys. Rev.* **B41**, 846 (1990).

[21] **Takagi, H. et al.** *Phys. Rev.* **B40**, 2254 (1990).

[22] **Gough, C. E. et al.** *Nature* **326**, 855 (1987) ; **Gross, R. et al.** *Physica* **C166**, 277 (1990) ; **Keene, M. N. et al.** *Nature* **340**, 210 (1989) ; **Lee, G. T. et al.** *Physica* **C161**, 195 (1989).

[23] **Van Bentum et al** *Physica C* **153**, 1718-1723 (1988).

[24] **Tsai, J. S. et al.** *Physica* **C 153-155**, 1385 (1988).

[25] **Thomas, G. A. et al.** *Phys. Rev. Lett.* **61**, 1313 (1988).

[26] **Braginsky, A.I et al.** *Proc. 5th Int. Workshop on Future Electron Devices - High Temperature Superconducting Devices*, pp 171-179 (1988).

[27] **Meservey, R. and Schwartz, B. B.** in *Superconductivity* , ed. by R. D. Parks, New York, pp 124-127 (1969).

[28] **Batlogg, B. et al.** *Phys. Rev. Lett.* **58**, 2333 (1987).

[29] **Bourne, L. C. et al.** *Phys. Rev. Lett.* **58**, 2337 (1987).

[30] **Lee, P.A and Read, N.** *Phys. Rev. Lett.* **58**, 2691, (1987).

[31] **Varma, C.M. et al** *Proceedings of the International Conference on New Mechanisms of Superconductivity*, ed. by V. Kresin and S. Wolf , Plenum, New York (1987).

[32] **Kresin, V.** *Phys. Rev.* **B35**, 8716 (1987).

[33] **Ruvalds, J.** *Phys. Rev.* **B35**, 8869 (1987).

[34] **Prelovsek, P. Rice, T. M. and Zhang, F. C.** *Jou. Phys. C : Solid State Phy.* **20**, L229 (1987).

[35] **Vaknin, D. et al** *Phys. Rev.* **B41**, 1926 (1990).

[36] **Tranquada, J. M. et al.** *Phys, Rev. Lett.***60**, 156 (1988).

[37] **Tranquada, J. M. et al.** *Phys. Rev.* **B38**, 2477 (1988).

[38] **Torrance, J. B. et al.** *Phys. Rev.* **B40**, 8872 (1989).

[39] **Johnston, D. C.** *Phys. Rev. Lett.* **62**, 957, 1989; **Greene, R. L. et al.** *Solid State Comm.* **63**, 379 (1987).

[40] **Lee, W. C. et al.** *Phys. Rev. Lett.* **63**, 1012 (1989).

[41] **Cheong, S - W. et al.** *Solid Stat. Comm.* **65**, 111 (1988).

[42] **Johnston, D. C. et al.** *Phys. Rev.* **B36**, 4007 (1987).

[43] **Cava, R. J. et al.** *Phys. Rev.* **B36**, 5719 (1987).

[44] **Ganguly, P. et al.** *Pramana J. Phys.* **28**, L321, (1987).

[45] **Grant, P. M. et al.** *Phys. Rev.* **B35**, 7242 (1987).

[46] **Hazen, R. M. et al.** *Phys. Rev.* **B35**, 7238 (1987).

[47] **Qadri, S. B. et al.** *Phys. Rev.* **B35**, 7235 (1987).

[48] **Jorgensen, J. D. et al.** *Phys. Rev. Lett.* , **58**, 1024 (1987).

[49] **Hass, K.C** *Solid State Phys.* , 42 (1989).

[50] **Takigawa, M. et al.** *Phys. Rev.* **B39**, 7371 (1989).

[51] **Alloul, H. et al.** *Phys. Rev. Lett.* **61**, 746 (1988).

[52] **Mitsuda, S. et al.** *Phys. Rev.* **B36**, 822 (1987) ; **Freltoft, T. et al.** *Phys. Rev.* **B36**, 826 (1987) ; **Kastener, M. A. et al.** *Phys. Rev.* **B38**, 6636 (1988)

[53] **Stassis, C. et al.** *Phys. Rev.* **B38**, 9291 (1988).

[54] **Uemura, Y. J. et al.** *Phys. Rev. Lett.* **59**, 1045 (1987).

[55] **Harshman, D. R. et al.** *Phys. Rev.* **B38**, 852 (1988).

[56] **Birgeneau, R. J. and G. Shirane in** *Physical Properties of High Temperature Superconductors I*, edited by D.M. Ginsberg (World Scientific, Singapore) (1989).

[57] **Brewer, J. H. et al.** *Phys. Rev. Lett.* **60**, 1073 (1988).

[58] **Preyer, N. W. et al.** *Phys. Rev.* **B42**, 11563, (1989).

[59] **Chen, C. Y. et al.** *Phys. Rev.* **B43**, 1 (1991).

[60] **Watanabe, I. et al.** *J. Phys. Soc. Jpn.* **46**, 3028 (1987).

[61] **Birgeneau, R. J. et al.** *Phys. Rev. Lett.* , **59**, 1329 (1987).

[62] **Chakravarty, S.** *High temperature Superconductivity* ed. Bedell et al. (Addison-Wesley, 1990) pp 136 and **Batlogg**, *ibid*, pp 37.

[63] **Manousakis, Efstratios** *Rev. Mod. Phys.* **63**, 1 (1991).

[64] **Lyons, K. et al.** *Phys. Rev.* **B37**, 2353 (1988).

[65] **Sulewski, P. E. et al.** *Phys. Rev.* **B41**, 225 (1990).

[66] **Aeppli, G. et al.** *Phys. Rev. Lett.* **62**, 2052 (1988).

[67] **Chakravarty, S. Halperin, B. I. and Nelson, D. R**, *Phys. Rev. Lett.* **60**, 1057 (1988).

[68] **Arovas, D. P. and Auerbach, A.**, *Phys. Rev.* **B38**, 316 (1988).

[69] **Takahashi, M.** *Phys. Rev.* **B40**, 2494 (1989).

[70] **Hirch, J. E and Tang, S** *Phys. Rev.* **B40**, 4769 (1989).

[71] **Soukoulis, C. M. et al.** *Phys. Rev.* **B44**, 446 (1991).

[72] **Singh, A. and Tesanovic, Zlatko** *Phys. Rev.* **B43**, 11445 (1991).

[73] **Yablonskiy, D. A.** *Phys. Rev.* **B44**, 4467 (1991).

[74] **Majlis, N. Selzer, S and Strinati, G. C.** *Phys. Rev.* **B45**, 7872 (1992) ; *Phys. Rev.* **B48**, 957 (1993).

[75] **Liu, Bang-Gui** *Phys. Rev.* **B41**, 9563 (1990).

[76] **Singh, Avinash et al.** *Phys. Rev. Lett.* **64**, 2571 (1990).

[77] **Oguchi, T.,***Phys. Rev.* **117**, 117 (1960); **Kubo, R.**, ibid **87**, 568 (1952).

[78] **Ding, H. Q and Makivic, M. S.** *Phys. Rev. Lett.* **64**, 1449 (1990).

[79] **Singh, R. R. P. et al.** *Phys. Rev. Lett.* **62**, 2736 (1989).

[80] **Lynn, J. W.** *High Temperature Superconductivity* ed. J.W.Lynn (Springer-Verlag, 1990) pp 268.

[81] **Li, Q. et al.** *Phys. Rev. Lett.* **64**, 3086 (1990).

[82] **Chen, Hao et al.** *Phys. Rev.* **B41**, 267 (1990).

[83] **Jolicoeur, Th. et al.** *Phys. Rev.* **B42**, 4800 (1990).

[84] **Ohkawa, Fusayoshi J.** *Phys. Rev.* **B42**, 4163 (1990).

[85] **Diep, H. T.** *Phys. Rev.* **B40**, 4818 (1989).

[86] **Li, W. H. et al.** *Phys. Rev.* **B37**, 9844 (1988).

[87] **Kadowaki, H. et al.** *Phys. Rev.* **B37**, 7932 (1988).

[88] **Moudden, A. H. et al.** *Phys. Rev.* **B38**, 8893 (1988).

[89] **Dgotto, E.** *Int Journal of Mod. Phy.* **5**, 77 (1991).

[90] **Lu, J. P.** *Phys. Rev. Lett.* **68**, 125 (1992).

[91] **Nori, F. et al.** *Phys. Rev. Lett.* **68**, 240 (1992).

[92] **Borsa, F.** *Phys. Rev. Lett.* **68**, 698 (1992).

[93] **Bulut, N. and Scalapino, D. S.** *Phys. Rev. Lett.* **68**, 706 (1992).

[94] **Canneli, G. et al.** *Phys. Rev.* **B45**, 931 (1992).

[95] **Ghatak, S. K. et al.** *Phys. Rev.* **B45**, 951 (1992).

[96] **Boolchand, P. et al.** *Phys. Rev.* **B45**, 921 (1992).

[97] **Collcott, S. J. et al.***Phys. Rev.* **B45**, 945 (1992).

[98] **Guskos, N.** *Phy. stat. solidi (b)* **163**, k113 (1991).

[99] **Chandra, P. et al.** *Int. Jour. Mod. Phy.* **5**, 171 (1991).

[100] **Martinez, G. and Horsch, P.** *Int. Jour. Mod. Phy.* **5**, 207 (1991).

[101] **Sachdev, S. and Read, N.** *Int. Jour. Mod. Phy.* **5**, 219 (1991).

[102] **Moriya, T.** *Physica C* **114**, 80 (1991).

[103] **Pines, D.** *Physica C* **120**, 80 (1991).

[104] **Garcia, J. L. et al.***Physica C* **80**, 1085 (1991).

[105] **Singh, M.** *Solid Stat. Communication* **70**, 751 (1989).

[106] **Fleming, R. M. et al.** *Phys. Rev.* **B35**, 7191 (1987).

[107] **Shafer, M. W. et al.** *Phys. Rev.* **B36**, 4047 (1987).

[108] Kumagai, K. et al. *Phys. Rev. Lett.* **60**, 724 (1988).

[109] **Rossat-Mignod, J. et al.** *Proc. Int'l Conf. on the physics of highly correlated systems, Santa Fe, NM* (Sept 1989).

[110] **Mermin, N. D. and Wagner, H.** *Phys. Rev. Lett.* **17**, 1133; 1307 (1966).

[111] **Tahir-Kheli, R. A. and ter Haar, D.** *Phys. Rev.* **127**, 88 (1962).

[112] **Jou, D. and Chen, H.** *Phys. Lett.* , **45A**, 239 (1973).

[113] **Marshell, W. and Lovesey, S. W.** *Theory of Thermal neutron scattering: The use of neutron for the investigation of Condensed Matter* (Clarendon, Oxford, 1971); **Liu, S. H.** *Phys. Rev* , **142**, 267 (1966).

[114] **Keimer, B. et al.** *Phys. Rev.* **B45**, 7430 (1992).

[115] **Phillips, J. C** *Physics of High-T_c Superconductors, Academic Press Inc. (1989)* ; *Phys. Rev Lett.* **59**, 1856 (1987).

[116] **Tang, H. et al.** *Jour. Appl. Phys.* **67**, 4518 (1990).

[117] **Nishihara, Y. et al.** *Jpn J. Appl. Phys. Lett.* **26**, L1416 (1988).

[118] **Tang, H. et al.** *J. Appl. Phys.* **64**, 5950 (1988).

[119] **Kopietz, Peter** *Phys. Rev. Lett.* **68**, 3480 (1992); **Kopietz, Peter** *Phys. Rev. Lett.* **71**, 655 (1993).

[120] **Singh, A. et al.***Phys. Rev.* **B41**, 11457 (1990).

[121] **Anderson, P. W.** *Phys. Rev.* **86**, 694 (1952).

[122] **Imbert, P. et al.***Phys. Rev. Lett.* **71**, 654 (1993).

[123] **Saylor, J. et al.** *Phys. Rev.* **B40**, 6854 (1989).

[124] **Rosov, N.** *Phys. Rev. Lett.* **67**, 1938 (1991).

[125] **Johnston, D. C. et al.** *in Chemistry of High-temperature superconductivity* , edited by D. L. Nelson, M. S. Wittingham and T. F. George, ACS symposium series No. 351 (American Chemical society, Washington, DC) (1987).

[126] **Nishida, N. et al.** *Jpn. J. Appl. Phys.* **26**, L1856 (1987); *J. Phys. Soc. Jpn.* **57**, 722 (1988).

[127] **Tranquada, J. M. et al.** *Phys. Rev. Lett.* **60**, 1567 (1988).

[128] **Troc, R. et al.** *Phys. Lett. A* **125**, 222 (1987).

[129] **Vier, D. C. et al.** *Phys. Rev.* **B36**, 8888 (1987).

[130] **Jacobson, A. J. et al.** *in IUPAC Symposium on Chemistry of oxide superconductors* , edited by C. N. R. Rao (IUPAC/ Blackwell, Oxford) (1988).

[131] **Lines, M. E.** *J. Phys. Chem. Solids* **31**, 101 (1970); *Phys. Rev.* **139**, A1304, 1965; 164, 736 (1967).

[132] **Bloch, M.** *Phys. Rev. Lett.* **9**, 268 (1962); *J. Appl. Phys.* **34**, 1151 (1963).

[133] **Hewson, A. C. and Ter Haar, D.** *Physica* **30**, 890 (1964); **Hewson, A. C, Ter Haar, D. and Lines, M. E.** *Phys. Rev.* **137**, A1465 (1965).

[134] **Callen, H. B.** *Phys. Rev.* **130**, 890 (1963).

[135] **Haas, C. W. and Jarret, H. S.** *Phys. Rev.* **135**, A1089 (1964).

[136] **Zubarev, D. N.** *Sov. Phys. Usp.* **3**, 320 (1960).

[137] **Glasser, M. L. and Zucker, I. J.** *Proc. Natl. Acad. Sci.* USA **74**, 1800 (1977) and references therein.

[138] **de Jongh, L. J.** in *Magnetism and Magnetic materials* ed. by Graham, C D. and Rhyne, J. , AIP Conference Proceedings No. 10 (AIP, New York 1972).

[139] **Auerbach, A. et al.***Phys. Rev. Lett.* **61**, 617 (1988).

[140] **Hohenemser, C. et al.***Physica* **C162**, 1283 (1989).

[141] **Singh, R. P. Tao, Z. C. and Singh, M.** *Phys. Stat. Solidi (b)* **179**, 539 (1993).

[142] **Wei, G. Z. and Du, A.** *Phys. Stat. Solidi (b)* **175**, 237 (1993).

[143] **Lynn, J. W. et al.***Phys. Rev.* **B36**, 2374 (1987).

[144] **Chattopadhyay, T.** *Europhys. Lett.* **6**, 363 (1988).

[145] **Bogoliubov, N. N. et al.** *Sov. Phy. Dokl.* **4**, 604 (1959).

[146] **Hewson, A. C and D. Ter Haar** *Physica* **30**, 890 (1964).

[147] **Ding, H. Q. and Makivic, M.** *Phys. Rev.* **B43**, 2662 (1991).

[148] **Hasenfratz, P. and Niedermayer, F.** *Phys. Lett. B* , **168**, 231 (1991).

[149] **Muramatsu, A.** *Phys. Rev. Lett.* **65**, 2909 (1990).

[150] **Yanagisawa, T.** *Phys. Rev. Lett.* **68**, 1026 (1992).

[151] **Fischer, H. E. et al.** *Comments on Cond. Mat. Phys.* **14**, 65 (1988).

[152] **Uher, B.** *Superconductivity and it's Applications* , ed. H. S. Kwok et al., Plenum Press, NY (1990).

[153] **Lyons, K. B. Fluery, P. A. Singh, R. R. P. and Sulewski, P. E**, in *Dynamics of magnetic fluctuations in High temperature superconductors* edited by G. Reiter et al., Plenum Press, New york (1991).

[154] **Borodin, V. A. et al.** *JETP Lett.* **52**, 469 (1990) ; **Lutgemeier, H. and Pieper, M. W.** *Solid Stat. Comm.* **64**, 267 (1987) ; **MacLaughlin, D. E. at al.** *Phys. Rev. Lett.* **67**, 525 (1991).

[155] **Singh, R. P. and Singh, M.** *Phys. Stat. Solidi (b)* **169**, 571 (1992).

[156] **Singh, R. P. and Singh, M.** *Phys. Rev.* **B46**, 14069 (1992).

[157] **Singh, R. P. Tao, Z. C. and Singh, M.** *Phys. Rev.* **B46**, 1244 (1992).

[158] **Carlson, J.** *Phys. Rev.* **B40**, 846 (1989).

[159] **Callaway, J.** *Quantum theory of the Solid State*, (Academic), New York (1976).

[160] **Peters, C. J. et al.** *Phys. Rev.* **B37**, 9761 (1988).

[161] **Micnas, R. et al.** *Rev. Mod. Phys.* **62**, 113 (1990).

[162] **Chakravarty, S. et al.** *Phys. Rev.* **B39**, 2344 (1989).

[163] **Tyc, Stephane and Halperin, Bertrand** *Phys. Rev.* **B42**, 2096 (1990).